U. S. DEPARTMENT OF COMMERCE
W. Averell Harriman, Secretary
NATIONAL BUREAU OF STANDARDS
E. U. Condon, Director

APRIL 1948
VOLUME 40
NUMBER 4

JOURNAL OF RESEARCH

of the

NATIONAL BUREAU OF STANDARDS

Contents

RP		Page
1871.	Determination of sulfur in bone char. Victor R. Deitz, Helen R. Higginson, and Cola Parker. (Price 15 cents)	263
1872.	Effect of support on the performance of vane anemometers. Galen B. Schubauer and Gerald H. Adams. (Price 10 cents)	275
1873.	Heat of combustion of phenyl-beta-naphthylamine (*N*-phenyl-2-naphthylamine). Donald E. Roberts and Ralph S. Jessup. (Price 5 cents)	281
1874.	Calibration of X-ray measurement of strain. John A. Bennett and Herbert C. Vacher. (Price 15 cents)	285
1875.	Magnetic measurement of the thickness of composite copper and nickel coatings on steel. Abner Brenner and Eugenia Kellogg. (Price 10 cents)	295
1876.	Behavior of experimental zinc-steel couples underground. Irving A. Denison and Melvin Romanoff. (Price 15 cents)	301
1877.	Disintegration of antimony-124. Irving Feister and Leon F. Curtiss. (Price 10 cents)	315
1878.	Stabilization of austenitic stainless steel. Samuel J. Rosenberg and John H. Darr. (Price 15 cents)	321

For sale by the Superintendent of Documents, U. S. Government Printing Office, Washington 25, D. C. - Price 45 cents
$4.50 per year on subscription

UNITED STATES GOVERNMENT PRINTING OFFICE, WASHINGTON : 1948

U. S. Department of Commerce
National Bureau of Standards

Research Paper RP1871
Volume 40, April 1948

Part of the Journal of Research of the National Bureau of Standards

Determination of Sulfur in Bone Char[1]

By Victor R. Deitz, Helen R. Higginson,[2] and Cola Parker

In sugar technology the established analytical procedures were found to give erroneous results for the "sulfide" sulfur and "total" sulfur in bone char. The error was found to be caused by the presence of organic sulfur in the carbonaceous component. Solution of the total sulfur in bone char was obtained by three independent methods: (1) After oxidation with nitric and perchloric acids, (2) after air oxidation in an intimate mixture with sodium carbonate and magnesium oxide, (3) after oxidation with nitric acid in a modified Carius tube. The precipitate of barium sulfate was found to be contaminated with calcium and phosphate from the bone char. It was discovered in the present work that barium sulfate was easily and completely soluble in hot 70-percent perchloric acid, thus making possible a purification by reprecipitation. Quantitative precipitation was verified by using known mixtures of calcium chloride, phosphoric acid, and sulfuric acid. The distribution of the total sulfur between the carbonaceous residue and the filtrate resulting from the conventional acid treatment of bone char was determined after digestion in three mixtures: nitric and hydrochloric acids, potassium chlorate and hydrochloric acid, and hydrochloric acid alone. It was shown that the sulfur contained in the gases evolved with hydrochloric acid (determined by combustion with air followed by gravimetric barium sulfate) was greater in most samples than that determined as sulfide-sulfur (precipitated as cadmium sulfide and determined iodometrically). The distribution of the total sulfur between filtrate, residue, and evolved gases was influenced by deliberate variations in the acid leaching process.

I. Introduction

In sugar technology the established methods of determining sulfur in bone char have been concerned with the calcium sulfate and calcium sulfide. The general procedure outlined by Spencer and Meade [1][3] is substantially the same as that of the original methods outlined in 1881 by Tucker [2]. Discordant results obtained by these methods made it desirable to make a critical study of the procedures for determining sulfur in bone char.

According to the old procedure, a sample of bone char was heated with hydrochloric acid, cooled, and diluted to a known volume. The residual carbonaceous matter was removed by filtration. A barium sulfate determination was then made in an aliquot part of the filtrate. The result was calculated as percentage "calcium sulfate" of the original sample of char. In order to determine "calcium sulfide", a sample of the original char was first digested with either nitric acid or a mixture of potassium chlorate and hydrochloric acid. The subsequent procedure was the same as that given for the calcium sulfate. Subtracting from the result of this determination, the barium sulfate already found in the calcium sulfate determination gave the barium sulfate equivalent to the calcium sulfide. One object of this paper is to show that these methods may give erroneous results for the sulfide sulfur and the total sulfur in bone char. It will also be shown that this is due to a significant quantity of organic

[1] This investigation has resulted from a joint research project undertaken by the United States Cane Sugar Refiners and Bone Char Manufacturers, a greater part of the refining industry of the British Commonwealth, and the National Bureau of Standards.

[2] Research Associate at the National Bureau of Standards, representing the United States Cane Sugar Refiners and Bone Char Manufacturers and the greater part of the refining industry of the British Dominion.

[3] Figures in brackets indicate the literature references at the end of this paper.

sulfur contained in the carbonaceous component of bone char.

An accurate determination of the sulfur in bone char is important in a study of its revivification. In kilns using direct firing, the bone char is in contact with the products of combustion of the fuel, which may have several possible effects on the char.

The total sulfur content of service bone char may be of the order of magnitude of 1 percent, when expressed as SO_4. The gross heterogeneity of char and the difficulty of obtaining uniform samples are factors that limit the reproducibility of the analytical results. For aliquot parts of a given well-mixed powdered sample, it is possible to realize a precision adequate for this work.[4]

II. Precipitation of $BaSO_4$ in the Presence of Ca and PO_4 Ions

Many investigations with contaminated barium sulfate precipitates in analytical chemistry have shown the difficulties attending the exact determination of sulfur as barium sulfate. An interesting discussion of the possible compensation of considerable plus and minus errors has been given by Hillebrand and Lundell [3]. Kolthoff and Sandell [4] have also reviewed the evidence for the contamination of barium sulfate precipitates by coprecipitation under various conditions.

A great deal of difficulty was experienced in precipitating the sulfate quantitatively from known solutions containing the sulfate, calcium, and phosphate ions. For bone char the problem is that of determining about 1 percent of total sulfur, expressed as SO_4 in the presence of about 40 percent of calcium ion and 50 percent of phosphate ion. The extensive literature on the barium sulfate determination has unfortunately not dealt with this situation.

The precipitation of barium sulfate from known solutions of calcium chloride, phosphoric acid, and sulfuric acid was first investigated in some detail. The weights of calcium chloride and phosphoric acid in each solution were maintained constant, and the values were chosen so as to give 1.75 g of calcium ion and 2.75 g of phosphate ion in each test solution. These weights correspond approximately to the weight of calcium and phosphate ions contained in a solution of 5 g of a bone char.

In these investigations, the precipitation of barium sulfate was conducted at an acidity between pH 1 and 2. It was found possible to obtain an easily filterable precipitate and to avoid excessive loss of barium sulfate by solution. This value for acidity is in agreement with the value of 0.05 *N* hydrochloric acid recommended by Kolthoff and Sandell [4]. Fortunately, the solutions prepared from the bone char samples were readily filterable at pH 1, although they were almost nonfilterable at pH 2. A glass electrode and pH meter, calibrated with a buffer of pH 3.0, were used in determining the pH of all solutions.

Data for the weights of barium sulfate precipitated from known amounts of sulfuric acid in mixtures of calcium chloride and phosphoric acid are given in table 1. The precipitation was made by the slow addition of 50 ml of a 5-percent solution of barium chloride. The first four determinations were with mixtures of the sulfuric acid in calcium chloride only, and the results indicate a

TABLE 1. *Weights of barium sulfate derived from a single precipitation in a mixture of sulfuric acid, calcium chloride, and phosphoric acid, adjusted with hydrochloric acid to* pH *1*

Conditions of precipitation	Weight of precipitate		
	Found	Theory	Difference
CALCIUM CHLORIDE AND SULFURIC ACID			
	g	*g*	*Percent*
4 hr stirring at 30° C	0.3273	0.3239	+1.05
Do	.3228	.3239	−0.33
Do	.3263	.3239	+.74
Do	.3278	.3239	+1.20
PHOSPHORIC ACID AND SULFURIC ACID			
4 hr stirring at 30° C	0.3346	0.3239	+3.30
Do	.3440	.3239	+6.21
CALCIUM CHLORIDE, PHOSPHORIC AND SULFURIC ACIDS			
4 hr stirring at 50° C, stood overnight	0.3044	0.2790	+9.10
Do	.3081	.2790	+10.43
6 hr stirring at 90° C, stood overnight	.3375	.3244	+4.04
Do	.3387	.3244	+4.41
4 hr stirring at 50° C, stood overnight	[a] .2961	.2790	+6.13
Do	[a] .3009	.2790	+7.85
Do	[a] .2979	.2790	+6.77
Do	[a] .3010	.2790	+7.88
Do	[a] .3056	.2790	+9.52

[4] A coefficient of variability of 1.65% as a measure of the precision was calculated from the data of table 5.

[a] Saturated barium hydroxide used instead of 5-percent solution of barium chloride.

percentage difference of about 1 percent. With sulfuric acid in solutions of phosphoric acid, the indicated contamination was greater. With mixtures of calcium chlroride, phosphoric acid, and sulfuric acid the positive error has been found to be as much as 10 percent. Qualitative examination showed that the precipitates from the phosphate mixtures were contaminated with phosphate ion.

In the course of the experiments to be described on the total oxidation of the carbonaceous matter in bone char, it was discovered that the barium sulfate precipitate was freely soluble in hot perchloric acid.[5] [6] It was thus possible to purify the precipitate by a reprecipitation from perchloric acid. The only other solvent for barium sulfate to which reference has been found is hot concentrated sulfuric acid. Its use here is obviously not feasible.

The procedure for reprecipitating the barium sulfate was as follows: The first precipitate was obtained from a known volume of the standard solution of sulfuric acid in solutions of calcium chloride and phosphoric acid by the slow addition in drops of 50 ml of a 5-percent solution of barium chloride to the stirred mixture at 50° C. The pH was adjusted with ammonium hydroxide with the aid of a glass electrode to either pH 1 or 2, as designated in table 2. The precipitate was separated by filtration through analytical-grade filter paper and washed with 200 ml of distilled water. Both precipitate and paper were digested with concentrated nitric acid until the paper was decomposed. Perchloric acid was then added, and the mixture boiled in a covered beaker until a clear colorless solution was obtained. Distilled water was added slowly to the warm solution until the volume was approximately 400 ml; 5 ml of a 5-percent solution of barium chloride was added, and the stirred mixture was adjusted to pH 1 with ammonium hydroxide. The precipitate was allowed to stand overnight at room temperature and then filtered through a porcelain filtering crucible. It was ignited at 600° C for at least 2 hours.

TABLE 2. *Weights of barium sulfate after double precipitation*

pH	Weight of precipitate		
	Found	Theoretical	Difference
	g	*g*	*Percent*
2.0	0.1336	0.1298	+2.93
2.0	.1306	.1298	+0.62
1.0	.1283	.1298	−1.16
1.0	.1348	.1298	+3.85
1.0	.2907	.2790	+4.19
1.0	.2912	.2790	+4.37
1.0	.2923	.2790	+4.77
1.0	.2897	.2790	+3.84
2.0	.3286	.3244	+1.29
2.0	.3328	.3244	+2.59
2.0	.3360	.3244	+3.58
2.0	.3333	.3244	+2.74
1.0	.3384	.3244	+4.31
1.0	.3376	.3244	+4.06
1.0	.3352	.3244	+3.33
2.0	.6478	.6488	−0.15
2.0	.6506	.6488	+.28
2.0	.9873	.9732	+1.44
2.0	1.0000	.9732	+2.75

The results for the double precipitation are shown in table 2. The quantity of standard sulfuric acid was varied over a wide range. An analysis of the results in table 2 was made, disregarding the two values for pH. A measure of precision and also of accuracy was obtained and found to be very satisfactory. A very slight contamination of the barium sulfate precipitate was found equal to about 1 percent.[7]

The better agreement realized on double precipitation could be attributed to either a purging of the barium sulfate of the contaminants or to the closer compensation of the minus errors (for example, the possible loss of barium sulfate in the acid solution because of the additional analyti-

[5] Throughout this paper, whenever acids are mentioned, perchloric acid will mean the concentrated acid of commerce 70 to 72 percent; hydrochloric acid, the concentrated acid of specific gravity 1.18; nitric acid, the concentrated acid of specific gravity 1.42. Diluted acids will be designated as follows: For example, diluted hydrochloric acid (1+20) will mean 1 volume of the concentrated acid of specific gravity 1.18 diluted with 20 volumes of water. Ammonium hydroxide will mean the concentrated solution of specific gravity 0.90.

[6] Because of the possible explosive nature of perchloric acid mixtures, care must be taken that excess nitric acid be always present before adding perchloric acid.

[7] The authors are indebted to J. Mandel and W. V. Loebenstein for the following analysis of the data in table 2. They have plotted the weight of the precipitate found against the corresponding weight as calculated from the volume and the normality of the standard sulfuric acid. The plot of 19 points appeared to be sufficiently linear to warrant a fit by the method of least squares. The intercept of the resulting line was not significantly different from zero as indicated by a "Student's" t value of 1.64. This is smaller than the 2.11 value, corresponding to the 5-percent significance level for 17 degrees of freedom (R. A. Fisher, Statistical Methods for Research Workers). The slope of the fitted line was found to be only slightly different from 1, since the t value in this case was 2.14 compared to 2.11. This might indicate a contamination in the second precipitation of the order of 1 percent of the theoretical value. The standard deviation from regression is 0.0062 when expressed in grams of precipitate.

cal step) with the plus errors (the gain due to contamination). In order to test the latter possibility, an additional precipitation of the barium sulfate was made. The procedure for the second reprecipitation was exactly the same as for the first. The results are shown in table 3 where a comparison is made with those for a single and for a double precipitation. The results of a spectro-chemical analysis of the second and third precipitates did not show any appreciable difference in the presence of calcium or any other possible contaminants. This would indicate that the observed smaller plus error obtained in the third precipitation might be attributed to a closer compensation of the plus and minus errors.

TABLE 3. *Triple precipitation of the barium sulfate from known solutions of sulfuric acid containing calcium chloride and phosphoric acid*

Method	Weight of precipitate		
	Found	Theoretical	Difference
	g	*g*	*Percent*
Three precipitations	0.2845	0.2790	+1.97
Do	.2798	.2790	+0.29
Do	.2837	.2790	+1.68

The best procedure for the reprecipitation of barium sulfate from its solution in hot perchloric acid has yet to be established. It is, of course, most desirable to avoid the addition of any reagent that will recontaminate the barium sulfate. A few determinations were made in which the precipitate was dissolved in 15 ml of perchloric acid and reprecipitated by dilution with 600 ml of distilled water only (pH of the resulting mixture, 0.3). The results obtained by this procedure are low, as may be seen in table 4. Since barium sulfate was known to be soluble in strong acids, a few determinations were made in which the diluted mixture from the perchloric acid solution was adjusted to pH 1 with ammonium hydroxide. The very low results so obtained indicate the relatively strong effect of ammonium salts. This may have affected the solubility of the barium sulfate or the ammonium ion may have replaced some barium in the precipitate. The results were also low when only 1 ml of a 5-percent solution of barium chloride was added to the mixture containing ammonium hydroxide at pH 1. However, it was possible to obtain a positive error from the diluted mixture with ammonium hydroxide at pH 1 by the addition of sufficient barium chloride (see table 4). The addition of saturated barium hydroxide solution to the diluted mixture (instead of ammonium hydroxide and barium chloride) was tried in order to raise the pH and to depress the solubility by the common ion effect. Unfortunately, a considerable amount of barium hydroxide was required to decrease the acidity to pH 1 and the corresponding amount of barium ion introduced (50 times that contained in 5 ml of a 5-percent solution of barium chloride) was found to yield a large positive error (see table 4).

It would be of interest to ascertain how much barium hydroxide should be added to the diluted mixture in order to compensate for the negative error caused by the solubility. The addition of the barium ion would depress the solubility by the common ion effect alone. Another mode of attack would be to raise the pH by addition of the base of a large organic group and to furnish the barium ion by the barium salt of an organic acid (for example, barium salicylate). The use of large ions that do not coprecipitate has recently been used for the purpose of preparing a crystallographically pure barium sulfate [8]. The precision so far indicated by the work described appears to be sufficient for the present purposes.

TABLE 4. *Effect of some variations in the conditions employed to reprecipitate barium sulfate from solutions in hot concentrated perchloric acid*

[All first precipitates made in same manner]

Method	pH	Weight of precipitate		
		Found	Theory	Difference
		g	*g*	*Percent*
Dilution with water only	0.3	0.2732	0.2790	−2.08
Do	.3	.2688	.2790	−3.66
Dilution+NH_4OH	1.0	.0904	.1298	−30.4
Do	1.0	.1017	.1298	−21.6
Dilution+NH_4OH+1 ml $BaCl_2$	1.0	.3069	.3244	−5.39
Do	1.0	.3076	.3244	−5.18
Dilution+NH_4OH+10 ml $BaCl_2$	1.0	.3384	.3244	+4.31
Do	1.0	.3376	.3244	+4.06
Do	1.0	.3352	.3244	+3.33
Dilution+saturated $Ba(OH)_2$ (600 ml)	1.0	.2990	.2790	+7.17
Do	1.0	.2994	.2790	+7.31
Do	1.0	.2980	.2790	+6.81
Do	1.0	.2925	.2790	+4.84

III. Total Sulfur Content of Bone Char

In order to obtain the complete solution of a sample of bone char, it is necessary to decompose the insoluble carbonaceous component under conditions that insure no loss of the sulfur. Some of the total sulfur is contained as sulfate-sulfur, some as sulfide-sulfur, and some in combination with the carbonaceous component. Three different methods have been employed in this investigation to prepare a complete solution of the sulfur free of organic matter: (1) complete oxidation with nitric and perchloric acids, (2) the Eschka method, i. e., air oxidation in a muffle furnace of the intimate mixture with sodium carbonate and magnesium oxide, (3) nitric acid treatment in a modified Carius bomb.

1. Complete Oxidation With Nitric and Perchloric Acids

The destruction of organic matter by heating with concentrated nitric and perchloric acids has been incorporated in a number of analytical schemes. A 72.4-percent perchloric acid solution in water boils at 203° C (1 atm). This is approximately 100 deg lower than the temperature reached in a boiling sulfuric acid solution at atmospheric pressure. In these experiments, as well as as many others, it has been shown that the oxidation with a mixture of nitirc and perchloric acids can be performed without fear of dangerous explosions. The only precaution needed is first to heat the mixture at about 100°C until subsidence indicates the destruction of the more easily decomposable portion of the organic matter.

The detailed procedure for the analysis of a bone char for total sulfur by this method follows. A screen test of samples for analysis indicated that 90 percent passed through a U. S. Standard Sieve 80 and that 60 percent passed through a U. S. Standard Sieve 140. The procedure is divided into the numbered paragraphs for convenience in cross reference when the other methods are described. The following procedure is designated as method 1.

1.1. Five grams of the powdered bone char was placed in a weighing bottle and was dried between 105° to 110° C in an air oven for at least 4 hours. The bottle containing the sample was tightly stoppered upon removal from the oven and cooled in a desiccator. The stoppered bottle was weighed, the contents then transferred to an 800-ml beaker, and the bottle weighed again.

1.2. The sample was wetted with about 10 to 15 ml of distilled water, and 25 ml of nitric acid was added. This mixture was boiled gently for 1½ hours in a covered beaker. Fifteen milliliters of perchloric acid (see footnotes 5 and 6) was added and the beaker heated until all fumes of nitric acid had disappeared and the carbonaceous residue was completely oxidized. During this process the mixture changed from the original black to orange, then to brilliant yellow, and finally to a clear solution with a slightly pinkish tinge.

1.3. The clear solution was cooled and diluted with about 100 ml of distilled water. The small residue (insoluble silica) was removed by filtration through a Whatman No. 40 filter paper or its equivalent. The residue was washed thoroughly with 150 to 200 ml of distilled water, and all filtrates were collected in a 1,500-ml beaker.

1.4. Water was added until the volume of filtrate was 750 to 800 ml. The pH of this solution was adjusted to 1.0 by adding ammonium hydroxide dropwise during mechanical stirring (add hydrochloric acid if the pH is greater than 1.0 at first). A glass electrode and pH meter were used in determining the pH.

1.5. The solution was heated to a temperature of 50° C, and 50 ml of a 5-percent solution of barium chloride was added dropwise, the solution being stirred mechanically during the entire process. The temperature was maintained at 50° C for 4 hours.

1.6. The solution was then filtered through a Whatman No. 42 filter paper or its equivalent and the precipitate washed with distilled water until only a faint test for chloride was obtained with silver nitrate.

1.7. The filter paper containing the barium sulfate precipitate was transferred to an 800-ml beaker, and 25 ml of nitric acid was added. It was heated gently until the paper had decomposed; 15 ml of perchloric acid was added, and the solution was boiled until the nitric acid had been eliminated and the residue had dissolved. The covered beaker at this point became filled with white fumes, and the constant boiling mixture of perchloric acid and water condensed on the wall of the beaker. This state of reflux was continued for at least 15 minutes. The solution was perfectly clear and colorless or slightly yellow.

1.8. The solution was cooled to room temperature and 400 ml of distilled water was added; 5 ml of a 5-percent barium chloride solution was added, and the pH readjusted to 1.0. It was allowed to stand overnight. The mixture was filtered through a porcelain filtering crucible, washed with 100 ml of distilled water, and ignited for about 2 hours at 600° C, then cooled in a desiccator and weighed. The precipitate was weighed as barium sulfate, and the result was expressed as percentage of SO_4.

2. Eschka Method Applied to Bone Char

The Eschka method is commonly used in the determination of sulfur in coal. An intimate mixture of the sample with sodium carbonate and magnesium oxide is heated to convert all the sulfur into water-soluble sulfate. The method

can be readily applied to the determination of sulfur in bone char. There is little danger of losing oxides of sulfur, since the quantity of sulfur expressed as SO_4 contained in the organic matter to be oxidized is usually less than 1 percent of the weight of bone char.

A modification of the Eschka method described by Treadwell and Hall [5] was used. The following procedure is designated as method 2.

2.1. A 5-g sample of powdered bone char was taken. However, the sample in this case was transferred to a 200-ml evaporating dish instead of an 800-ml beaker.

2.2. The sample was mixed thoroughly in the dish with 10 g of magnesium oxide and 5 g of sodium carbonate. A second mixture containing 6 g of magnesium oxide and 3 g of sodium carbonate was sprinkled over the top of the mixture in the dish. The mixture with the sample should be completely covered. The dish was placed in an electric muffle furnace at room temperature, heated slowly to 600° C, and left overnight.

2.3. The sample was removed from the furnace and allowed to cool. The mixture was transferred to a 1,500-ml beaker with distilled water, stirred mechanically, and 100 ml of saturated bromine water added. The mixture was heated to boiling on a hot plate while continuously stirring; 50 to 80 ml of diluted hydrochloric acid (1+1) was added until the solution was acid to litmus, and the hot mixture was stirred for about an hour. Concentrated hydrochloric acid was then added dropwise until the solids dissolved and the solution became clear yellow with only a small insoluble residue of silica remaining. The amount of hydrochloric acid needed to make the solution clear varied from 100 to 200 ml. After the final addition of hydrochloric acid, the solution was kept on the hot plate an additional hour while continuously stirring.

2.4. The solution was allowed to cool and the silica residue filtered according to the procedure used in paragraph 1.3. The analysis of the filtrate was performed exactly as in paragraphs 1.4 through 1.8 of the perchloric-acid method (method 1).

3. Complete Oxidation in a Modified Carius Tube

A Carius combustion tube as modified by Gordon [6] and the technique described by Gordon, Schlecht, and Wichers [7] for the use of sealed tubes in preparing acid solutions of samples for analysis were employed in these analyses. The sealed tube was placed in a protective shell of cold-rolled steel, made by drilling a 1-in. hole into 1 4-in. length of 1¼-in. hexagonal stock and surrounded with solid carbon dioxide to provide a compensating pressure that served to reduce the probability of bursting the tube. It was found possible to oxidize the carbonaceous matter in bone char completely with fuming nitric acid and to reuse the tubes for several analyses.

The following analytical procedure is designated as method 3:

3.1. A 5-g sample of powdered bone char was taken. However, the sample in this case was transferred to a Carius tube [6]. The tube was cooled in liquid air, and 5 ml of fuming nitric acid was added. This was done to freeze the acid in order to delay any reaction. The tube was sealed while it was still immersed in the cooling mixture. The tube was placed in the steel shell and surrounded with 50 g of dry ice and the top screwed on securely. The steel shell was tested for leaks by immersing it in water to note the escape of gas bubbles. It was then placed in a muffle furnace at 215° C, slightly inclined so that the seal of the glass tube was elevated. The tube was left overnight in the furnace.

3.2. The steel shell was cooled to room temperature (about 2 hours) and the carbon dioxide cautiously released by unscrewing the cap. The Carius tube was taken out and the contents frozen by placing it in liquid air.[8] It was opened by heating with a tiny gas flame from a blow torch at the very end of the seal. The material inside the Carius tube usually had a deep blue color that disappeared soon after the tube was opened. The residue in the tube was transferred to an 800-ml beaker with a stream of hydrochloric acid. The analysis was continued exactly as in paragraphs 1.3 through 1.8.

4. Percentage of Total Sulfur

The method of determination for a given service bone char (Y–1) was further tested by making a number of determinations with the addition of known quantities of standard sulfuric acid to the bone char. The determinations were made according to method I in which the total sulfur was oxidized to sulfate-sulfur with a mixture of nitric and perchloric acids. The results are summarized in table 5. The amount of standard sulfuric acid was varied from 5 to 25 ml (0.1112*N*). With the smallest addition of sulfuric acid, approximately 20 percent of the barium sulfate came from the acid and 80 percent from the char. With the largest addition of sulfuric acid, approximately 60 percent came from the acid and 40 percent from the char. The average value of the total sulfur for the eight determinations was 1.91 percent expressed as SO_4. There is no apparent correlation of the individual results with the total amount of barium sulfate involved in the determination.

In view of the consideration already given to the reprecipitation of the barium sulfate (derived from known solutions of sulfuric acid, calcium chloride, and phosphoric acid) after solution in perchloric

[8] As a safety precaution, it is recommended that the steel shell be cooled in dry ice and the transfer of the Carius tube to the liquid air be made behind a window of safety glass.

TABLE 5. *Determinations by the nitric-perchloric acid method of the total sulfur in samples of a service bone char (Y–1) with additions of standard sulfuric acid*

Volume of standard H_2SO_4 (0.1112 N)	Weights of barium sulfate			Weight of char	Total sulfur in char expressed as SO_4
	Total	From the H_2SO_4[a]	From the char		
ml	*g*	*g*	*g*	*g*	*Percent*
5	0.2901	0.0649	0.2252	4.8465	1.91
10	.3645	.1298	.2347	4.9098	1.96
20	.4883	.2596	.2287	4.8037	1.92
25	.5545	.3244	.2301	4.8797	1.94
5	.2920	.0649	.2271	4.9799	1.88
10	.4447	.1298	.3149	6.9572	1.86
20	.5169	.2596	.2573	5.5377	1.91
25	.5497	.3244	.2253	4.8260	1.92
Avg					1.91

[a] Weights calculated from the normality and quantity of the standard sulfuric acid in column 1.

acid, it is important to study the effect of multiple precipitation employing bone char alone. Accordingly, several determinations were made of the total sulfate after a nitric-perchloric acid oxidation of the char sample in which the barium sulfate was reprecipitated twice. The results are contained in table 6, in which a comparison is made with the results from a single and double precipitation. Included, also, are some determinations in which the initial oxidation of the bone char was effected by the Eschka method already described. It is apparent from table 6, and can be shown by statistical considerations, that a significant difference exists between the average values for single and double precipitations, namely, 1.97 and 1.91 percent, respectively. The average value for the determinations employing triple precipitation is 1.89 percent, which can be shown not to be significantly smaller than 1.91 percent. It appears, therefore, that while a single reprecipitation of the barium sulfate precipitate is justified, there is not much to be gained by another similar operation.

Table 7 contains the results for the determination of total sulfur (expressed as SO_4) in six different service bone chars. The sulfur in each char was completely oxidized to sulfate-sulfur by the three methods already outlined. The results by initial oxidation with nitric acid in a Carius tube (method 3) appear to be higher than the results by methods 1 and 2. This may be due to unknown factors inherent in the methods of analysis

TABLE 6. *Single, double, or triple precipitation of the barium sulfate in the determination of total sulfur in bone char (expressed as SO_4)*

[All determinations were made with a service bone char, Y–1]

Single precipitation	Double precipitation	Triple precipitation
COMPLETE OXIDATION OF THE SAMPLE WITH NITRIC AND PERCHLORIC ACIDS		
Percent	*Percent*	*Percent*
[a] 2.01	1.89	1.89
[a] 1.97	1.90	1.90
1.97	1.91	1.88
1.96	1.92	----
ESCHKA'S METHOD APPLIED TO BONE CHAR		
1.98	1.92	----
1.96	1.92	----
Avg. 1.97	1.91	1.89

[a] Standard sulfuric acid added, and the corresponding amount of barium sulfate subtracted from the quantity determined experimentally.

TABLE 7. *Total sulfur (expressed as SO_4) in six service bone chars by three methods*

[Values in italic type are average values]

Char	method 1	method 2	method 3	Average of methods 1, 2, and 3
	Percent	*Percent*	*Percent*	*Percent*
Y–1	*1.91*	*1.92*	*1.96*	1.93
36	*1.98*	1.99	2.04	2.00
P–1	1.01	*0.95*	*1.00*	0.99
P–2	0.80	.81	0.85	.82
R–22	.96	.95	*1.00*	.97
R–23	.97	.94	*1.04*	.98

rather than to loss of sulfur during the oxidation step.

Further discussion of these results will be postponed until presentation of the analyses according to methods 4, 5, and 6.

IV. Sulfur in the Residue and in the Filtrate From Acid Leaching

When bone char is digested with nitric acid, it is well known that the carbonaceous residue takes on a different appearance than when hydrochloric acid alone is used. The treatment with nitric acid leaves a definite brownish residue that has been attributed to organic oxidation reactions. It is also known that the inorganic sulfides or sulfites are completely oxidized to sulfates. It is possible

778365—48——2

also to oxidize sulfides and sulfites to sulfates with a dilute mixture of potassium chlorate and hydrochloric acid. This does not appear to alter the carbonaceous matter to the extent that the nitric acid treatment does. Dilute hydrochloric acid alone may be expected to oxidize the carbonaceous matter to the least extent. The extent to which the above three acid mixtures oxidize the carbonaceous residue in bone char should determine the amount of sulfur that is extracted from the residue, providing, of course, there is appreciable sulfur in the residue. Thus, the sulfate-sulfur contained in the filtrate need not be derived solely from the inorganic salts in bone char.

Three independent analytical procedures will now be described in which the sulfur may be determined in both the residue and the filtrate obtained in acid leachings of bone char.

1. Digestion With Nitric Acid and Hydrochloric Acid

The following procedure will be designated as method 4 for the determination of sulfur in bone char:

4.1. A 10-g sample of finely powdered bone char was taken.

4.2. The sample contained in the 800-ml beaker was wetted with 25 ml of distilled water; 25 ml of concentrated nitric acid was added dropwise and the mixture allowed to evaporate slowly to dryness on the hot plate. It was necessary to remove the mixture from the hot plate immediately after the evaporation was completed so that no carbonaceous matter would be lost by oxidation. Three additional evaporations to dryness were then made using 15 ml of diluted hydrochloric acid (1+1) each time. This was done in order to expel the nitric acid completely. After the third evaporation, 40 ml of diluted hydrochloric acid (1+1) was added and the mixture boiled gently for about 1 hour.

4.3. The mixture was cooled and transferred to a volumetric flask, where it was made up to exactly 250 ml. The mixture was filtered through a No. 40 Whatman filter paper or its equivalent and exactly 200 ml collected in a second volumetric flask. The remaining solution, the residue and filter paper, and the funnel washings were transferred to an 800-ml beaker.

4.4 The filtrate contained in the 200-ml volumetric flask was transferred to a 1,500-ml beaker and this part of the analysis concluded according to paragraphs 1.4 through 1.8.

4.5. Twenty-five milliliters of nitric acid was added to the beaker containing the residue, the paper, and remaining filtrate and heated until the filter paper had disintegrated; 15 ml of perchloric acid was added, and the procedure outlined in paragraphs 1.2 through 1.8 was then followed.

4.6. The percentage total sulfate in the sample was calculated from the sum of the weights of barium sulfate obtained in 4.4 and 4.5. The volume of the residue was estimated from the weight of the residue and a value of 1.8 for the density. The weight of the residue was determined by the acid washing of independent samples. Subtracting the small volume of the residue from 250 ml yielded the total volume of the filtrate. The total sulfur in the filtrate, expressed as SO_4, was the value obtained for 200 ml (paragraph 4.4) multiplied by the ratio of the total volume of filtrate to 200 ml, approximately 1.25. The total sulfur expressed as SO_4 in the residue was calculated by subtracting the value for the filtrate from the value for the total sulfate.

2. Digestion With Potassium Chlorate and Hydrochloric Acid

The following procedure is designated as method 5 for the determination of sulfur in bone char:

5.1. A 10-g sample of finely powdered bone char was taken.

5.2. The sample contained in the 800-ml beaker was wetted with 25 ml of distilled water and 50 ml of a solution of potassium chlorate (10 g of potassium chlorate in a liter of water) was slowly added. The solution was heated to about 80° to 90° C, and 100 ml of diluted hydrochloric acid (1+1) was added dropwise from a buret, while stirring mechanically. The acid must not be added too rapidly lest sulfur escape as hydrogen sulfide. After the addition of all the acid, the mixture was boiled gently in the covered beaker for 1½ hours.

5.3. The analysis was concluded according to paragraphs 4.3 through 4.6.

3. Digestion With Hydrochloric Acid

The following procedure is designated as method 6 for the determination of sulfur in bone char:

6.1. A 10-g sample of finely powdered bone char was taken.

6.2. The sample contained in the 800-ml beaker was wetted with 25 ml of distilled water and 100 ml of diluted hydrochloric acid (1+1) slowly added. The solution was heated in a covered beaker for about 1½ hours at 80° to 90° C.

6.3. The analysis was concluded according to paragraphs 4.3 through 4.6. However, when separating the residue from the 200 ml of filtrate, No. 42 Whatman filter paper, or its equivalent was used.

4. Distribution of the Sulfur Between Residue and Filtrate

The results of a number of analyses by methods 4, 5, and 6 have shown good checks for the *sum* of the sulfur contained in the residue and that contained in the filtrate. The data for the six service bone chars already mentioned are given in table 8. The values for total sulfur contained

TABLE 8. *Distribution of the total sulfur (expressed as SO_4) between the residues and filtrates derived from the acid-leaching of service bone chars*

Char	Average total sulfur	HNO_3 and HCl			$KClO_3$ and HCl			HCl (alone)			
		Filtrate	Residue	Total	Filtrate	Residue	Total	Filtrate	Residue	Evolved[a] gases	Total
	Percent	*Percent*	*Percent*	*Percent*	*Percent*	*Percent*	*Percent*	*Percent*	*Percent*	*Percent*	*Percent*
Y-1	1.93	1.78	0.13	1.91	1.65	0.22	1.87	0.99	0.68	0.17	1.84
					1.65	.26	1.91	1.09	.58	.17	1.84
36	2.00	1.77	.23	2.00	1.53	.48	2.01	1.41	.35	.13	1.89
P-1	0.99	0.94	.04	0.98	0.98	.05	1.03	0.78	.16	.07	1.01
P-2	.82	.66	.15	.81	.72	.12	0.84	.32	.30	.05	0.87
		.73	.09	.82				.54	.25	.05	.84
R-22	.97	.88	.10	.98	.76	.23	.99	.48	.40	.08	.96
		.86	.06	.92							
R-23	.98	.89	.08	.97	.83	.11	.94	.57	.29	.10	.96
								.54	.33	.10	.97

[a] Determined by combustion of evolved gases in air.

in column 2 are those given in table 7, and these are inserted for comparison. The use of nitric and hydrochloric acids (method 4) resulted in the least value for the sulfur in the residue. It is of interest to note that the sulfur contained either in the residue or in the filtrate was found to vary considerably for individual determinations. When the sulfur was lower in the residue, it was higher in the filtrate; however, as mentioned above, the sum of that in the residue and that in the filtrate was constant.

Without exception the sulfur contained in the residue was greatest when the char was extracted with hydrochloric acid (method 6). There is evidence which points to some oxidation of the sulfur contained in the carbonaceous matter even when this acid alone is used. Samples of the same char (P–2) were digested in diluted hydrochloric acid (1+1) for different periods of time. Three samples after digestion for 1½ hours gave residues in which the result for sulfur (as SO_4) were 0.307, 0.262, and 0.246; two values after 8 hours were 0.234, and 0.222; one value after 50 hours was 0.226. These results indicate that for contact periods up to approximately 8 hours the hot hydrochloric acid is gradually leaching the sulfur from the carbonaceous residue. Because of the loss of volatile sulfur compounds (principally hydrogen sulfide) during the hydrochloric-acid leaching, the sum of the sulfur contained in the residue and in the filtrate does not equal the total sulfur.

V. Analysis of Gases Evolved With HCl

The presence of hydrogen sulfide is readily apparent in the gases evolved from bone char by the action of hydrochloric acid. The hydrogen sulfide has been attributed to the decomposition of inorganic sulfides in the char. Some may possibly result from an acid hydrolysis of an organic-sulfur component in the carbonaceous residue. If the latter possibility exists, there may be other volatile sulfur-containing gases in those evolved with hydrochloric acid.

With this possibility in mind, the gases derived from bone char by evolution with hydrochloric acid were analyzed by two methods. First, the hydrogen sulfide was determined alone; second, the evolved gases were burned in air and a gravimetric determination for barium sulfate made in the products of the reaction.

1. Iodometric Determination of the Hydrogen Sulfide

The sulfide sulfur was separated from the char by evolution with hydrochloric acid in a closed apparatus and by washing the gases in ammoniacal cadmium sulfate solution.[9] A schematic apparatus is illustrated in figure 1. The cadmium sulfide was determined without removal from the gas wash bottle by a subsequent titration with standard iodine in the acidified solution.

[9] The stock solution of ammoniacal cadmium sulfate contained 168 g of cadmium sulfate, 960 ml of concentrated ammonium hydroxide, and 1,046 ml of distilled water.

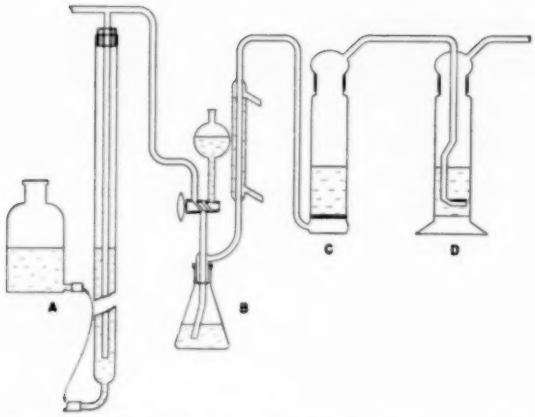

FIGURE 1. *Apparatus for the evolution of hydrogen sulfide.*
A, Pressure regulator for carrier gas; *B*, evolution unit with Erlenmeyer flask equipped with interchangeable ground joint; *C* and *D*, gas-wash bottles with fritted disks charged with solution of ammoniacal cadmium sulfate.

Two gas-wash bottles with fritted disks were used in series and charged with a dilute solution of ammoniacal cadmium sulfate made by diluting 1 ml of the stock solution to 100 ml of water. A 5-g sample of bone char was introduced into the Erlenmeyer flask, the interchangeable joint wetted, and the apparatus assembled. A test for possible leaks was made by application of air pressure. Fifty milliliters of diluted hydrochloric acid (1+1) was slowly added, and, as soon as the reaction slowed down, the system was swept with a flow of compressed air. The flask was heated gently for 20 minutes. The first gas-wash bottle was cooled with ice water. If the first gas-wash bottle alone contained a yellow precipitate of cadmium sulfide, then only this mixture was titrated with iodine. Before titration the mixture was acidified with 25 ml of hydrochloric acid. The heat evolved was usually sufficient to bring the solution to room temperature. The titration with standard iodine solution was made after adding 5 ml of a freshly made starch solution. As the end point was approached the solution appeared yellowish red, orange, purplish red, and finally a deep permanent blue. A blank was run to determine the amount of iodine necessary to color a similar solution containing no sulfide.

A number of results for six service bone chars are given as part of table 9. Considerable fluctuations were observed in repeated runs with aliquot parts of the same sample. A possible explanation will be given after the presentation of the second method for determining sulfur in the evolved gases. A number of measurements of the hydrogen sulfide liberated from steel (National Bureau of Standards Samples 9d and 8g) were made. The average of 10 determinations for samples of 9d was 0.036 percent of sulfur as compared with the standard value of 0.036 percent of sulfur. The average of five determinations of 8 g was 0.024 percent of sulfur as compared with the standard value of 0.026 percent of sulfur.

The results of table 9 indicate a possible oxidation of the sulfur gases with the carrier gas used to sweep out the apparatus. It appears that the results are higher when the carrier gas contains oxygen. However, the differences may also be due to variable action of the hydrochloric acid on the carbonaceous component of the bone char.

TABLE 9. *Determination of sulfur (expressed as SO_4) in the gases evolved from bone char by treatment with hydrochloric acid*

Sample	Iodometric determination of the hydrogen sulfide displaced with carrier gas noted		Gravimetric determination after combustion in air in a quartz furnace
	Percent		*Percent*
Y-1	0.135	Air	0.176
	.118	Commercial N_2	.151
	.105	do	.199
	.108	do	.217
	.117	do	.183
	[a].148	N_2 and O_2	.174
			.151
			Avg .170
36	.102	Commercial N_2	.158
	.103	do	
	.131	do	.192
	[a].126	N_2 and O_2	
P-1	.028	Air	
	.040	Commercial N_2	.072
	[a].035	N_2 and O_2	
P-2	.031	Commercial N_2	.096
	[a].036	N_2 and O_2	
R-22	.046	Commercial N_2	.077
	[a].071	N_2 and O_2	
R-23	.047	Commercial N_2	
	.062	Air	.085
	[a].057	N_2 and O_2	

[a] Independent values by R. M. Thompson.

2. Gravimetric Determination of the Evolved Sulfur by Combustion in Air

In this determination the gaseous products of evolution were directed by a stream of air to pass through a quartz tube, 1-cm inside diameter and 10 cm long, in which pieces of solid quartz rod were packed snugly. The quartz tube covered with wire gauze was heated to about 800° C with two Meker gas burners for at least 15 minutes before the reaction was allowed to take place in the evolution flask. While the quartz tube was heating, the system including two gas-wash bottles containing a 5-percent solution of sodium hydroxide was swept with air.

An attempt was made to get a very slow evolution of gases by the following procedure for the addition of the hydrochloric acid: (a) The sample was wetted with a few milliliters of distilled water, (b) ten 1-ml portions of diluted hydrochloric acid (1+20) were added during a period of about 20 minutes, (c) ten 2 ml portions of diluted hydrochloric acid (1+20) were added in about 20 minutes, (d) 20 ml of concentrated hydrochloric acid was added in one portion. Finally, the flow of air was increased, and the contents of the flash was boiled gently for 40 minutes. During this process the quartz tube was continually heated with two Meker burners.

At the conclusion of the experiment the quartz tube was allowed to cool. All the connecting Pyrex tubing was washed with 200 ml of distilled water into the first gas-wash bottle. The contents of both gas-wash bottles were transferred to a 2-liter beaker; 100 ml of saturated bromine water was added to oxidize any sulfites to sulfates and concentrated hydrochloric acid added until the solution turned a definite orange. The solution was boiled until colorless, cooled, adjusted to pH 1, and a single precipitation of barium sulfate made.

The results for the six service chars are contained in the last column of table 9. Although definite fluctuations were observed in repeated determinations with aliquot parts of the same sample, the sulfate values so determined are greater than those corresponding to simple evolution of hydrogen sulfide. In one case, sample 36, the two values are the same.

A reasonable explanation of the fluctuations, apart from inherent inaccuracies in the determinations, is the variable action of the hydrochloric acid on the carbonaceous residue of the char. It would be very difficult to control the extent of the acid hydrolysis of the organic-sulfur component in the residue. It is important, therefore, in the analysis of a bone char by method 6, to determine first the sulfur in the evolved gases, and to use the mixture remaining in the flask to determine the sulfur in the residue and the filtrate. Unfortunately, the values in table 8 were obtained by method 6 with two samples of char, one for the evolution experiment and the other for the distribution of sulfur between residue and filtrate.

Three service chars, however, were analyzed by method 6 with the precaution of using but one sample for analysis. The results for these chars are given in table 10. A satisfactory agreement was obtained between the total sulfate deduced from method 1 (column 2) and the total sulfate derived as the sum of that in the residue, in the filtrate, and in the gases evolved with hydrochloric acid. Independent data for these three samples are available for the sulfate content of the filtrate after hydrochloric acid treatment. These were furnished through the courtesy of H. I. Knowles, chief chemist, Atlantic Sugar Refineries, Ltd., Saint John, N. B., Canada.

TABLE 10. *Determination of sulfur (expressed as SO_4) in service bone chars*

Char	Total sulfur (perchloric acid method)	Digestion of sample with HCl				
		Filtrate	Residue	Evolved gases	Total	Filtrate only [a]
	Percent	*Percent*	*Percent*	*Percent*	*Percent*	*Percent*
A	1.07	0.70	0.32	0.049	1.07	0.60
B	1.48	1.00	.45	.051	1.50	.99
C	1.53	1.13	.34	.056	1.53	1.10

[a] Samples and the results in this column were furnished through the courtesy of H. I. Knowles, chief chemist, Atlantic Sugar Refineries, Ltd.

VI. Discussion of Results

The results of analysis of the several bone chars for sulfur show clearly the errors in the existing methods used by sugar refining laboratories. The major error is in the value for so-called calcium sulfide, which is based on a fallacy contained in its definition. The sulfur reported as calcium sulfide is in reality that contained in the sulfides liberated by evolution with hydrochloric acid and a part of the combined organic sulfur in the carbonaceous residue. Other errors are due to the variable

amount of organic sulfur removed from the carbonaceous residue that depends on the oxidation media employed in the analysis.

It is recommended that for practical purposes the sulfur contained in bone char be defined as follows:

Total sulfur.—This value may be determined from either methods 1, 2, or 3. Method 1 is preferred for its convenience.

Inorganic sulfate-sulfur.—The nearest value to this quantity is the sulfate found in the filtrate of a dilute hydrochloric acid treatment of the bone char, method 6.

Sulfide-sulfur.—This value may be obtained from a determination of the hydrogen sulfide evolved by treatment of the char with hydrochloric acid, see section V, 1.

Combined organic sulfur.—The sulfur in the carbonaceous residue may be determined by either of two alternative procedures: the residue obtained after digestion with dilute hydrochloric acid may be so analyzed (method 6); or, the *total sulfur* may be obtained (method 1) and the sum of the *inorganic sulfate-sulfur* and the *sulfide-sulfur* subtracted.

Any proposed definition of the sulfur content of bone char must take into account the rather complex chemical composition. Research purposes, of course, require the best available methods of analysis, and the data obtained thereby may not fit into the three simple categories defined above. For practical considerations of sugar technology work, however, it may suffice to know the sulfur content of bone char with a precision and accuracy sufficient to warrant the proposed definitions.

Interesting changes take place in the sulfur content of bone char during cane-sugar refining operations, and the contrast in the percentage of sulfur of service bone char with that of new bone char should be briefly mentioned. The order of magnitude of the total sulfur expressed as SO_4 in new bone char is 0.15 percent as compared with a maximum of 1 to 2 percent in service char. This would indicate that an important source of the sulfur during char operations in sugar refining is the adsorbed impurities removed from the sugar liquors.

Some of the adsorbed impurities contain protein matter composed in part of sulfur-bearing amino acids. The sulfur could be retained by the carbonaceous residue formed in the reactions that occur in the char kiln. It is also possible that some sulfate-sulfur may be introduced if phosphate defecation was used in the refining operations. Even good technical phosphoric acid may contain approximately 0.3 to 0.5 percent of sulfate. If manufactured by the wet method (sulfuric acid and phosphate rock), it may contain more sulfate than if manufactured by the furnace method (oxidation of phosphorus). The latter product may be preferred for sugar refining. The two mentioned sources of sulfur are independent of the type of kiln used to revivify the char.

VII. References

[1] G. L. Spencer and G. P. Meade, Cane sugar handbook, p. 348, 8th ed. (John Wiley & Sons, Inc., New York, N. Y., 1945).

[2] John Henry Tucker, A manual of sugar analysis, p. 320–322, 1st ed. (D. Van Nostrand Co., Inc., New York, N. Y., 1881).

[3] W. F. Hillebrand and G. E. F. Lundell, Applied inorganic analysis, p. 575–579 (John Wiley & Sons, Inc., New York, N. Y., 1929)

[4] I. M. Kolthoff and E. B. Sandell, Textbook of quantitative inorganic analysis, revised ed., chap. 20, Determination of sulfur as barium sulfate, p. 329–344 (The Macmillian Co., New York, N. Y., 1943).

[5] F. P. Treadwell and W. T. Hall, Analytical chemistry **2**, 322, 6th ed. (John Wiley & Sons, Inc., New York N. Y., 1924).

[6] C. L. Gordon, J. Research NBS **30**, 107 (1943) RP1521.

[7] C. L. Gordon, W. G. Schlecht, and E. Wichers, J. Research NBS **33**, 457 (1944) RP1622.

[8] G. Walton and G. H. Wahlen, Jr., J. Am. Chem. Soc. **68**, 1742 (1946).

Washington, November 19, 1947.

U. S. Department of Commerce
National Bureau of Standards

Research Paper RP1872
Volume 40, April 1948

Part of the Journal of Research of the National Bureau of Standards

Effect of Support on the Performance of Vane Anemometers

By Galen B. Schubauer and Gerald H. Adams

One of the more important factors affecting the accuracy of a measurement of air speed with a vane anemometer is the manner in which the instrument is supported. An awareness of this fact is important, because the user must devise his own support. It is shown that seemingly minor changes in the support may change the indicated speed by 5 percent, and that holding an anemometer in the hand may increase the indicated speed by as much as 17 percent. In order to insure the reliability of a speed measurement, an interference-free type of support is recommended.

I. Introduction

The accurate measurement of air speed with a vane anemometer depends on an accurate calibration and on conforming strictly to the conditions for which the calibration will be valid. These conditions involve primarily the manner in which the anemometer is supported.

For many years calibrations were conducted at the National Bureau of Standards by means of a whirling arm, a device that moves the instrument along a circular path through the air at constant speed. The instrument was simply fastened to a flat plate at the end of the arm as shown in figure 1, and the arm was rotated at a series of known rates. The accuracy of a calibration by this method was limited by the so-called swirl correction, a necessary but rather uncertain correction applied to the peripheral speed of the arm to take account of the rotation of the air in the room produced by the rotating arm.

In June 1947, it was decided to conduct all calibrations of vane anemometers in the wind tunnel where absolute speed measurements could be based entirely on the standard pitot-static tube. In making the change to the wind tunnel, the question of the proper means of supporting an anemometer was brought to the fore. It was already known that the support could affect the rate of an instrument and that the best way to avoid possible error was to use the same type of support at all times. The flat plate, formerly used with the whirling arm, could be defended only on the grounds that manufacturers in failing to supply a supporting member of any sort presumably left the user free to adopt any support that suited his convenience—even to holding the anemometer in his hand. To throw some light on the importance of this question, it was decided to investigate the performance of several sizes of vane anemometers of the type shown in figures 1 to 5 on the various types of support shown in the figures. The investigation was conducted in the Bureau's 4½-foot wind tunnel.

II. Interference-Free Mounting

If an anemometer is suspended in a wind stream on wires so fine that they are incapable of producing interference, a performance free from support interference may be obtained. By comparing the performance obtained in this way with that obtained on the rod type of support shown in figure 2, it has been found that a rod no greater than ½ in. in diameter produces no measurable interference when it extends directly downstream. Effects from members supporting the rod itself may be made negligible by placing them at a sufficient distance downstream. This requires a minimum distance of the order of 16 times the diameter or cross-stream width of such members. In the mounting shown in figure 2 ample margin has been allowed, and the mounting is interference free. The portion of the rod directly under the anemometer is flattened to about ⅛ in. in thickness. In the investigation of the interference produced

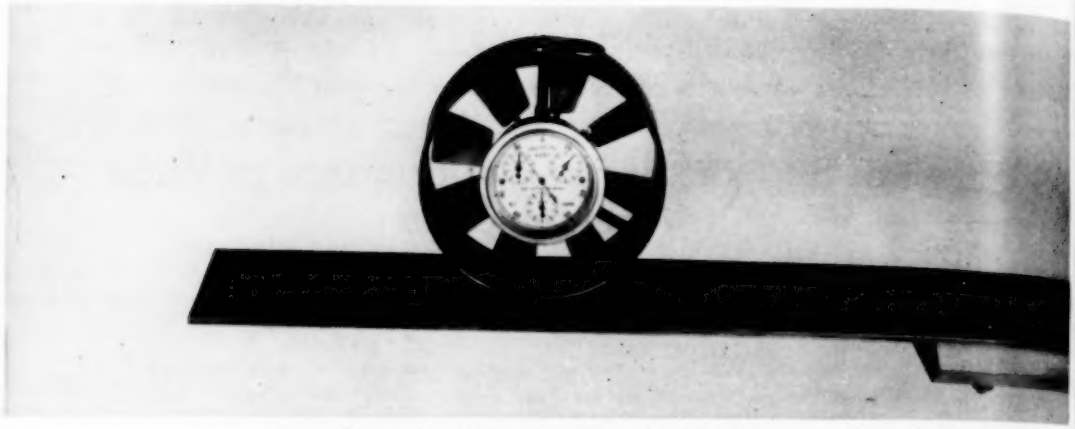

FIGURE 1. *Anemometer supported on flat plate.*

FIGURE 2. *Anemometer supported on rod.*

by other types of support, the performance on the support in question was compared with that on the rod.

III. Other Supports Investigated

1. Whirling-Arm Mounting

The flat plate on which anemometers were mounted in the past for a whirling-arm test is shown in figure 1. A wooden member simulating the end of the arm is shown to the right. The plate is ⅛ in. thick and 3 in. wide. The distance from the end of the arm to the end of the plate is 12½ in. The wind moves normal to the face opposite the dial and parallel to the flat side of the plate.

2. Hand Support

The types of hand support shown in figures 3, 4, and 5 were chosen not as recommended methods of support, but rather as manners in which an observer might be inclined to hold an anemometer in making a measurement of air speed. The models are intended to respresent approximately an adult hand and arm. The arm length is not intended to be correct, and the body is not represented. This would correspond to the case where the observer's body is completely outside the wind stream. Figures 1 to 5 all show a 4-in. anemometer, the size referring to the inside diameter of the cylindrical housing.

Figure 3, hand 1, shows one finger through the ring of the anemometer and two fingers supporting the housing. The arm extends to the side and is at right angles to the wind.

FIGURE 3. *Hand 1 supporting anemometer.*

Figure 4, hand 2, shows one finger through the ring allowing the anemometer to hang down freely. The arm is at right angles to the wind. The thumb is on the downstream side.

Hand 3 in figure 5 shows an anemometer being held by means of a short handle. The arm is directly downstream inclined at an angle of 45 degrees to the wind.

III. Results

Curves showing the performance of a 3-, 4-, and 6-in. anemometer are given in figures 6, 7, and 8, respectively.

The speed indicated by an anemometer depends on the rate of rotation of the vane wheel, which in turn depends on the setting of the vanes, the diameter of the wheel, the speed and direction of the air through the wheel, and the friction of the instrument. The true speed is the speed of a uniform parallel flow of air that would exist if the anemometer and its supports were absent. The indicated speed may be less than, equal to, or greater than the true speed depending on the factors that control the rate of rotation of the vane wheel.

The performance given in figures 6, 7, and 8 is in terms of the ratio of the indicated speed to the true speed plotted against the true speed. Displacement of the various curves from that marked "rod" shows the altered performance due to the

FIGURE 4. *Hand 2 supporting anemometer.*

FIGURE 5. *Hand 3 supporting anemometer by short handle.*

interference of the support. It will be noted that the ratio of indicated to true speed is increased in every case. The reason for this is that the air speed through the instrument increases locally due to the fact that the air must flow around the support.

The changes in indicated speed due to interference are given in table 1 as percentages of the true speed at several values of the true speed. There is an indication that the percentages decrease slightly with increasing speed, but the change is scarcely outside the experimental error. The column of averages may therefore be used as a reliable index of the various interference effects. It will be seen that the interference effects are about the same on the 3- and 4-in. anemometers but somewhat less on the 6-in. anemometer. A decrease with increasing size is to be expected, because the anemometer becomes larger relative to its support. As hands 1 and 2 produced roughly the same effect, hand 1 was used only with the 4-in. anemometer.

TABLE 1. *Change in indicated speed due to interference, expressed as percentage of true speed*

Support	True air speed, fpm					Average
	400	600	800	1,200	1,600	
3-IN. ANEMOMETER						
	Percent	*Percent*	*Percent*	*Percent*	*Percent*	*Percent*
Rod	0	0	0	0	.....	0
Plate	5.6	5.6	5.4	5.0	.....	5.4
Hand 1	.....	.....	.....	.....	.....	.....
Hand 2	15.6	16.1	15.4	14.4	.....	15.4
Hand 3	14.6	14.5	14.1	13.4	.....	14.2
4-IN. ANEMOMETER						
Rod	0	0	0	0	0	0
Plate	5.5	5.3	5.4	5.1	4.7	5.2
Hand 1	18.1	17.1	16.8	16.2	15.9	16.8
Hand 2	18.1	16.9	16.5	16.5	16.8	17.0
Hand 3	11.5	11.8	11.9	11.7	.....	11.7
6-IN. ANEMOMETER						
Rod	0	0	0	0	0	0
Plate	5.6	4.3	3.7	3.3	.....	4.2
Hand 1	.....	.....	.....	.....	.....	.....
Hand 2	12.7	11.8	11.9	11.9	12.0	12.1
Hand 3	10.7	10.3	10.1	9.7	9.6	10.1

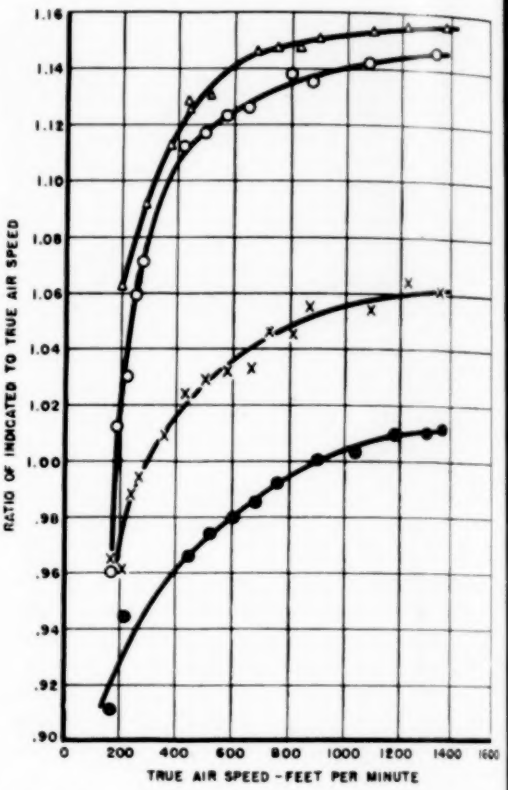

FIGURE 6. *Performance of 3-inch, eight-vane anemometer.* △, Hand 2; ○, hand 3; ×, plate; ●, rod.

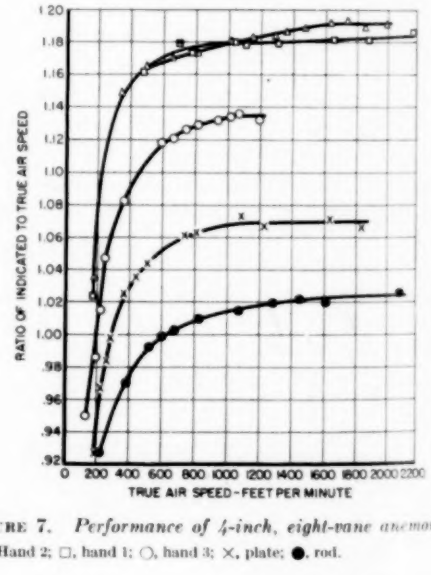

FIGURE 7. *Performance of 4-inch, eight-vane anemometer.* △, Hand 2; □, hand 1; ○, hand 3; ×, plate; ●, rod.

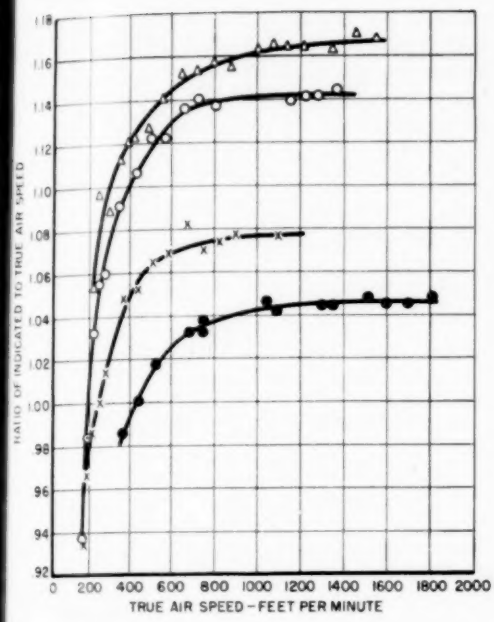

FIGURE 8. *Performance of 6-inch, 10-vane anemometer.*

△, Hand 2; ○, hand 3; ×, plate; ●, rod.

All of the effects demonstrated here are large compared to the inherent accuracy of a calibration curve. The scatter of the points about any one mean curve in figures 6, 7, and 8 shows that a calibration curve is defined to an accuracy of better than 1 percent. However, there may be systematic errors in the measurement of speeds below 400 feet per minute amounting to several percent, so that the scatter of observations is not a reliable indication of the absolute accuracy at the lower speeds. Nevertheless, interference effects are likely to be the major source of error unless the same support system is used at all times. The support, therefore, becomes in effect part of the instrument and changing it amounts to changing the instrument.

Not all interference effects will be as large as those shown here, for the effect depends entirely on the size, position, and shape of the support. If the bulk of the support is to the rear of the anemometer, the effect may be in the opposite direction. It is entirely possible that some disposition of the support may be made such that effects from the side and effects from the rear just cancel. However, proper balance might be difficult to obtain over the entire speed range of an instrument and also would be affected by wind direction. Directional effects on anemometers without support interference have been treated in a previous paper.[1]

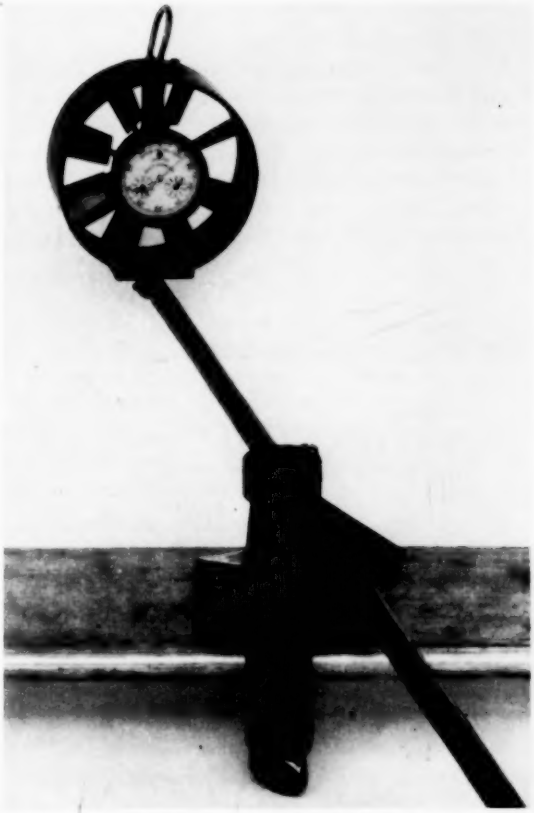

FIGURE 9. *Anemometer on rod clamped to strut.*

IV. Adoption of a Standard Mounting for Calibration Purposes

In considering the question of a standard mounting, it is helpful to keep in mind the fact that any mounting must be regarded as part of the instrument. As an anemometer supplied by a manufacturer should be regarded as a complete instrument, it is assumed that nothing should be added to it. Therefore, as the rod support is equivalent aerodynamically to adding nothing,

[1] Roy H. Heald and Paul S. Ballif, Effect of yaw on vane anemometers, J. Research NBS **19,** 685 (1937) RP1056.

the rod support of figure 2 has been adopted for the purpose of calibration.

Experience with vane anemometers at the National Bureau of Standards has shown that it is possible to employ the rod support under nearly all conditions of use. Even when it is necessary to use a short rod, the interference from the member holding the rod is likely to be small. According to Heald and Ballif (see footnote 1), for example, the clamping device and strut shown in figure 9 had a negligible effect at distances downstream of 1 foot or more. Even at 4 in., the interference effect was only of the order of 1 or 2 percent. The strut in this case was 1¼ in. thick and 3 in. wide and extended completely across the tunnel.

WASHINGTON, November 4, 1947.

U. S. Department of Commerce
National Bureau of Standards

Research Paper RP1873
Volume 40, April 1948

Part of the Journal of Research of the National Bureau of Standards

Heat of Combustion of Phenyl-Beta-Naphthylamine (N-Phenyl-2-Naphthylamine)

By Donald E. Roberts and Ralph S. Jessup

The heat of combustion of purified solid phenyl-beta-naphthylamine, (*N*-phenyl-2-naphthylamine) in forming gaseous carbon dioxide, liquid water, and gaseous nitrogen, has been determined from measurements with a bomb calorimeter. The value obtained ($-\triangle H_c^\circ$ at 25° C) is 37909.6 int j/g (1987.07 kcal/mole), with an estimated value of 8.3 int j/g (0.43 kcal/mole) for the standard deviation of the mean, obtained by making allowance for both accidental and systematic errors.

I. Introduction

Phenyl-beta-naphthylamine (*N*-phenyl-2-naphthylamine) is one of the most important materials used as stabilizers in the production of synthetic rubber. Stabilizers prevent continued polymerization, cross-linking, or cyclization, which would otherwise cause stiffening during storage of the unvulcanized synthetic rubber. The concentrations used range from 0.10 to 2.0 percent, depending on the type of rubber.

This material is also widely used as an antioxidant in the compounding of natural and synthetic rubbers prior to vulcanization. In this connection it retards oxidative deterioration of the product after vulcanization and improves its resistance to cracking and deterioration by heat. It is sold under the trade names Agerite Powder and Neozone D.

Data on the heat of combustion of phenyl-beta-naphthylamine are useful in interpreting the results of heat of combustion measurements on synthetic rubbers, and an accurate value may be desirable for other calculations.

II. Apparatus and Method

The measurements of the heat of combustion were made in a bomb calorimeter. The apparatus and procedure are the same as those described previously [1, 2, 3, 4, 5],[1] except in the following respects: (1) The firing electrode was sealed into the head of the bomb with soda glass instead of the special glass previously used [3], (2) the bomb has two valves, and the carbon dioxide remaining in it after the pressure was reduced to atmospheric following a combustion was flushed out by passing purified oxygen through the bomb, instead of by alternately filling it to a pressure of several atmospheres and releasing the pressure [5].

The calorimetric system was calibrated with Bureau Standard Sample 39f of benzoic acid. The value used for the heat of combustion of this sample under the conditions of the standard bomb process was reported previously [4].

The amount of the combustion reaction in each measurement of heat of combustion was derived from the mass of carbon dioxide formed. The determination of the carbon dioxide, tests for carbon monoxide, and corrections for ignition energy, and for nitric acid formed were the same as described previously [6]. No carbon monoxide was detected in the gaseous products of combustion. A value of 60 kj/mole of nitric acid was used in correcting for the aqueous nitric acid (about 0.5 molar) formed in the bomb. This correction amounted to about 0.12 percent of the heat of combustion. The nitric acid represented about 7 percent of the total nitrogen present.

Using the procedure described by Washburn [7], modified so as to apply to 30° C and to the energy content of the gases at zero pressure instead of 1 atmosphere, the observed heat of combustion in

[1] Figures in brackets indicate the literature references at the end of this paper.

each experiment was reduced to the value of $-\Delta U_c^\circ$, the decrease in intrinsic energy accompanying the combustion reaction:

$$C_{16}H_{13}N(c)+\frac{77}{4}O_2(g) \rightarrow 16CO_2(g)+\frac{13}{2}H_2O(l)+\frac{1}{2}N_2(g),$$

with each of the reactants and products in its thermodynamic standard state.

The energy unit used in the original calculation of the results is the international joule. Conversion of the results to terms of the conventional thermochemical calorie was made by use of the relation 1 calorie = 4.1833 int. j. Conversion to absolute joules may be made by use of the relation 1 int j = 1.000165 absolute j.

III. Material

The sample used was prepared by F. J. Linnig of this Bureau from a commercial grade material (Agerite Powder, supplied by the R. T. Vanderbilt Co.) by vacuum distillation and two recrystallizations from aviation gasoline. It consisted of nearly white needle crystals with a melting point of approximately 107° C.

Spectrochemical examination of the unpurified and purified samples of phenyl-beta-napthylamine was made by Martha E. Mayo of this Bureau to determine whether the recrystallized sample had been contaminated with lead from the aviation gasoline. Lead was not detected in either sample. Traces (less than 0.001%) of copper and silicon were found in the unpurified material.

IV. Results

The results of the calibration experiments with benzoic acid are given in table 1. The results of the measurements of heat of combustion of phenyl-beta-napthylamine are given in table 2, where $-\Delta U_B$ is the observed heat of combustion under the conditions of the bomb process [2], and $-\Delta U_c^\circ$ is the decrease in intrinsic energy accompanying the combustion reaction when the reactants and products are all in their thermodynamic standard states at 30° C. In table 3 are given values of heat of combustion per gram and per mole calculated from the mean value given in table 2, on the assumption that 16 moles (16 × 44.010 g) of carbon dioxide corresponds to 1 mole (219.272 g) of phenyl-beta-napthylamine ($C_{16}H_{13}N$).

[2] The conditions of the bomb process are specified by the temperature (30° C) to which the combustion reaction is referred, the mass of water (1 g) placed in the bomb before each experiment, the internal volume of the bomb (377 ml), and the data given in columns 1 and 2 of table 2.

TABLE 1. *Calibration of calorimeter with benzoic acid*

Observed energy equivalent at 28.5° C int j/° C
13724.7
13727.6
13723.9
13725.0
13723.1
13724.5
13727.5
13724.2
13730.4
13727.0
13723.2
13729.3
13726.8
Mean 13725.9
Standard deviation of the mean [1], s_E 0.6

[1] Standard deviation of the mean, as used here and in table 2, is defined as $[(\Sigma d^2)/n(n-1)]^{\frac{1}{2}}$, where d is the difference between a single observation and the mean, and n is the number of observations. In the case of the final values of heat of combustion given in table 3, the values given for the standard deviation include the effects of estimated systematic errors, as well as accidental errors. These values were calculated from the relation

$$s=Q[(s_E/E)^2+(s_Q/Q)^2+R^2+R^2]^{\frac{1}{2}},$$

where s_E is the standard deviation of the mean of the experiments with benzoic acid to determine E, the energy equivalent of the calorimetric system; s_Q is the standard deviation of the mean of the results of the experiments to determine Q, the heat of combustion of the sample; R is an allowance of 5×10^{-5} for the standard deviation of the value used for heat of combustion of benzoic acid; and R is an allowance of 2×10^{-4} for systematic errors associated with the impurities in the sample and the determination of the amount of the combustion reaction from the mass of carbon dioxide.

TABLE 2. *Bomb-calorimetric measurements on phenyl-beta-naphthylamine*

Mass of sample	Initial O_2 pressure at 30° C	Mass of CO_2	Heat of combustion at 30° C	
			$-\Delta U_B$	$-\Delta U_c^\circ$
g	*atm*	*g*	*int j/g CO_2*	*int j/g CO_2*
0.99480	32.4	3.19305	11802.8	11795.7
.99981	32.2	3.11248	11801.5	11794.4
.99304	32.0	3.09107	11799.7	11792.7
.98986	32.7	3.17725	11801.8	11794.9
Mean				11794.4
Standard deviation of the mean, [1] s_m				0.6

[1] See footnote 1, table 1.

TABLE 3. *Heat of combustion of phenyl-beta-naphthylamine*

	int J/g	int kJ/mole	cal/g	kcal/mole
$-\Delta U_c^\circ(30°C)$	37875.8	8305.10	9054.05	1985.30
$-\Delta H_c(30°C)$	37907.4	8312.03	9061.60	1986.96
$-\Delta H_c(25°C)$	37909.6	8312.51	9062.12	1987.07
Standard deviation of mean[1], σ	8.3	1.81	1.97	0.43

[1] See footnote 1, table 1.

The values obtained for the mass of carbon dioxide formed in combustion of phenyl-beta-naphthylamine were lower than the stoichiometric amounts calculated from the corresponding masses of sample burned by an average of 0.053 percent, indicating that some impurity was present in the samples. Several measurements of the carbon dioxide formed in combustion of Bureau Standard Sample 39f of benzoic acid yielded results in agreement with calculated values within less than 0.01 percent on the average. Both the benzoic acid samples and the phenyl-beta-naphthylamine samples were compressed into pellets, which burned completely, leaving no residue.

Two experiments on unpurified Agerite Powder yielded a value for heat of combustion per gram of carbon dioxide formed, which was 0.062 percent lower than that of the purified material. With the unpurified samples, the values obtained for the mass of carbon dioxide formed in combustion were lower than the stoichiometric amounts calculated from the corresponding masses of sample burned by an average of 0.135 percent.

The use of the mass of carbon dioxide formed as a measure of the amount of the combustion reaction is equivalent to assuming that the material burned consists of phenyl-beta-naphthylamine plus inert impurity. If this were true for both the purified and unpurified material, the same value of heat of combustion per gram of carbon dioxide formed would be obtained for both. The fact that different values were obtained for the purified and unpurified materials indicates that the assumption is not true for both materials, and it is not certain that it is true for either. It is possible, therefore, that the results for the purified material reported in tables 2 and 3 may be systematically in error by a few hundredths of a percent due to impurity in the material.

V. Previous Work

Lemoult [8] reported the values 9153.39 and 9166.79 cal/g (mean 9160.1 cal/g) as the results of calorimetric measurements of the heat of combustion of phenyl-beta-naphthylamine. His calorimeter was calibrated with naphthalene using 9,664 cal/g for its heat of combustion. No experimental details were given. His sample melted at 107.5° C and contained 6.18 percent of nitrogen (theoretical, by present atomic weights 6.39 percent). In terms of the energy unit used in the present work, the mean of Lemoult's results is calculated to be $-\Delta H_c = 1{,}999$ kcal/mole. This value was calculated with the aid of the values reported by Lemoult for naphthalene and phenyl-beta-naphthylamine, a value for the ratio of the heats of combustion of naphthalene and benzoic acid derived from the work of Dickinson [1], and the value [4] for the heat of combustion of benzoic acid used in the present work.

VI. References

[1] H. C. Dickinson, Bul. BS **11,** 189 (1914) S230.
[2] E. F. Mueller, Bul. BS **13,** 547 (1916) S288.
[3] R. S. Jessup and C. B. Green, J. Research NBS **13,** 469 (1934) RP721.
[4] R. S. Jessup, J. Research NBS **29,** 247 (1942) RP1499.
[5] R. S. Jessup, J. Research NBS **18,** 115 (1937) RP966.
[6] D. E. Roberts, W. W. Walton, and R. S. Jessup, J. Research NBS **38,** 627 (1947) RP1801.
[7] E. W. Washburn, BS J. Research **10,** 525 (1933) RP 546.
[8] P. Lemoult, Ann. chim. phys. [8] **10,** 395 (1907).

WASHINGTON, November 11, 1947.

U. S. Department of Commerce
National Bureau of Standards

Research Paper RP1874
Volume 40, April 1948

Part of the Journal of Research of the National Bureau of Standards

Calibration of X-Ray Measurement of Strain

By John A. Bennett and Herbert C. Vacher

In order to increase the precision of strain determination by X-ray methods, 12 measurements of ring radius were made on each of two patterns for the customary incidence angles of 90° and 45°. For a specimen to which uniaxial stress was applied, a method was developed for handling the data to give one value representative of these 24 readings. When these values (obtained on a flat steel specimen loaded in bending) were compared with mechanical strain measurements, it was found that the X-ray measurements were proportional to the maximum principal strain up to the beginning of plastic deformation, and the precision was such that a change corresponding to 1,000 lb/in.^{2} should be detectable.

I. Introduction

In an investigation at the National Bureau of Standards it was necessary to determine strain by means of X-rays. As the accuracy required was greater than that ordinarily obtained with this method, experiments were made to develop a technique for making the measurements with sufficient accuracy for the purpose intended. The method developed and some results obtained with it are described in this paper.

Deformation of metals can be of two types, elastic and plastic. Elastic deformation results in a change in the interatomic spacing of the crystals, whereas plastic deformation does not. It is possible, by means of X-ray diffraction, to measure the lattice spacing and thus determine elastic strain independently of plastic strain. Because of this and other advantages over mechanical extensometers, which measure over all changes in dimensions, X-ray diffraction has been widely used for the determination of strain and stress in metals. During the past 20 years the literature on the subject has become extensive [1, 2]. A very good general treatment is given by Barrett.[3]

The X-ray strain measurements are made on relatively few crystals oriented in particular directions, and it is possible that the deformation of these crystals is not representative of the behavior of the polycrystalline material as a whole. Also the strain cannot be measured in the direction of the applied stress, so the principal strains must be calculated by means of elastic theory. The uncertainty introduced by these two factors must be overcome by experiment to ensure the accuracy of the X-ray determination of strain. In order to do this and to evaluate the precision of the method, calibrating tests were made on a specimen to which uniaxial stress was applied.

II. X-Ray Diffraction Method of Measuring Strain

1. Precision of a Single Measurement

The mathematical relationships involved in the measurement of strain for the case of uniaxial stress will be reviewed before describing the method. In the back-reflection technique of X-ray diffraction, the collimated beam is passed through a photographic film placed at right angles to it. The beam strikes the specimen and is diffracted by those crystals which are so oriented as to satisfy the Bragg equation

$$n\lambda = 2d \sin \theta, \tag{1}$$

where n is the order, λ the wavelength of the X-rays, d the interplanar spacing, and θ the diffraction angle. If monochromatic X-rays are used, the incident beam is diffracted into a series of cones having a common axis coincident with the incident beam; if any one of these intersects

[1] Herbert R. Isenburger, Welding Research Supplement, Welding J. 23, 571-s (Nov. 1944).
[2] George Sachs, C. S. Smith, J. D. Lubahn, G. E. Davis, and L. J. Ebert, Welding Research Supplement, Welding J. 25, 400-s (July 1946).
[3] C. S. Barrett, Structure of metals, chap. 14, p. 267 (McGraw-Hill Book Co., Inc., New York, N. Y., 1943).

U. S. Department of Commerce
National Bureau of Standards

Research Paper RP1874
Volume 40, April 1948

Part of the Journal of Research of the National Bureau of Standards

Calibration of X-Ray Measurement of Strain

By John A. Bennett and Herbert C. Vacher

In order to increase the precision of strain determination by X-ray methods, 12 measurements of ring radius were made on each of two patterns for the customary incidence angles of 90° and 45°. For a specimen to which uniaxial stress was applied, a method was developed for handling the data to give one value representative of these 24 readings. When these values (obtained on a flat steel specimen loaded in bending) were compared with mechanical strain measurements, it was found that the X-ray measurements were proportional to the maximum principal strain up to the beginning of plastic deformation, and the precision was such that a change corresponding to 1,000 lb/in.^{2} should be detectable.

I. Introduction

In an investigation at the National Bureau of Standards it was necessary to determine strain by means of X-rays. As the accuracy required was greater than that ordinarily obtained with this method, experiments were made to develop a technique for making the measurements with sufficient accuracy for the purpose intended. The method developed and some results obtained with it are described in this paper.

Deformation of metals can be of two types, elastic and plastic. Elastic deformation results in a change in the interatomic spacing of the crystals, whereas plastic deformation does not. It is possible, by means of X-ray diffraction, to measure the lattice spacing and thus determine elastic strain independently of plastic strain. Because of this and other advantages over mechanical extensometers, which measure over all changes in dimensions, X-ray diffraction has been widely used for the determination of strain and stress in metals. During the past 20 years the literature on the subject has become extensive [1, 2]. A very good general treatment is given by Barrett.[3]

The X-ray strain measurements are made on relatively few crystals oriented in particular directions, and it is possible that the deformation of these crystals is not representative of the behavior of the polycrystalline material as a whole. Also the strain cannot be measured in the direction of the applied stress, so the principal strains must be calculated by means of elastic theory. The uncertainty introduced by these two factors must be overcome by experiment to ensure the accuracy of the X-ray determination of strain. In order to do this and to evaluate the precision of the method, calibrating tests were made on a specimen to which uniaxial stress was applied.

II. X-Ray Diffraction Method of Measuring Strain

1. Precision of a Single Measurement

The mathematical relationships involved in the measurement of strain for the case of uniaxial stress will be reviewed before describing the method. In the back-reflection technique of X-ray diffraction, the collimated beam is passed through a photographic film placed at right angles to it. The beam strikes the specimen and is diffracted by those crystals which are so oriented as to satisfy the Bragg equation

$$n\lambda = 2d \sin \theta, \qquad (1)$$

where n is the order, λ the wavelength of the X-rays, d the interplanar spacing, and θ the diffraction angle. If monochromatic X-rays are used, the incident beam is diffracted into a series of cones having a common axis coincident with the incident beam; if any one of these intersects

[1] Herbert R. Isenburger, Welding Research Supplement, Welding J. 23, 571-s (Nov. 1944).
[2] George Sachs, C. S. Smith, J. D. Lubahn, G. E. Davis, and L. J. Ebert, Welding Research Supplement, Welding J. 25, 400-s (July 1946).
[3] C. S. Barrett, Structure of metals, chap. 14, p. 267 (McGraw-Hill Book Co., Inc., New York, N. Y., 1943).

the photographic film, a circle will be recorded. When d is changed by the application of stress to the material, sin θ changes correspondingly, as the product $n\lambda$ is constant.

In considering the relationships involved in the determination of strain by X-ray diffraction, the assumptions are made that the material is isotropic and homogeneous, and that the applied stress is uniaxial. The coordinate system is set up with the X and Y axes in the surface of the specimen and the Z axis normal to the surface. The stress is applied parallel to the X axis. Figure 1 shows the relationship of various angles

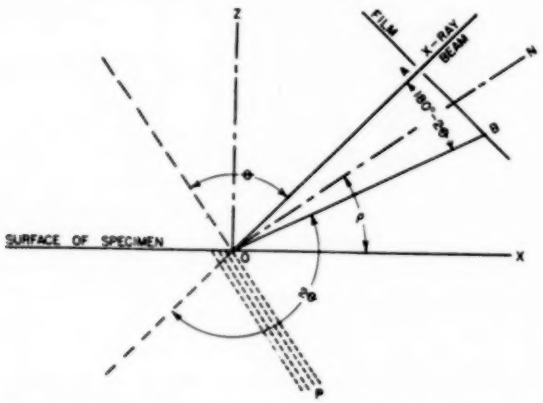

FIGURE 1. *Relationship of various angles in a plane normal to the surface of the specimen and parallel to the applied stress.*

Reflecting planes are shown at P, and the diffracted beam intersects the film at B.

in the XZ plane when the incident X-ray beam makes an oblique angle with the surface of the specimen. The diffracted beam is shown intersecting the photographic film at B, one set of reflecting planes is shown at P, and N is the normal to these planes. The intersection of the diffracted cone with the XZ plane on the other side of the incident beam has been omitted to avoid confusing the diagram. In order to determine θ, the distances OA and AB are measured.

Definitions of other symbols used are as follows:

S=Specimen-to-film distance (OA on fig. 1).

R=Radius of the diffraction ring on the photographic film (AB on fig. 1).

ρ=Angle between the X axis and the normal to the reflecting planes.

β=Longitude angle about the incident X-ray beam. The zero position is in the XZ plane on the side of the incident beam nearest the positive X direction.

ϵ=Strain in a direction making an angle ρ with the X axis.

ϵ_X, ϵ_Y, ϵ_Z=Strain in the X, Y, and Z directions, respectively.

ν=Poisson's ratio; assumed to equal 0.3.

Measurements of strain by the X-ray method are not made in the direction of the applied stress, therefore, it is necessary to know how the strain varies with direction. This is shown (for uniaxial stress parallel to the X-axis) in figure 2, which is a stereographic projection, the plane of projection being in the surface of the specimen (XY plane). The latitude lines connect points of equal strain ratio. Strain ratio, defined as the ratio of the strain in a given direction to that in the direction of the applied stress is designated as ϵ/ϵ_X.

The formula used in computing the strain ratios

$$\epsilon/\epsilon_X = \cos^2 \rho - 0.3 \sin^2 \rho, \qquad (2$$

was derived from the approximate equation for the ellipsoid of strain, the complete derivation being shown in section VI, 1.

Obviously it is desirable to make strain measurements at an angle such that the strain ratio will be as large as possible, but mechanical considerations limit the incident angle to a maximum of about 45° from the normal to the surface of the specimen. On figure 2 are shown the reflection circles (cones formed by the normals to the reflecting planes) for two positions of the incident beam; normal to the surface and at 45° to the surface in the XZ plane. The circles were calculated for cobalt $K\alpha$ radiation reflected from the 310 planes of iron, the diffracting angle, θ, being 80½°. Position on the reflection circle is defined by β. The point of maximum strain ratio coincides with the position β=0 when the beam is incident at 45°, and for this condition the strain ratio is 0.562, computed from eq. 2.

In order to calculate the change in tan 2θ (which is the quantity measured experimentally), that would be expected for a given strain, eq 1 is differentiated (see section VI, 2 for complete derivation), and it is found that for infinitesimal strains

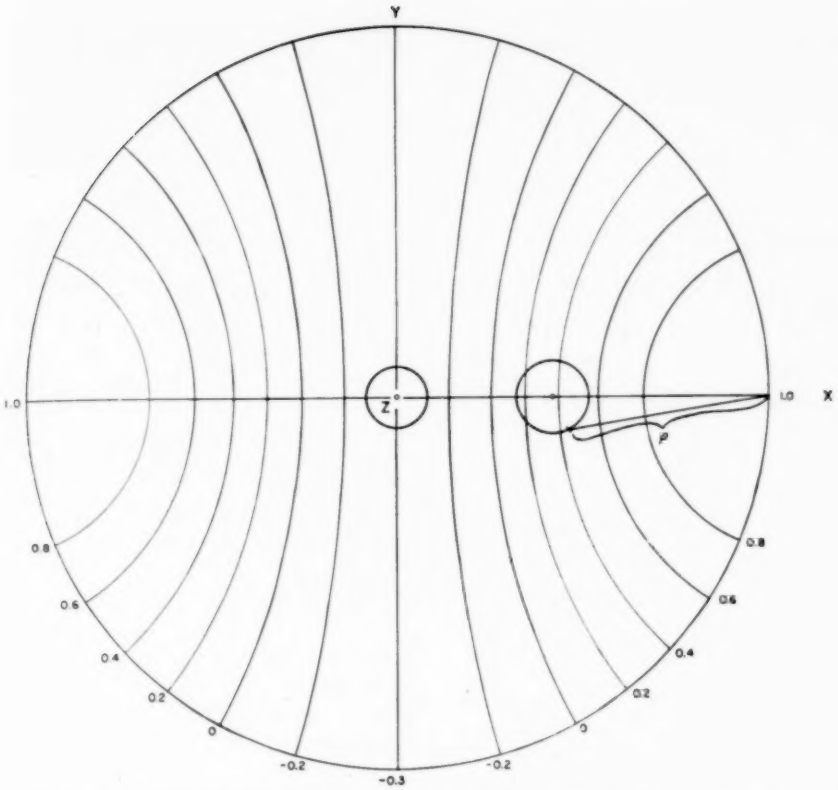

FIGURE 2. *Stereographic projection (plane of projection is the surface of the specimen) showing the variation of strain ratio with direction (latitude circles), for uniaxial loading in the X direction.*

The small circles are the reflection circles for X-ray beams incident at 90° and 45°. Cobalt $K\alpha$ radiation reflected from the 310 planes of iron.

$$\epsilon = -\left[\frac{(1-2\sin^2\theta)^2}{2\tan\theta}\right] d\tan 2\theta. \qquad (3)$$

The term in brackets is nearly constant [4] over the range of values of θ involved in this work, so tan 2θ can be considered to vary linearly with strain. Assuming that the maximum strain which annealed medium carbon steel can withstand without plastic deformation is about 0.001, the strain at the point of maximum available strain ratio would be 0.00056. Substituting this value in eq 3 and assuming $\theta = 80\frac{1}{2}°$, the change in tan 2θ is found to be 0.0075. In work of this kind the specimen-to-film distance is usually about 60 mm; at this distance the above change in tan 2θ would cause a change of 0.45 mm in the radius of the diffraction ring. As the radii of the sharpest diffraction rings cannot be measured more closely than about 0.05 mm, the sensitivity of a single measurement is greater than 10 percent of the maximum strain to be determined. This consideration made it obvious that the number of measurements used to determine a specific condition of strain would have to be farily large if the required precision were to be obtained.

2. Strain Determination From Multiple Measurements of Ring Radius

It will be noted on figure 2 that the reflection circles (particularly when the incident angle is 45°) intersect a wide range of values of strain ratio. This means that the radius of the diffraction ring from a stressed specimen will not be constant, as was shown by Stäblein.[5] Figure 2

[4] The errors involved in certain of the approximations made in this paper are evaluated in section VI, 4.

[5] Von F. Stäblein, Tech. Mitt. Krupp **2**, 29 (appendix, 1930).

shows that for all values of β the strain ratio is negative when the beam is normally incident, and positive for 45° incidence. This is shown in detail in figure 3, where the strain ratio is plotted as a function of position on the reflection circle. The values used in plotting these curves can be obtained either by determining ρ for various values of β on a stereographic projection or from the geometrical considerations shown in section VI, 3.

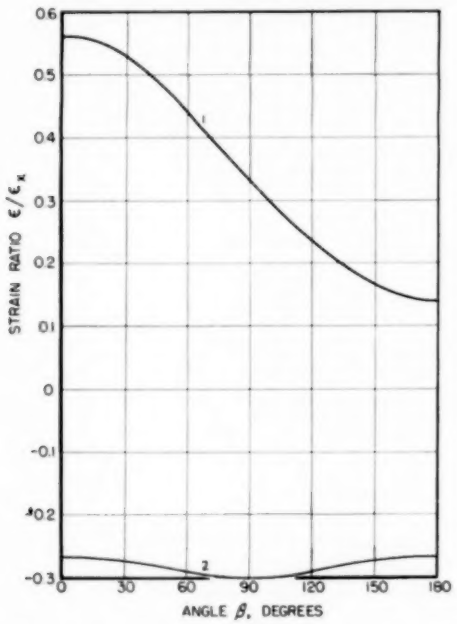

FIGURE 3. *Theoretical variation of strain ratio with position on the diffraction ring, for uniaxial stress.*

1, 45° incidence; 2, 90° incidence.

It should be pointed out that the curves of figure 3 are strictly true only for infinitesimal values of strain, since θ, and therefore ρ, change slightly with strain. As shown in section VI, 4 the effect of the maximum anticipated strain on the position of the curves of figure 3 is not significant.

As was shown above, tan 2θ can be considered to be a linear function of strain; therefore, if the measured values of tan 2θ for various positions on the ring are plotted against the corresponding values of the strain ratio, the points would be expected to lie on a straight line. The intercept of this line at $\beta=0$, for example, would provide a value representative of all the measurements taken on that diffraction ring. This method of analyzing the data was followed in the experiments described in this report in order to increase the precision over that obtainable with a single measurement. The results will be discussed after the experimental procedures have been described.

III. Procedure

1. Apparatus

The X-ray apparatus used in this work was a General Electric XRD unit, the tube having a cobalt target. The voltage was 45–47 KVP with a tube current of 7 ma. The collimator consisted of two 1-mm-diameter pinholes spaced 75 mm apart. Under these conditions an exposure of 1 hour on Eastman No-Screen film was satisfactory. Single-coated film was not found to be necessary in this work, as only the change in radius was important.

A flat specimen was used, the stress being applied by bending. The specimen was made from a ⅝-in. diameter rod of X4130 steel in the normalized condition. A flat central section, 1/16 in. thick by 1⅜ in. long was machined equidistant from the ends of the rod, the thickness of the reduced section being uniform within 1 percent. The surface on which strain measurements were to be made was polished with progressively finer abrasive papers, finishing with 400 Aloxite; then the specimen was normalized in vacuum at 1,625° F, and finally the surface was etched for 5 minutes in 1 percent nital.

Strain in the X-direction in the specimen was measured with two wire strain gages placed above and below the spot where the X-ray beam was incident. Baldwin-Southwark A–7 gages, having an effective length of ¼ in., were read on a type K strain indicator. The average difference between the readings of the two gages was about 15×10^{-6}.

The specimen was loaded in a jig (a top view of which is shown in fig. 4), which applied a uniform bending moment to a 1-in. length of the reduced section. This was accomplished by loading the specimen as a simple beam, with the load distributed symmetrically on the two knife edges. This symmetry was maintained by supporting the knife edges on two pins, which allowed rotation about both a vertical and a horizontal axis.

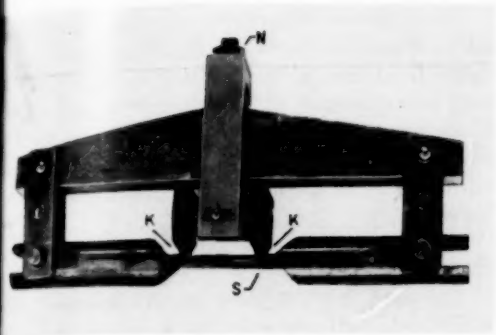

FIGURE 4. *Jig for applying a bending moment to the flat specimen used in this investigation.*

S, specimen; K, knife edges; *N*, loading nut.

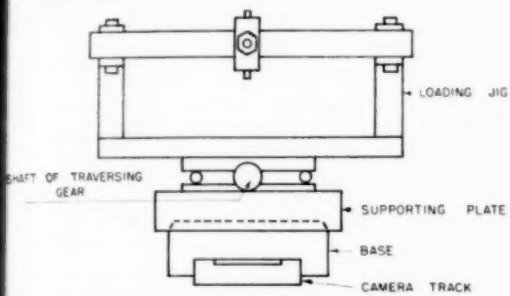

FIGURE 5. *Sketch of complete mounting assembly for loading jig, looking toward the X-ray tube.*

The loading jig was supported on three balls guided by steel V-blocks on the bottom plate of the jig and on the supporting plate below, as shown in the sketch of figure 5. The surface of the specimen was parallel to the V-blocks, so that the jig could be traversed while keeping the surface of the specimen accurately in the same plane. The supporting plate was mounted on a base in such a way that the specimen could be set either normal to the incident beam or at an angle of 45° to it when the base was in place on the track of the X-ray unit. During the exposure, the loading jig was translated horizontally about 3 mm by a clock mechanism operating through a flexible shaft.

2. Measurement of Film-to-Specimen Distance

Two measurements are required for a determination of the diffraction angle, namely, the film-to-specimen distance, S, and the radius of the diffraction ring, R, tan 2θ being R/S. Many investigators [6] have, in effect, made the first measurement by using a calibrating substance in the form of a powder dusted on the specimen. The diffraction ring from this standard is compared with that from the specimen so that no direct measurement of the specimen-to-film distance is required. Because of the uncertainty of measurement of a diffraction ring, the more precise method of determining S by micrometer measurement was adopted. These measurements were made on a separate camera track on which the complete specimen mount assembly was placed before making an exposure. A pointer controlled by a micrometer screw was mounted in a collimator mount on the camera track in such a way that the pointer was in the same position relative to the specimen as the X-ray beam. The spacing between the collimator mount and the supporting plate of the specimen mount was set by means of a gage block placed on the camera track between them.

After the specimen mount assembly and the collimator mount had been clamped firmly against the gage block, the pointer was advanced until it contacted the specimen, the contact being indicated electrically. The micrometer reading was recorded and the complete specimen mount assembly was then transferred to the camera track on the X-ray apparatus. The same gage block was used to adjust the spacing between the supporting plate and the camera mount, following which the exposure was made. After a few calibrating exposures had been made with substances of known diffraction angle, the micrometer readings could be converted directly to values of S. This distance was approximately 60 mm.

3. Measurement of Ring Radius

In order to provide a reference mark on the film from which to measure the radius of the diffraction ring, a calibrating ring was exposed on the film after the diffraction pattern. A circular mask having a diameter about 10 mm greater than the diffraction ring was held firmly against the light shield in such a way that the periphery of the mask was accurately concentric with the position of the collimated X-ray beam. A direct beam of X-rays, arranged to form a sharp shadow of the mask, produced a dark ring on the film, and this ring was used as a reference in all measurements of the diffraction ring. As the calibrating ring was exposed immediately after the diffraction

[6] See footnote 3.

pattern, any dimensional change in the film could be measured.

The diffuseness of the diffraction ring makes it difficult to measure the radii with the desired sensitivity of 0.05 mm, the total width of the line being 1½ to 2 mm, under the best circumstances. Preliminary measurements made for comparison on a recording microphotometer and with visual methods, indicated that the greater precision of the former justified the additional time which it required. The microphotometer used was of the Knorr-Albers type.

A film holder (fig. 6) was constructed which allowed the film to be rotated without being removed from the holder. The film was mounted between two circular glass plates which were held in a flanged ring by spring clamps. The ring was a close fit in a hole in a 4- by 10-in. brass plate and was beveled on the outer edge so that it could be held firmly against the plate by means of knurled clamping screws. The plate fitted into the plate holder of the microphotometer with the long axis of the plate horizontal. The calibrating ring on the film was made concentric with the ring of the film holder by means of ⅛-in.-diameter alinement holes in the center of the glass plates and in the film. Then the plate holder was adjusted so that the scanning light would pass through this common center. In this way the ring could be set quickly (using a graduated circle on the flange) for scanning any desired diameter of the diffraction ring. It was found by trial that the most satisfactory scanning speed was 10 mm a minute, which, with a chart speed of 2 in. a minute, gave a magnification of about × 5 on the chart.

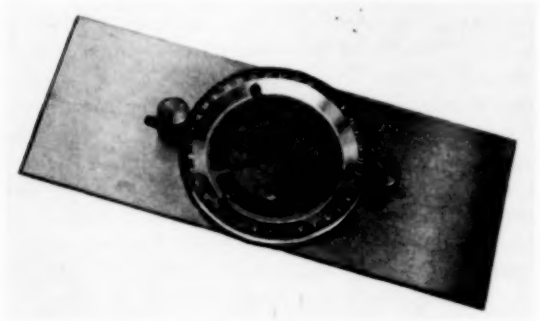

FIGURE 6. *Film holder for mounting and rotating the diffraction pattern in the microphotometer.*

The diameter of the calibrating ring was measured at three positions on the film, and the distance from the calibrating ring to the diffraction ring was measured at 12 points 30° apart. From these measurements the radii (corrected for film shrinkage) at 12 values of β could be obtained, as the diameter of the calibrating ring was accurately known.

4. Treatment of Data

For each load applied to the specimen, two diffraction patterns were made, one with the X-ray beam incident at an angle of 90° and the other with 45° incidence. As 12 measurments of ring radius were made on each pattern, there were a total of 24 measurements associated with each loading condition. Figure 3 shows that the strain ratio for normal incidence is sufficiently constant around the reflection circle so that all values of the radius may be averaged. However, in the case of 45° incidence a considerable loss in sensitivity would result if the readings were averaged, as the average strain ratio is significantly smaller than that at $\beta=0$. Instead, the values of $\tan 2\theta$ were plotted against strain ratio, and the intercept corresponding to $\beta=0$ was taken as the value representative of the group of readings. A typical set of data plotted in this way is shown in figure 7, in which the coordinate lines are drawn at each value of β where a measurement of radius was made. The strain in the X direction (ϵ_x) in this case was 0.06 percent. The straight line representative of the points was determined by least squares analysis.

Both the slope and the intercept of curves plotted as in figure 7 would be expected to vary with strain, but the intercept was used as it was more sensitive to strain changes and could be compared more readily with the results from the patterns taken at normal incidence.

A systematic error is indicated by the fact that the points in figure 7 for the radii from 0 to 180° are consistently higher than those from 180 to 360°. This discrepancy occurred in all patterns, regardless of angle of incidence, and is probably due to a slight misalinement of the pinhole collimator relative to the camera track or other parts of the apparatus. The error amounts to about 0.1 mm, and would occur if the angle between the collimated beam and the camera track were as large as 5 minutes.

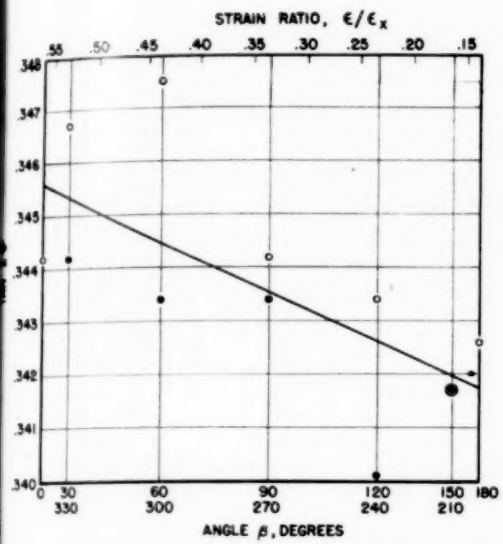

FIGURE 7. *Typical plot of the measurements on one diffraction pattern.*

The open circles represent values of δ from 0 to 180°, closed circles from 210 to 330°. For convenience, the ordinates are drawn at the values of δ where measurements were made, although the graph is actually constructed on a uniform strain ratio scale, as shown by the scale at the top.

IV. Results and Discussion

The results obtained from a series of diffraction patterns from the flat specimen stressed by bending are shown in figure 8. The values representing the 45° incidence patterns are the intercepts for $\beta=0$, obtained as explained above, (fig. 7). The values for normal incidence are the averages of twelve readings from each diffraction pattern.

During the first stressing after normalizing, the specimen was inadvertently deformed enough to cause plastic deformation; consequently the surface layer of the specimen contained some residual compressive stress, as shown by the fact that the curves of figure 8 do not start together, but cross after the surface has been strained somewhat in tension.

It is interesting to note that the curve for 45° incidence flattens off at a strain value of about 9×10^{-4}, indicating that plastic deformation occurred when the strain was greater than this value. However, the 90° curve shows no flattening up to the maximum applied strain. From this it appears that plastic deformation in one direction in a crystal does not affect the atomic spacing or elastic properties in other directions where the strain is not great enough to cause slip.

In order to minimize systematic errors and utilize all of the data to obtain a single curve, the difference between values of tan 2θ for the two angles of incidence are plotted against strain in figure 9. (The subscripts A and B indicate values obtained with 90° and 45° incidence, respectively). Below the start of plastic deformation, the maximum deviation of any point from a linear relationship is 0.0035-percent strain. This deviation corresponds to a stress of about 1,000 lb/in^2. The dashed line on the figure is the theoretical relationship obtained from eq 1 and 2 on the assumption that Poisson's ratio $=0.3$, and that the stress is purely axial.

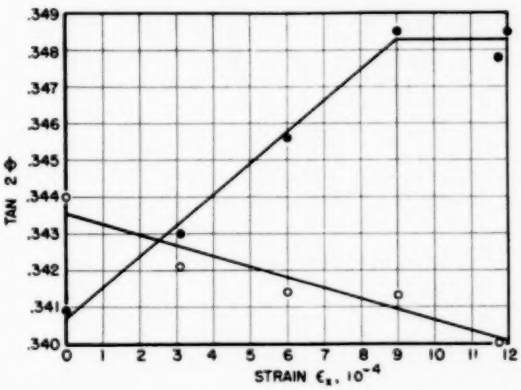

FIGURE 8. *Effect of strain on the diffraction angle as measured with the X-ray beam incident at 90 and 45°.*

Strain was measured with wire strain gages. Each of the points represents the data derived from one diffraction pattern. ○, 90° incidence; ●, 45° incidence.

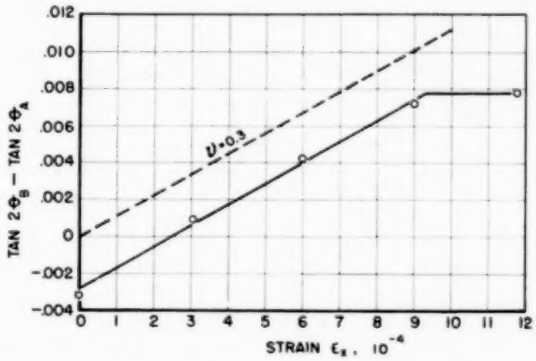

FIGURE 9. *Difference between the 90 and 45° points shown in figure 8.*

The subscripts A and B indicate values of tan 2Θ obtained with 90 and 45° incidence, respectively. The dashed line is the theoretical curve calculated for Poisson's ratio $=0.3$.

The slope of this theoretical curve is not changed greatly by change in the assumed value of Poisson's ratio, so that it is not possible to draw any conclusions regarding the correctness of the value assumed. However, the fact that the slope of the experimental curve is nearly the same as that of the theoretical curve shows that X-ray measurements can be used to give a reliable determination of strain in the direction of the applied stress.

V. Conclusions

For the condition of uniaxial stress, the precision of X-ray strain measurements can be improved by increasing the number of measurements of diffraction ring radius. This investigation showed that is was possible to determine elastic strain sufficiently accurately so that a change of stress of 1,000 lb/in.^{2} could be detected.

VI. Appendix

The following symbols, not used in the body of the paper, will appear in the derivations below.

a_1, a_2, a_3, Direction cosines of the direction in which ϵ is measured with respect to the X, Y, and Z axes, respectively. ψ, Angle between the X axis and the incident X-ray beam.

1. Derivation of Equation 2

Under the loading conditions described in section II, a, the directions of the principal strains coincide with the coordinate axes. The equation for the ellipsoid of strain can therefore be written

$$\epsilon = a_1^2\epsilon_X + a_2^2\epsilon_Y + a_3^2\epsilon_Z. \tag{4}$$

As the stress is uniaxial, $\epsilon_Y = \epsilon_Z = -\nu\epsilon_X$. Also $a_1^2 + a_2^2 + a_3^2 = 1$, so that eq. 4 becomes $\epsilon = \epsilon_X[a_1^2 - \nu(1-a_1^2)]$. Or, assuming $\nu = 0.3$

$$\epsilon/\epsilon_X = \cos^2\rho - 0.3\sin^2\rho$$

2. Derivation of Equation 3

To avoid confusion, the interplanar spacing in eq. 1 will be symbolized by x rather than d:

$$n\lambda = 2x\sin\theta.$$

Differentiating

$$x\cos\theta d\theta = -\sin\theta dx,$$

$$\frac{dx}{x} = \epsilon = -\cot\theta d\theta. \tag{5}$$

This equation shows the advantage of the back-reflection method (i. e., large value of θ), for stress measurement. The relationship desired is that between ϵ and $d\tan 2\theta$, since the latter is the term measured experimentally

$$d(\tan 2\theta) = 2\sec^2 2\theta d\theta,$$

$$d\theta = \frac{(1-2\sin^2\theta)^2}{2} d\tan 2\theta,$$

$$\epsilon = -\cot\theta d\theta = -\left[\frac{(1-2\sin^2\theta)^2}{2\tan\theta}\right] d\tan 2\theta.$$

3. Formulas for ϵ/ϵ_X

Figure 10 shows the geometry for obtaining strain ratio as a function of β. The sides of the spherical triangle XAC are related as

$$\cos\rho = \cos(90-\theta)\cos\psi + \sin(90-\theta)\sin\psi\cos\beta. \tag{6}$$

For $\psi = 45°$ and $\theta = 80\frac{1}{2}°$:

$$\cos\rho = 0.697 + 0.117\cos\beta. \tag{7}$$

For $\psi = 90°$:

$$\cos\rho = 0.165\cos\beta. \tag{8}$$

Equation 2 can be written:

$$\epsilon/\epsilon_X = 1.3\cos^2\rho - 0.3. \tag{9}$$

Substituting eq 7 and eq 8, respectively,

$$\epsilon/\epsilon_X = 0.332 + 0.212\cos\beta + 0.018\cos^2\beta. \tag{9}$$

$$\epsilon/\epsilon_X = 0.035\cos^2\beta - 0.3 \tag{10}$$

These are the equations of the curves shown in figure 3.

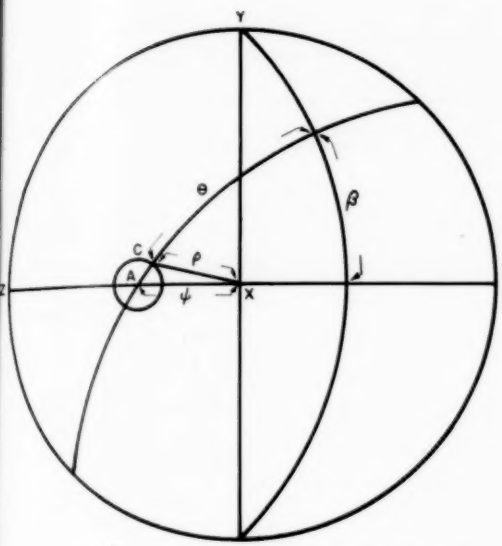

FIGURE 10. *Stereographic projection in the YZ plane showing the geometrical considerations involved in the determination of strain ratio as a function of δ.*
(See section VI, 3).

4. Evaluation of Errors of Approximation

The assumptions made in the following evaluations were $\theta=80\frac{1}{2}°$. Maximum $\epsilon_X=10^{-3}$, $\psi=45°$, $\beta=0$; therefore $\epsilon/\epsilon_X=0.56$ $\epsilon=0.00056$.

In the following, a prime (′) indicates that the value refers to the strained metal. From eq 1

$$d \sin \theta = d' \sin \theta'$$

$$\frac{d'}{d}=\frac{\sin \theta}{\sin \theta'}=1+\epsilon=1.00056$$

$$\theta'=80°19'$$

(a) Variation of the Term in Brackets in Equation 3 with Strain

$$\frac{(1-2 \sin^2 \theta')^2}{2 \tan \theta'}=0.0748$$

$$\frac{(1-2 \sin^2 \theta)^2}{2 \tan \theta}=0.0760$$

That is, the change in tan 2θ is a linear function of strain within 1 percent over this range.

(b) Effect of Strain on Strain Ratio

From eq 6 and 2 the strain ratios for the above conditions are

$$\epsilon/\epsilon_X=0.562$$

$$\epsilon'_X=0.566$$

This change of less than 1 percent has a negligible effect on the determination of the intercept for $\beta=0$.

WASHINGTON, October 3, 1947.

778305—48——3

U. S. Department of Commerce
National Bureau of Standards

Research Paper RP1875
Volume 40, April 1948

Part of the Journal of Research of the National Bureau of Standards

Magnetic Measurement of the Thickness of Composite Copper and Nickel Coatings on Steel

By Abner Brenner and Eugenia Kellogg

A magnetic method has been developed for measuring the thickness of composite coatings of copper and nickel, electrodeposited on steel. The method consists in measuring the attractive force between the specimen and two permanent magnets of different strengths. The total thickness of the deposit and the relative thickness of copper and nickel layers can be determined from a set of calibration curves.

In the plating industry composite coatings of copper and nickel are extensively used, although they do not generally yield as good a protective value as an equal thickness of pure nickel. These composite coatings on steel consist of two layers—the first, copper, which is electrodeposited directly on the steel, and the second, nickel, deposited on the copper. The copper is less expensive than nickel, and it may be readily buffed as an undercoat for bright nickel. The present trend is toward the use of heavier composite coatings to secure increased protective value. The automotive industry commonly uses copper-nickel deposits up to 0.002 in. thick on steel parts. It is therefore desirable to obtain a nondestructive method of measuring the total thickness and the relative thicknesses of the copper and nickel layers such as described in this paper.

An instrument known as the Magne-gage has been used to measure the thickness of nonmagnetic and of nickel coatings on steel.[1] This instrument measures the attractive force between a small permanent magnet and the plated sample. This attractive force is dependent upon the thickness of the coating and the magnetic properties of the coating and base material. When a coating is interposed between the magnet and the magnetic base material, the attractive force is decreased, provided that the coating is less magnetic than the base material, the decrease being greater the thicker the coating.

[1] Abner Brenner, J. Research NBS **20**, 357 (1938) RP1081.

The Magne-gage is a spring balance, on one arm of which the magnet is suspended. A helical spring is attached in such a manner that as the knob is turned, the spring is wound up. The force required to detach the magnet is a measure of the attraction between the magnet and the specimen. The attractive force of the magnet for the sample is read from a dial attached to the turning knob. The thickness of the coating is determined from this reading with the aid of a calibration curve made with coatings of known values of thickness. To determine the thickness of composite coatings, two magnets of different strengths are used. In order to compensate for the difference in the attractive force of the two magnets, it would be necessary to use two different gages unless different springs were used or two magnets were hung at different distances from the pivot on the balance arm. For the measurements here reported, the stronger magnet was hung nearer to the pivot. The modified gage is shown in figure 1.

Nickel is somewhat magnetic, although not as much so as steel, hence the calibration curve for the nickel coatings differs from that for copper coatings as copper is practically nonmagnetic. As can be seen from figure 2, the calibration curve for pure nickel coatings of given values of thickness falls considerably to the left of the curve for pure copper, and is steeper. The calibration curve for any composite coating must fall within the boundaries of these two curves as, for ex-

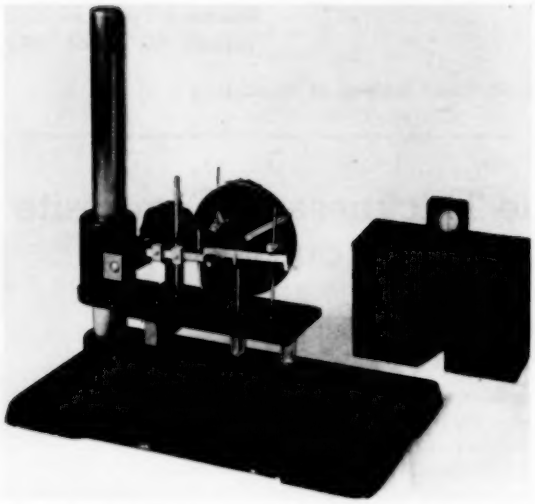

FIGURE 1. *Magne-gage for measuring thickness of composite coatings.*

ample, does the curve for equal thickness of copper and nickel. In the absence of knowledge of the relative thickness of copper and nickel, the total thickness cannot be determined from a single reading as a certain reading can represent a number of thicknesses. For instance, in figure 2, a dial reading of 70 would represent a total thickness of 0.00049 in. of pure copper; 0.00085 in. of a half copper and half nickel coating; or 0.00168 in. of a pure nickel coating.

It is possible, by making measurements on a coating with two magnets of different strengths, to determine not only the total thickness but also the relative thickness of the two layers. This method is based on the fact that the calibration curves of magnets of different strengths have quite different curvatures. This is illustrated in figure 3, where the stronger magnet has about three times the magnetic strength of the weaker magnet. Curves for composite coatings of different compositions, such as 100-percent copper, half copper-half nickel, and 100-percent nickel were prepared, as shown in figures 4 and 5. Suppose that on a given sample a dial reading of 78 was obtained with the weaker magnet, and a reading of 80 was obtained with the stronger

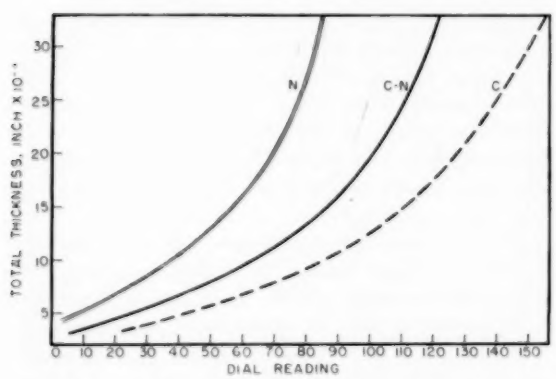

FIGURE 2. *Calibration curves for coatings of various percentages of copper and nickel on steel.*

N, 100-percent-nickel coating; *C-N*, 50-percent-copper–50-percent-nickel coating; *C*, 100-percent-copper coating.

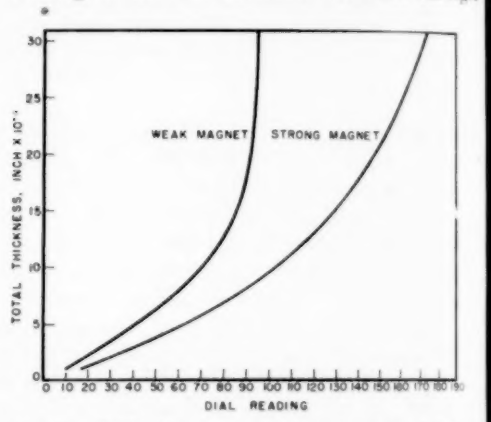

FIGURE 3. *Calibration curves for two magnets of different strengths with copper coatings on steel.*

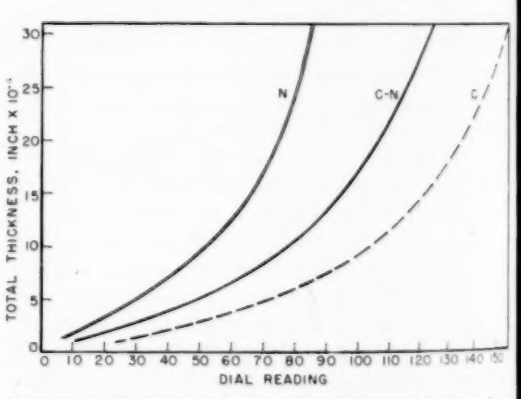

FIGURE 4. *Calibration curves of coatings containing various percentages of copper and nickel on steel for the strong magnet.*

N, 100-percent-nickel coating; *C-N*, 50-percent-copper–50-percent-nickel coating; *C*, 100-percent-copper coating.

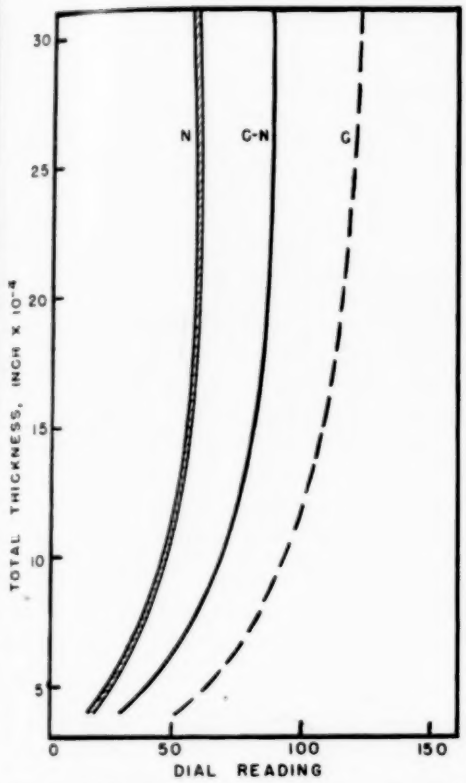

FIGURE 5. *Calibration curves of coatings containing various percentages of copper and nickel on steel for the weak magnet.*

N, 100-percent-nickel coating; *C–N*, 50-percent-copper–50-percent-nickel coating; *C*, 100-percent-copper coating.

magnet. Assuming that the sample has percentages of copper and nickel represented by one of the calibration curves, there are six possibilities as to the thickness as follows:

	Thickness, inch × 10^{-4}	
	Magnet 1	Magnet 2
If 100% copper	7.2	9.0
If 50% copper–50% nickel	13.4	13.4
If 100% nickel	>30.0	26.2

The thickness must be the same when measured by each magnet and in this case is 0.00134 in. The percentage of copper or nickel is defined by the point where the thickness readings for the two magnets coincide. Therefore in the above case half the total thickness must be copper. If the relative percentage of copper does not correspond to a specified curve, it becomes necessary to interpolate between the curves.

To avoid cumbersome, lengthy tabulations, the following graphical method has been developed. The method involves the superposition of the graphs for one magnet on those for the other so that the pertinent gage readings coincide. The points of intersection of the curves are noted. In figure 6, the reading of 78 with the weaker magnet is superposed on the reading of 80 with the stronger magnet, at the line *AB*. Although the curves intersect at a number of points, those of like composition cross at only three points, *X*, *Y*, and *Z*. Through those points line *XZ* is drawn. The intersection *Q* of the line *AB* and the line *XZ* defines the total thickness, in this case 0.00134 in., measured on the left scale. As the thickness falls on the calibration curve for half copper and half nickel, it is not necessary to interpolate to determine the percentage of copper or nickel. If the interpolation is necessary, it may be done in the following manner. Suppose that a reading

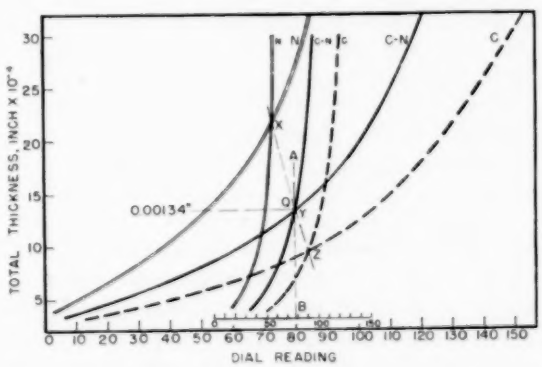

FIGURE 6. *Superposition of calibration curves of the weak (fig. 5) and strong (fig. 4) magnets.*

Intersection occurs on the half-copper–half-nickel curve. *N*, 100-percent-nickel coating; *C–N*, 50-percent-copper–50-percent-nickel coating; *C*, 100-percent-copper coating.

of 68 is obtained with the weak magnet and a reading of 75 with the strong, and the curves are superposed as above. In figure 7, the two dial readings are represented by line AB. A line XZ is drawn through the points X, Y, and Z where curves of like percentages of copper intersect. The position of point Q, where AB cuts XZ, defines the thickness (0.00172 in.), which is read off from the ordinate, and also the percentage of the total thickness that is copper. Point Q lies somewhere between points X and Y, i. e., between the calibration curves for pure nickel and half copper and half nickel, hence the percentage of copper must fall between these two. As Q lies along line XZ about 40 percent of the distance from the half copper curve to the nickel curve, the copper content is $(40/100)\times 50=20$-percent copper. Although the variation in composition is not linear along line XZ, we may assume it to be linear, without appreciably increasing the error in the determination of the percentage of copper of the coating.

The gage as designed will measure with a satisfactory accuracy composite coatings with total thicknesses from 0.0005 to 0.0030 in. Below and above this range the superimposed curves for the two magnets run virtually parallel. Within this range the error of the gage was found to be about 10 percent for the total thickness and 15 percent for the copper percentage determination, as shown in table 1. Measurements were made with the composite magne-gage on especially prepared specimens and on commercially plated coatings to determine their thickness; and the thicknesses were checked by microscopic and chemical analysis. The chemical analyses were made by dissolving the coatings and analyzing the solutions by standard methods. As the gage was calibrated with samples plated with standard Watts nickel, a study was made of the effects of bright nickel. It was found that the bright nickel deposits caused no error beyond the experimental errors of the gage itself. The accuracy of the gage may be seen in figure 8 and table 1, which include bright nickel coatings as well as Watts nickel.

The sample must meet certain requirements to yield satisfactory measurements. An area at least 1-in. square is required, especially for the stronger magnet. If this area is unobtainable, the sample

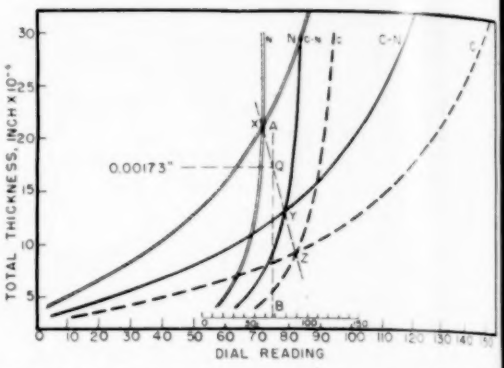

FIGURE 7. *Superposition of calibration curves of the weak and strong magnets.*

Intersection interpolated between curves. *N*, 100-percent-nickel coating; *C-N*, 50-percent-copper-50-percent-nickel coating; *C*, 100-percent-copper coating.

TABLE 1. *Accuracy of composite gage*

The percentage deviation is based on the total thickness obtained by chemical analysis. In most cases microscopic thickness measurements were made on areas adjacent to those used for the chemical analyses. Where the sample was found to be uniform, the microscopic determinations were concordant with the chemical results.

Specimen			Total thickness		Deviation	Thickness of copper, percentage of total		
No.	Plating by [a]	Type of nickel [b]	Chemical analysis	Composite gage results		Chemical analysis	Composite gage results	Difference in percentage of copper
			Inch	*Inch*	*Percent*			
1	Com	B	40×10^{-4}	31×10^{-4}	−23	63	100	37
2	do	B	61	52	−15	44	50	6
3	do	B	63	62	−2	21	30	9
4	do	B	66	109	+65	84	76	−8
5	NBS	B	71	73	3	0	10	+10
6	do	B	76	72	−6	38	45	10
7	Com	B	77	72	−7	38	54	16
8	NBS	B	78	76	−3	35	40	5
9	Com	B	87	86	−1	86	76	−10
10	do	B	86	87	+1	38	30	−8
11	do	B	93	82	−12	24	30	+6
12	do	W	97	93	−4	57	60	3
13	do	W	102	86	−16	56	70	14
14	NBS	W	105	100	−4	76	75	−1
15	do	B	113	132	+17	24	25	+1
16	Com	B	130	128	−2	20	8	−12
17	do	W	136	134	−1	59	55	−4
18	NBS	W	148	152	+3	75	80	+5
19	do	W	149	166	11	75	60	−15
20	Com	W	150	145	−3	59	55	−4
21	NBS	W	191	185	−3	25	25	0
22	do	W	190	205	+3	75	80	+5
23	do	W	201	235	17	25	33	8
24	do	W	247	222	−10	25	40	15

[a] Com refers to commercially plated samples; NBS to those plated at the National Bureau of Standards.

[b] B refers to bright nickel; W to Watts nickel.

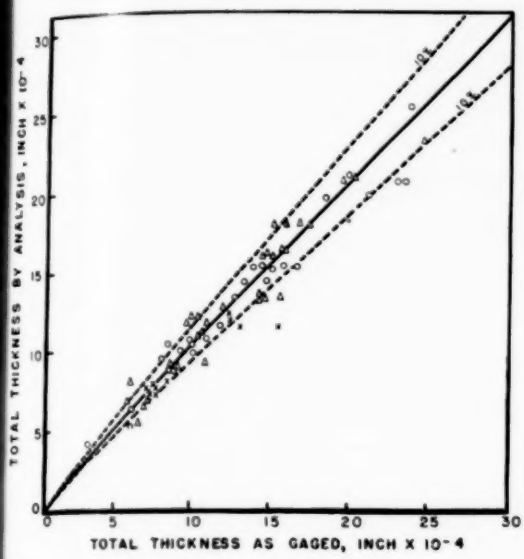

FIGURE 8. *Accuracy of the composite coating Magne-gage.*

The dotted lines represent a 10-percent deviation of thickness obtained by gaging from the thickness obtained by analysis. Watts nickel, ○, chemical analysis; △, metallurgical analysis; bright nickel, ×, chemical analysis.

should be placed on a larger steel backing. The specimen should have a radius of curvature of not less than half an inch. An error of one dial division will cause an appreciable error in thickness. For example, with the weaker magnet in the range from 0.001 in. to 0.0020 in., one dial division will cause an error of 0.00014 in., or about 8 percent, if the sample is pure nickel; and with the stronger magnet an error of 0.00006 in., or about 5 percent. Care therefore must be taken in making the readings, and in providing an adequate area and a sufficient radius of curvature.

For the initial calibration and subsequent checking of this gage, standard-thickness samples will be provided. For each composition of coating, each set will consist of four specimens with different thicknesses of coating on steel. It is probable that all requirements can be met by three sets of specimens, consisting respectively of (a) pure nickel, (b) half copper and half nickel, and (c) pure copper.

WASHINGTON, October 20, 1947.

U. S. Department of Commerce
National Bureau of Standards

Research Paper RP1876
Volume 40, April 1948

Part of the Journal of Research of the National Bureau of Standards

Behavior of Experimental Zinc-Steel Couples Underground

By Irving A. Denison and Melvin Romanoff

The behavior of zinc anodes for the protection of iron and steel cathodically was investigated in eight diverse soil environments. The experimental unit consisted of a small steel ring to which was connected from one to three zinc cylinders to provide different area ratios of zinc to steel. Corrosion of the steel cathodes was prevented over the test periods of from approximately 3 to 6 years except in one poorly conducting soil and in a very alkaline soil. Measurements of galvanic current and open- and closed-circuit potentials made on the experimental couples during the course of the test are interpreted in terms of the extent cathodic protection received. Measurements of the apparent current required for cathodic protection as indicated by current-potential curves are compared with the currents actually required to prevent corrosion.

I. Introduction

Prior to the present investigation, which was started in 1941, zinc anodes had been employed more or less experimentally by a number of corrosion engineers for the cathodic protection of iron and steel pipe lines in local regions with corrosive soils. Several successful installations [1][1] had been described in the literature, but other reports of the use of zinc anodes were less favorable, raising the question whether differences in environment might not account for the reported differences in behavior. In order to study the effectiveness of zinc for the cathodic protection of iron and steel in different soils, the National Bureau of Standards in 1941 organized a series of field tests in cooperation with eight pipe line companies. The plan called for the installation of eight test sites, selected to represent a diversity of soil conditions, of galvanic units, consisting of an iron or steel cathode connected to from one to three zinc anodes. By varying the number of anodes, the current density on the corresponding cathodes was subject to some control. At the conclusion of the test the couples were to be returned to the laboratory for measurement of the degree of protection provided and to obtain other pertinent information.

[1] Figures in brackets indicate the literature references at the end of this paper.

Although measurement of the loss in weight of the steel cathodes after a given period of exposure would establish the degree of cathodic protection provided by the zinc anodes in the environments selected, it was planned also to make several electrical measurements as possible alternative indications of the protection obtained. Provision was made for measurement, whenever the opportunity offered, of galvanic currents and electrode potentials, and for study of the potential of the cathode as a function of applied current.

Subsequent to the installation of these experimental couples, a number of installations of zinc anodes on pipe lines have been made. In these recent installations attention has been directed chiefly toward maintenance of the most favorable environment around the anodes for the maximum output of current [2, 3, 4].

II. Properties of Soils at Test Sites

The properties of the soils at the test sites, recorded in table 1, indicate that the soils are highly diversified. The reaction of the soils ranges from the very acid Susquehanna clay, pH 4.3, to the strongly alkaline Chino silt loam, pH 9.2. The data indicate that the soils cover a wide range of composition and total content of

soluble salts. For example, in the Otero clay (site 74), calcium sulfate is present in high concentration, but in the silt loam at Albuquerque, N. M. (75), sodium sulfate predominates. The Chino silt loam (76) is unique in containing sodium carbonate, the presence of which accounts for the relatively strong alkaline reaction of this soil (pH 9.2).

TABLE 1. *Properties of the soils at the test sites*

Site	Soil type	Location	Aeration	pH	Resistivity at 60° F	Total acidity (mg-eq/100 g of soil)	Composition of water extracts—milligram equivalents per 100 g soil[a]								
							SiO_2	Na+K as Na	Ca	Mg	CO_3	HCO_3	Cl	SO_4	NO_3	Other
					ohm-cm											
71	Mahoning silt loam.	West Austintown, Ohio.	Fair	7.1	2,582	4	0.37	0.22	0.37	0.28	.....	0.33	0.030	0.27	0.24	
72	Papakating silty clay loam.	Deerfield, Ohio	Very poor	7.2	762	17	.34	3.11	7.49	.95	.....	.....	.....	11.58	.....	Fe, 1.32 Al, 0.25 Mn, .40
73	Wabash silty clay loam.	East St. Louis, Ill	do	6.8	521	6	.67	0.44	2.80	.68	.....	1.75	0.020	1.99	.....	
74	Otero clay loam	Rocky Ford, Colo	Fair	7.3	436	5	.90	4.72	18.42	4.24	.....	0.77	.38	26.22	.....	
75	Silt loam	Albuquerque, N. Mex.	do	8.4	379	Alkaline	.47	5.80	0.87	0.16	.....	.56	.70	5.58	.....	
76	Chino silt loam	Los Angeles, Calif	Good	9.2	2,650	do	.40	1.54	.065	.....	0.16	1.23	.068	0.15	.....	
77	Susquehanna clay.	Louisville, Miss	Fair	4.3	9,390	42	.30	0.39	.14	.....	.....	.....	.40	.047	0.081	
78	Caddo fine sandy loam.	Latex, Tex	Poor	4.5	821	24	.70	1.06	.18	0.31	.....	.....	.82	.74	.....	

[a] Analyses of water extracts by L. Schubert, Chemistry Division, National Bureau of Standards.

With respect to aeration, wide differences are exhibited. Marked reducing conditions, as shown by measurements of oxidation-reduction potential, are represented by the Papakating silt loam (72). The soil at the test site at East St. Louis, Ill. (73), is also very poorly aerated, the water table being close to the surface. Oxidizing conditions are represented by the test sites at Albuquerque, N. Mex. (75), and Los Angeles, Calif. (76).

III. Experimental Zinc-Steel Couples

A zinc-iron couple for use in field tests should be so designed that the data obtained may be applied to practical installations. Although the circuit resistance of a small test couple will necessarily differ greatly from that of a practical installation, it can be shown that if the appropriate dimensions are maintained in a medium of large extent and with the same resistivity, the current densities on the cathodes will be the same for the two installations.

The design of the experimental cathode and the installation of the couple at the test sites were based on theoretical considerations and measurements of current distribution as affected by the form of the cathode, horizontal spacing, and depth of the cathode below the surface of the ground. All of these measurements were made in a tank of such size relative to the size of the test couple that the effect of the walls and bottom of the tank on current distribution could be neglected. End effects were avoided by bending a steel rod in the form of an open ring, forming essentially what is known as a toroid or anchor ring (fig. 2). For distances from a small anode equal to or greater than the diameter of the ring, the maximum difference in current density over the cathode was about 10 percent. The effect of variations in the horizontal spacing between cathodes on current distribution was negligible at distances greater than the diameter of the ring. Similarly, at this distance from the surface, no effect of the surface on current distribution could be detected.

Cathodes for the field tests were constructed by bending a sufficient length of steel rod 0.5 in. in diameter to form a ring having an external diameter of 10 in. A small hole was drilled through one end of the curved rod, and, after the ring had been weighed, the end of a No. 14 rubber-covered copper wire was soldered into the hole. A coating of a bituminous material was then applied to the soldered joint. The surface area of the ring was 48 sq in. Because field tests had shown that the composition of the low-carbon steels commonly

used in the manufacture of pipe for underground service has a negligible effect on corrosion rate, no effort was made to secure steel conforming to some definite specification for the preparation of the cathodes, and steel that was readily available from stock was used.

Another problem in the design of a suitable experimental couple is the maintenance of definite ratios of the areas of zinc and steel throughout the duration of the test. This condition is difficult to produce in experimental couples, because the change in area of a small anode for a given rate of penetration by corrosion would be relatively greater than the change in area of the large anode in a practical installation for the same rate of penetration. However, by exposing only the base of a cylindrical zinc anode to the soil, the area of the zinc and hence the zinc-steel area ration could be held reasonably constant. This result was accomplished by covering each cylindrical zinc anode with a housing, which consisted of a wide-mouthed glass bottle, slightly larger in diameter than the anode, from which the base had been removed. With a zinc cylinder of sufficient weight, firm contact with the soil was assured, the cylinder being free to move downward as its base corroded.

The cylindrical anodes were 1.75 in. in diameter and 3.75 in. in height. The exposed area of the base of the anodes was 2.4 sq in. After the anodes had been weighed, the cylindrical surface was coated with a bituminous paint to prevent local corrosion, and a length of insulated copper wire was soldered to one end. The nominal percentage composition of the zinc used for the anodes was: Pb, 0.007; Fe, 0.005; Al, 0.00; Zn, 99.98 (by difference).

The plan of installation of the couples at the test sites is shown in figure 1. As is shown in the figure, the electric circuit was completed by means of binding posts attached to a copper strip. To protect the terminals from corrosion, the copper strip was placed in a glass bottle from which it could be removed when electrical measurements were to be made.

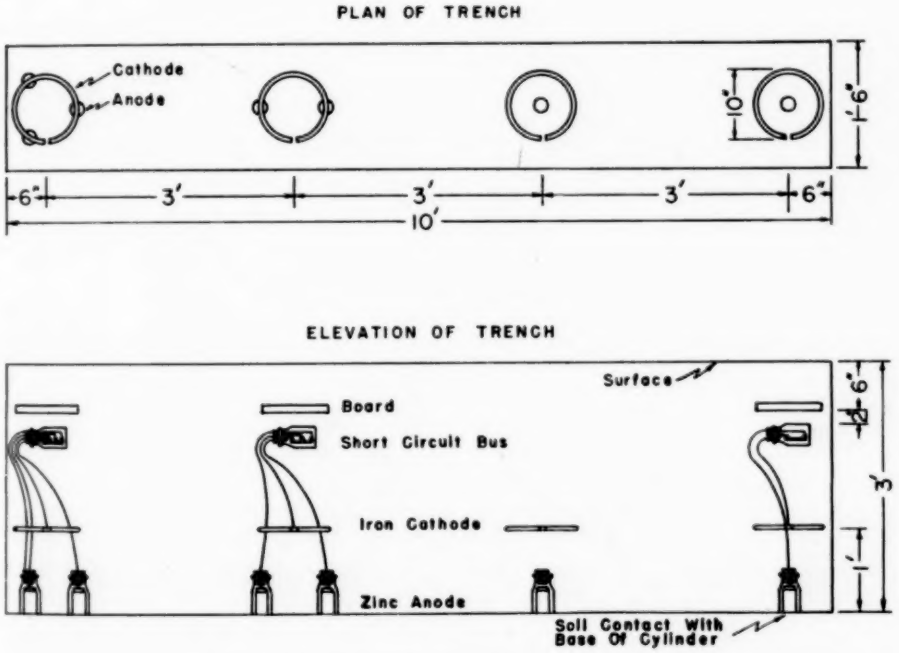

FIGURE 1. *Arrangement of zinc-steel couples at the test sites.*

IV. Cathodic Protection as by Indicated Corrosion Measurements

The losses in weight and the depths of the deepest pits on the steel cathodes connected to the zinc anodes are shown in table 2, together with similar data for the unconnected steel rings and zinc cylinders. It is evident that over the test periods of from 3 to nearly 6 years, practically complete protection was obtained at six of the eight test sites, namely 71 to 75, inclusive, and 78. Although a zinc-steel area ratio of 1:20 was sufficient for protection at sites 74, 75, and 78, an area ratio of 1:10 was required at sites 71, 72, and 73. The condition of the connected and unconnected steel rings and the bases of the zinc cylinders from sites 73 and 78 is shown in figure 2.

TABLE 2. *Weight losses and maximum pit depths on connected and unconnected electrodes*

P, Deepest pit less than 6 mils; *M*, shallow metal attack—no definite pits; *S*, uniform corrosion—no reference surface for pit measurements

Site		Duration of exposure	State of couple	Number of zinc anodes	Weight loss		Maximum penetration of cathode	Effectiveness of protection[a]
No	Location				Cathode	Total loss of anodes		
SITES AT WHICH PROTECTION WAS OBTAINED WITH A 1:20 ZINC-STEEL AREA RATIO								
		Years			*g*	*g*	*Mils*	*Percent*
75	Albuquerque, N. Mex.	5.80	Unconnected	1	109.2	0.8	135	
			Connected	1	3.2	229.9	P	
			do	2	2.0	283.6	P	
			do	3	0.6	309.0	P	
78	Latex, Tex.	3.14	Unconnected	1	67.3	0.8	84	
		3.14	Connected	1	1.8	43.1	7	
		4.26	do	2	0.8	88.3	P	
		3.14	do	3	1.4	63.6	4	
74	Rocky Ford, Colo.	5.82	Unconnected	1	28.9	0.6	P	
			Connected	1	0.6	40.1	P	
			do	2	[b] 25.2	[b] 28.7	[b] 48	
			do	3	0.2	29.1	P	
SITES AT WHICH PROTECTION WAS OBTAINED WITH A 1:10 ZINC-STEEL AREA RATIO								
73	East St. Louis, Ill.	5.83	Unconnected	1	235.0	0.2	70	
			Connected	1	32.6	184.9	35	
			do	2	1.7	135.9	P	
			do	3	5.2	260.4	P	
71	West Austintown, Ohio	5.12	Unconnected	1	57.1	0.0	38	
			Connected	1	13.2	25.1	30	
			do	2	7.6	37.8	16	
			do	3	7.4	45.0	22	
72	Deerfield, Ohio	5.18	Unconnected	1	26.8	0.6	118	
			Connected	1	29.0	16.1	42	
			do	2	2.9	33.0	M	
			do	3	2.9	43.1	P	
SITES AT WHICH INCOMPLETE PROTECTION WAS OBTAINED EVEN WITH A 1:6.7 ZINC-STEEL AREA RATIO								
76	Los Angeles, Calif.	1.49	Unconnected	1	45.9	0.4	70	
			Connected	1	27.3	33.8	78	
			do	2	17.1	39.1	35	
			do	3	15.3	72.8	41	
77	Louisville, Miss.	5.67	Unconnected	1	58.3	0.7	58	
			Connected	1	47.2	8.8	98	
			do	2	29.1	19.1	84	
			do	3	28.0	34.6	65	

[a] Based on weight loss of unconnected ring.
[b] Couple on open circuit for an indefinite period.

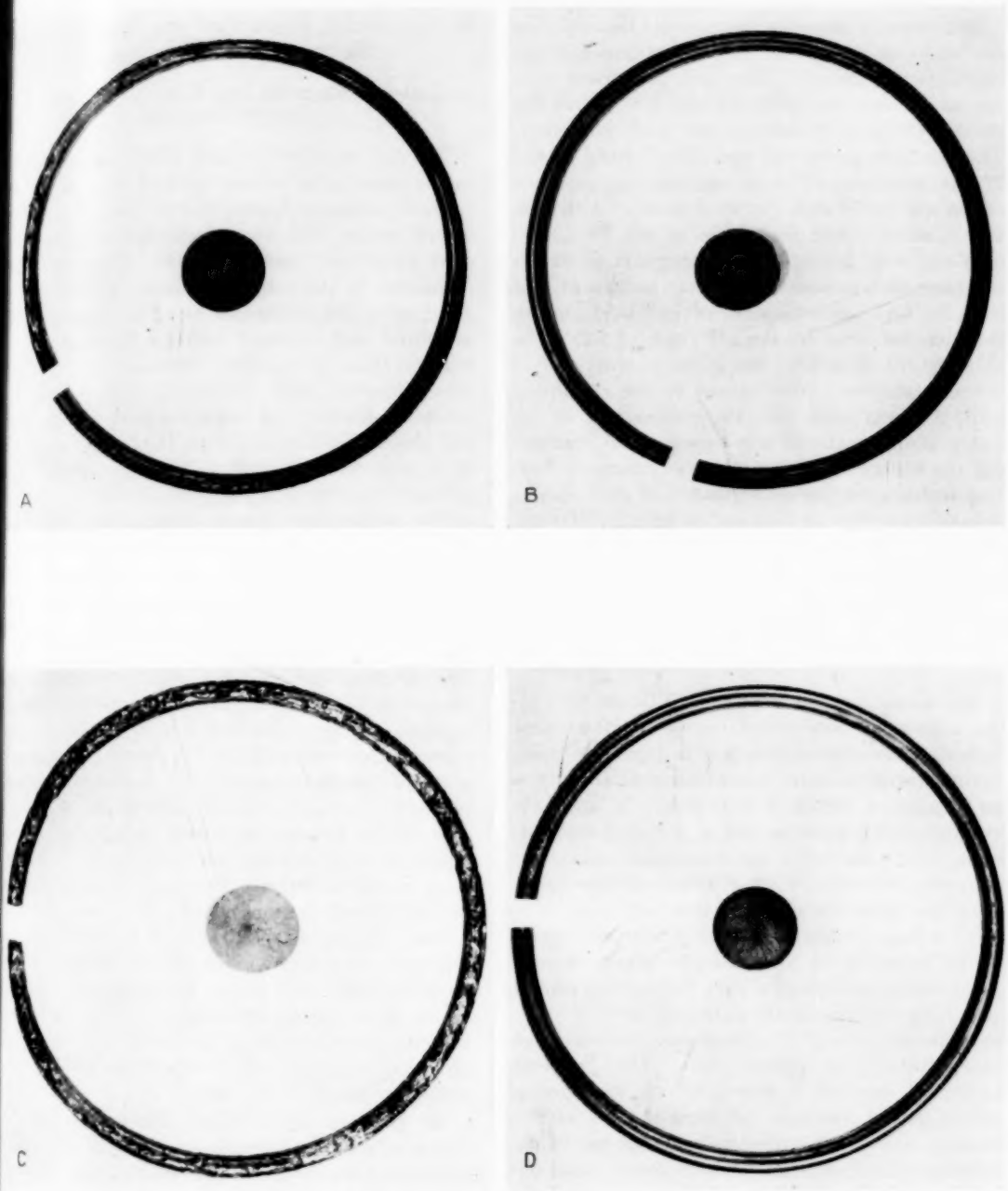

FIGURE 2. *Condition of connected and unconnected steel cathodes and zinc anodes at two test sites.*

A, Unprotected steel ring and zinc cylinder exposed at site 78 for 3.1 years; *B*, ring connected to zinc anode at site 78 for 3.1 years. Zn-Fe area-ratio 1:20; *C*, unprotected steel ring and zinc cylinder exposed at site 75 for 5.8 years; *D*, ring connected to zinc anode at site 75 for 5.8 years. Zn-Fe area-ratio 1:20.

778265—48——4

The primary environmental factors that affected the behavior of the zinc anodes are indicated by the data of table 1. The soil properties that appear to have the most inhibitive effect on the anodes are high resistivity and high alkalinity. The fact that protection was not obtained at site 77 is no doubt caused by the high specific resistance of the soil, 9,370 ohm-cm, at this site. Although the relatively high resistivity of soil 76 (2,650 ohm-cm) was probably an important factor in the poor performance of the zinc anodes at this site, the high concentration of hydroxyl ions in this soil, indicated by the pH value of 9.2, probably tended to inhibit the galvanic corrosion of the zinc anodes. With regard to the remaining soils, it would seem that the composition of the water soluble material was unimportant, providing the resistivity of the soil was relatively low. Improvement in the performance of zinc anodes in poorly conducting soils and in strongly alkaline soils deficient in chloride and sulfate ions can probably be obtained by surrounding the anodes with materials, such as calcium sulfate, which produce soluble corrosion products of zinc. This practice is advocated by Mudd [3], Morgan [5], and others.

The data obtained from site 72 throw light on the somewhat controversial subject of whether cathodic protection is practical in highly reducing environments in which microbiological activity is an important factor in corrosion. In such environments it is assumed that high-resistance oxide films, which normally cover cathodic areas, are converted to sulfide films of relatively low resistance, and that the effect of this conversion is to cause a large proportion of the protective current to be bypassed by the cathodic areas, thereby requiring an abnormally high current for protection. By referring to the data in table 1, it is seen that the soil at site 72 contains a relatively high concentration of sulfate ions. The reducing nature of this soil is shown by the presence of sulfide in the corrosion products of steel at this location and also by measurements of the oxidation-reduction potential. Under these conditions it is noteworthy that adequate protection of the steel cathodes was obtained with a moderate area-ratio of zinc to steel.

V. Cathodic Protection as Indicated by Electrical Measurements

1. Galvanic Currents and Open-and-Closed-Circuit Potentials

The data reported in table 3 consist of measurements made after various periods of exposure, of galvanic currents, potentials of the couples on closed circuit, and open-circuit potentials of the steel rings and zinc cylinders. Currents were measured by the zero-volt-loss method [6, 7], the *IR* drop in the millimeter being compensated by an equal and opposite voltage by means of a battery and a variable resistance. Potential measurements were measured with a potentiometer-voltmeter. A copper-copper sulfate half cell placed about 10 feet from the couple was used as a reference electrode. After measuring the galvanic currents and the closed-circuit potentials of the couples, the circuits were opened for 15 to 20 minutes, and the open-circuit potentials of the zinc anodes and steel cathodes were measured.

In the absence of polarization and mutual influence of the anodes, the galvanic currents produced by connecting, to a steel cathode, one, two, or three zinc anodes in parallel would be expected to be in the same ratio as the number of anodes. An approach to this ratio is shown by the currents that were measured at site 75 immediately after the installation was made, the currents standing in the ratio of 1:2:2.6. Similarly, the averages of the currents measured at site 72 for the entire period of the test are in the ratio 1:1.9:2.7. As a matter of interest, the total losses in weight of the respective numbers of zinc anodes for the 5-year test period are in the ratio 1:2.0:2.7, showing that the entire loss in weight of the anodes could be accounted for by the galvanic currents, as has been previously indicated. The fact that the currents were not in the exact ratio of 1:2:3 indicates some influence between the anodes connected to the same cathode.

At the test sites where polarization of the cathodes was marked, the couples that contained three anodes produced little, if any, more current than the couples that contained only two anodes. Furthermore, two anodes often produced considerably less than twice the current produced by

TABLE 3. *Potential and current measurements*

Site	Duration of exposure	Potentials: Steel rings having Zn:Fe area ratio of—			Potentials: Zinc cylinders having Zn:Fe area ratio of—			Potentials: Zinc-steel couples having Zn:Fe area ratio of—			Galvanic currents having Zn:Fe area ratios of—		
		1:20	1:10	1:67	1:20	1:10	1:6.7	1:20	1:10	1:6.7	1:20	1:10	1:6.7
PROTECTION WITH 1:20 ZINC-STEEL AREA RATIO													
	Years	*v*	*v*	*v*	*v*	*v*	*v*	*v*	*v*	*v*	*ma*	*ma*	*ma*
	0.00	0.71	0.70	0.74	1.11	1.15	1.17				5.9	11.7	15.2
75	.53	.80	.82		1.08			0.92	1.00	1.02	4.7	5.4	5.4
	5.80		.88	.93		1.00	1.10		1.03	1.04		1.32	1.30
	0.00	.59	.58	.58	0.91	0.92	0.92				3.80	5.35	6.80
	.27	.95	.96	.96	1.04	1.06	1.05	1.00	1.00	1.01	0.86	2.00	1.61
	.48	.91	.93	.93	1.09	1.10	1.10	1.05	1.05	1.05	.80	1.79	1.41
78	.84	.80	.78	.82	1.10	1.10	1.06	1.00	1.05	1.05	2.40	4.90	3.68
	1.17	.76	.83	.74		1.14	1.15	0.96	0.96	1.20	1.50	1.89	1.40
	3.14							.68	.91	0.96	2.00	1.62	1.95
	4.26		.81			1.08			.91			1.8	
	0.0	.74			1.18						7.26		
	[a].54							1.04	1.08	1.08	0.28	0.55	0.45
74	2.23							1.04	1.05	1.08	.58	1.11	.49
	5.82	.90	[a].72	1.03	1.08	[a]1.09	1.10			1.08	.66	[a]6.00	.38
PROTECTION WITH 1:10 ZINC-STEEL AREA RATIO													
	0.0										2.6	4.6	4.60
73	.68	0.94	0.95	0.85	1.10	1.11	1.14	1.01	1.03	1.03	0.58	1.00	1.02
	5.83	.68	.84	.68	1.05	1.09	1.06		0.90	0.76	3.45	2.40	5.00
	0.0	.59	.58	.60	1.09	1.10	1.10				0.44	0.48	0.66
	.32	.62	.55	.60	1.11	1.12	1.13	0.76	.80	.94	.93	1.33	1.30
71	.77							.79	.84	.92	.62	1.15	1.48
	3.02	.50	.58	.56	1.04	1.26	1.28	.55	.69	.73	.43	1.12	2.00
	5.12	.63	.74	.93	1.04	1.08	1.11	.76	.86	1.00	.21	0.27	0.35
	0.0	.73	.73	.73	1.14	1.14	1.14				.73	1.46	2.65
	.31	.78	.85	.75	1.02	1.06	1.05	.79	.80	.83	.24	0.41	1.14
72	.73	.76	.80	.77	1.02	1.07	1.05	.77	.83	.82	.35	.66	1.17
	1.04	.71	.76	.76	1.02	1.06	1.06	.72	.80	.81	.54	.97	1.34
	3.01	.62	.71	.73	0.91	1.05	1.06	.64	.72	.77	.52	.84	0.08
	3.18	.58	.63	.75	.82	1.08	1.04	.58	.65	.79	.14	.31	.49
INCOMPLETE PROTECTION													
	0.0	0.52	0.49	0.50	0.95	0.93	0.97	0.55	0.50	0.51	0.19	0.58	1.44
	.26	.68	.63	.72	1.07	1.05	1.07	.70	.67	.79	.87	2.30	3.27
76	.47	.66	.50	.67	1.05	1.03	1.03	.70	.66	.78	1.39	4.49	3.43
	.80	.47	.54	.56	1.05	1.03	1.04	.57	.63	.71	3.05	1.98	6.15
	1.28	.45	.45	.35	1.03	1.03	1.03	.59	.57	.61	2.25	1.69	4.09
	1.49	.83	.63	.83	1.07	1.02	1.03	.86	.67	.89	1.55	1.42	0.62
	0.0	.58	.55	.57	1.08	1.09	1.09				0.52	0.61	.71
77	.54							.58	.66	.69	.10	.53	.93
	5.67	.14	.20	[a].25	1.08	1.06	[a]1.07	.16	.22	[a]1.06	.12	.31	[a]1.25

[a] Couple found on open circuit.

one anode. These observations are illustrated by the ratio of the average currents at site 78 for one, two, and three anodes, namely, 1.0:1.5:1.5. As would be inferred from this relation, cathodic protection was readily accomplished at this site, a zinc-iron ratio of 1:20 being sufficient to prevent corrosion of the cathode (table 2).

The open-circuit potentials of the cathodes are seen to be highly variable, ranging at various sites from 0.14 to 0.96 volt. This is in marked contrast to the potentials of the zinc anodes, which, with a few exceptions, were remarkably constant. The marked differences in the potentials of the steel cathodes can be interpreted in terms of the local cell theory of Müller [8]. According to Müller, the potential of a self-corroding surface is given by the equation.

$$E = E_A \frac{Rc}{Rc+Ra} + E_c \frac{Ra}{Rc+Ra},$$

where

E = observed potential
E_A = potential of the anodic areas
E_c = potential of the cathodic areas
Rc = resistance of the cathodic film
Ra = resistance of the anodic areas, i. e., at pores.

This equation shows that if the resistance of the cathodic areas is very high relative to the resistance of the anodic areas, the potential of the anode only, E_A, is measured, and vice versa.

On the basis of Müller's equation one might reasonably interpret the relatively high values of potential measured in soils 73, 74, 75, and 78 as indicating that the potential of the anodic areas, E_A, was being approached. Similarly, the relatively low values for the potential of the rings in soils 76 and 77 would be taken to indicate that these values were influenced to a somewhat greater extent by the potential of the local cathodes E_c.

According to the criterion of Mears and Brown [9] for cathodic protection, namely, that corrosion is prevented when the potential of the local cathodes is brought to the open-circuit potential of the local anodes, one might infer that a slight increase in the relatively high potentials of the iron cathodes in soils 73, 74, 75, and 78 would be sufficient to prevent corrosion, because the observed potentials are already probably very close to the open-circuit potentials of the local anodes. By the same reasoning, a proportionately greater change in the nobler potentials of the cathodes in soils 76 and 77 would be necessary to prevent corrosion.

By comparing the open-circuit potentials of the cathodes in soils 73, 74, 75, and 78 with the corresponding closed-circuit potentials, it can be seen that by connecting the zinc anodes to the steel cathodes, the potentials of the latter were brought close to the potentials of the zinc anodes. As these latter potentials are almost certainly more anodic than the potentials of the local anodes on the steel rings, the criterion for cathodic protection suggested by Mears and Brown has apparently been satisfied. However, because of the inclusion of some IR drop, the values of closed-current potential indicated are probably somewhat greater than the true potentials of the local anodes. Because of the more cathodic potentials of the steel rings at sites 76 and 77, small changes in potential are seen to have been insufficient to polarize the rings to the potentials of the local anodes, and as a consequence, corrosion was not prevented. The relatively low closed-circuit potentials of the couples at sites 76 and 77 indicate that polarization of the zinc anodes was also an important factor in the failure to achieve cathodic protection in these soils.

2. Current-Potential Curves for the Steel Cathodes

In addition to the electrical measurements described in the preceding section, current-potential curves for the cathodes were obtained at most of the test sites. The relation between the potential of a corroding element and the applied current has been suggested as a practical means of measuring the current required for the protection of iron and steel cathodically. As increasing currents are caused to flow toward a corroding surface, the potential remains constant over a range of currents after which the potential changes in proportion to the logarithm of the current. Consequently, if the values of potential are plotted on the vertical axis against the logarithm of the corresponding currents on the horizontal axis, the points up to a certain value of current will lie along a horizontal line. Beyond this value of current and after more or less transition, the points fall along a second straight line having an appreciable slope. The current corresponding to the point at which

the potential departs from the horizontal relation and follows the curve for hydrogen overvoltage has been taken by Evans, Bannister and Britton [10], Pearson [11], and Ewing [12] as the minimum current that will prevent corrosion at least under the particular experimental conditions. However, as many current-potential curves depart considerably from the ideal curve, the interpretation of current-potential curves generally in terms of the current required for protection is uncertain. As it seemed probable that at least one of the three cathodes at each test site would be just protected cathodically, comparison of the values of the minimum protective current estimated from the current-potential curves and the galvanic currents that flowed to such protected cathodes would indicate the manner in which current-potential curves had best be interpreted in terms of the current required for cathodic protection.

Before proceeding with the interpretation of the current-potential curves of the experimental couples, it is preferable to consider similar curves obtained under conditions that permit direct comparison between the values of the protective current indicated by the curves and the currents actually required to prevent corrosion. In figure 3 are shown current-potential curves for steel electrodes in contact with two soils contained in a specially designed corrosion cell. The electrodes of the cell consisted of two segments cut from a disk of low-carbon sheet steel. The segments, separated by a thin bakelite strip, were placed side by side in the end of a Bakelite tube having the same internal diameter as the disk from which the segments were cut. The segments were aerated differentially by covering one segment with soil which, after being moistened had been mechanically worked to remove all air spaces, the other segment being covered with soil in its natural condition. After bringing the soil to a definite moisture content, the cell was placed on closed circuit. The potential of the electrodes connected externally was measured free of *IR* drop by the method of Hickling [13] the measurements being made during very short interruptions of the polarizing current. The reference electrode was so placed that further separation from the test electrodes being measured had no effect on the observed values. In addition to the potential of the electrodes, the cell current was measured as the applied current was increased, a "zero-resistance" milliammeter being used. The open-circuit potentials of the anode initially and after reduction of the cell current to zero are indicated in the figure for cells *A* and *B*.

In addition to the horizontal part previously referred to, the curves are seen to consist of two straight sections that differ in slope. Taking the lower curve to represent the overvoltage curve for evolution of hydrogen, it would seem to follow that the middle curve represents the cathodic reduction of oxygen. This interpretation of cur-

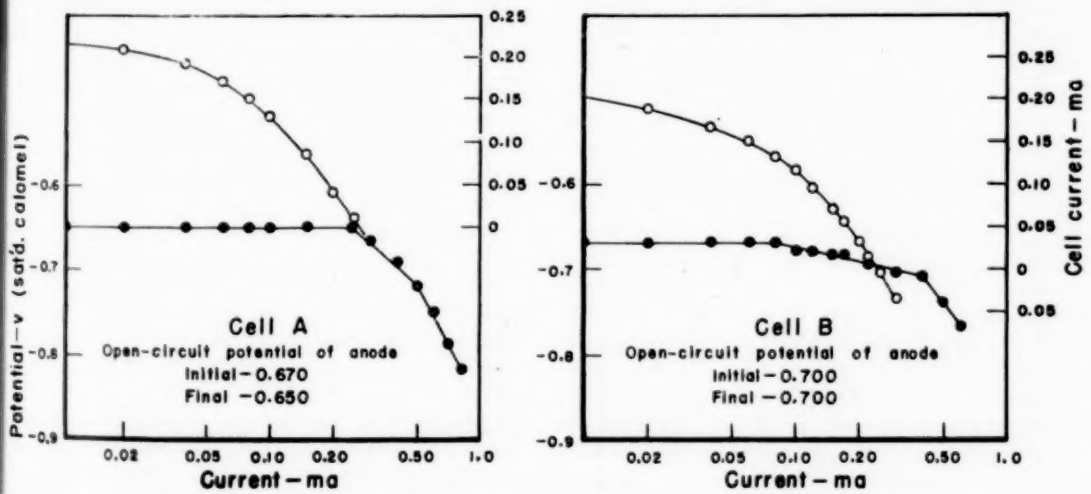

FIGURE 3. *Current-potential relation for differential-aeration cells with steel electrodes.*

● Potential; ○ cell current.

rent-potential curves for the cathode is essentially that of Evans, Bannister, and Britton [10].

It will be noted in the curves representing the behavior of cell *A* that the value of applied current that was required to reduce the cell current to zero coincided exactly with the discontinuity in the current-potential curve. In cell *B*, on the other hand, considerably more current was required to bring the cell current to zero than is indicated by the discontinuity in the current-potential curve. By referring to the values of the open-circuit potentials of the anodes, it is seen that if the open-circuit potential at the anode corresponds to the over-all potential of the combined anode and cathode, as in cell *A*, the protective current is indicated by the first discontinuity in the current-potential curve. However, if the over-all potential assumes lower or more cathodic values, the first discontinuity indicates a lower value of applied current than that actually required to prevent corrosion. Incidentally, it should be noted that no more current was required to reduce the cell current to zero than that which flowed originally in the corrosion circuits.

On the basis of a priori considerations and the laboratory measurements that have been described, it seems reasonable to consider the minimum protective currents as corresponding to the departures of the potential from the constant values indicated by the horizontal parts of the curves. Although these values of current would be insufficient to protect initially those cathodes whose potentials were considerably less than the potentials of the local anodes, this deficiency would be compensated for by the tendency of the current, applied continuously over a long period, to reduce the corrosiveness of the environment and hence the current requirement. Because of this tendency, for which evidence will be given later, the value of current indicated by the discontinuity in the current-potential curve might actually overestimate the current required over a long period for the special case in which the observed potential is determined by the potential of the local anodes.

The method used in obtaining the first series of current-potential curves, at sites 71 and 72, involved measuring the potential including the *IR* drop between the cathode and the reference electrode, calculation of the resistance for each value of applied current by observing the change in potential corresponding to an increment of current, and subtraction from each value of $E+IR$ the calculated value of the *IR* drop. All subsequent measurements were made with the null method described by Pearson [11], in which the *IR* drop is balanced out of the circuit and the true potential read directly. Typical current-potential curves obtained with the cathodes of the zinc-steel couples are shown in figure 4.

In the curves obtained at most of the test sites, the middle linear sections referred to in the discussion of figure 3 are well defined. It is possible that this section is obscured in the curves for sites 71 and 72 because of the successive changes in potential, which may have been required to eliminate the local currents in corroding areas in which, because of their geometrical configuration, the protective current density was not readily attained.

For comparison with the values of the minimum protective current obtained from the current-potential curves, the average galvanic currents that flowed toward the protected cathodes were calculated from the following sources of data: (1) Periodic direct measurements of current, (2) losses in weight of the unconnected iron ring, and (3) losses in weight of the connected zinc anodes. The total quantity of electricity that flowed in each couple during the test period was first calculated, and from these values the average currents were obtained. Fortunately, the losses in weight of the unconnected zinc anodes were very low (table 2) so that no appreciable error was made in calculating the galvanic current from the gross loss in weight of the anodes. The calculated values of average current are shown in table 4 for comparison with the minimum protective currents. Because the cathodes at sites 73 and 75 had received cathodic protection for nearly 6 years before the protective currents were measured, comparisons between the minimum and average currents at these sites are not valid for evaluating the accuracy of the protective currents. The data for these sites are included in the table in order to illustrate the effects of time and current on the protective currents, which will be discussed later.

The data for the test sites at which comparisons between the minimum protective currents and the respective average currents are valid, namely, sites 71, 72, and 78, are seen to be of the same order of magnitude, the average currents being generally

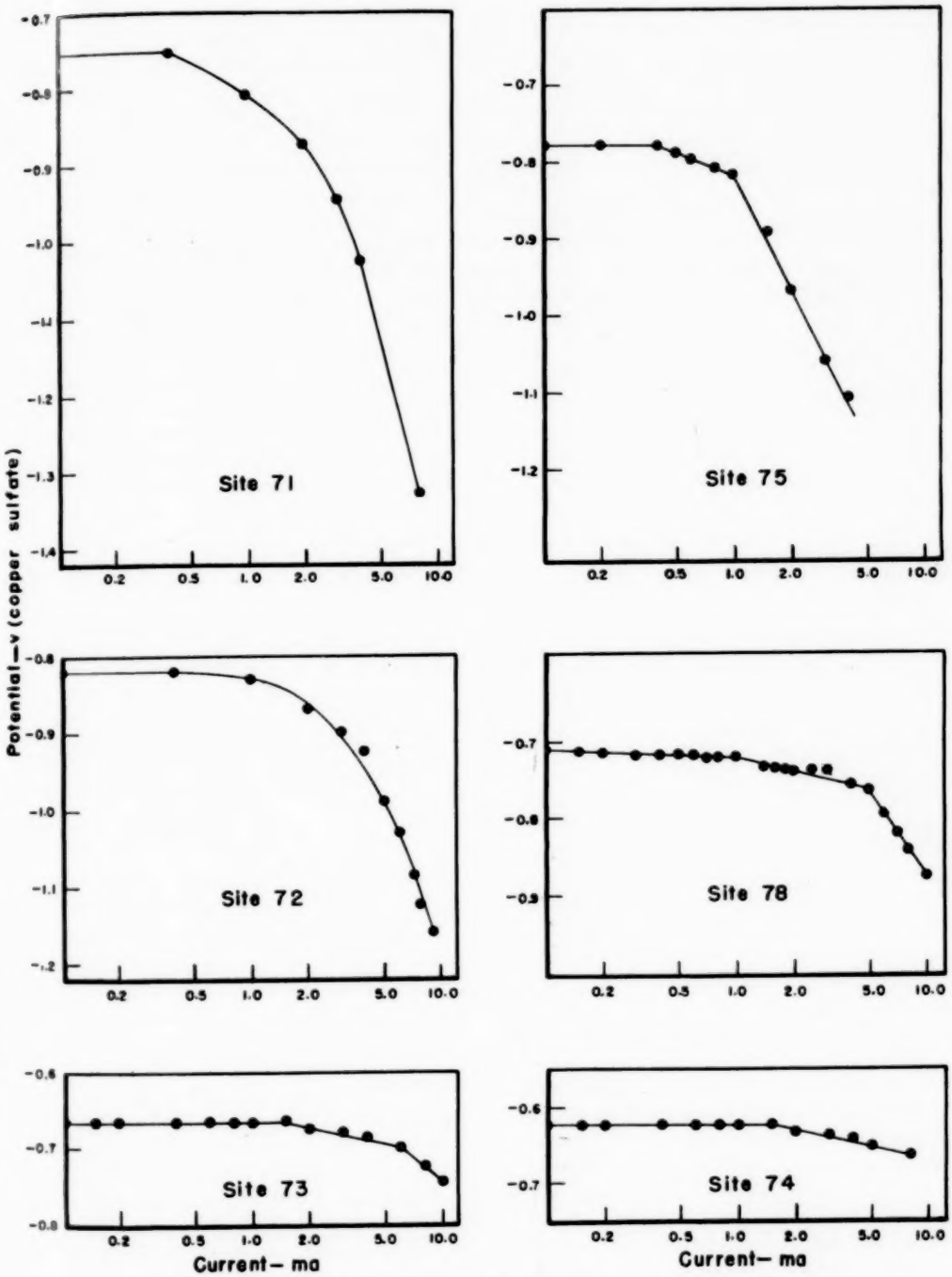

FIGURE 4. *Current-potential curves of the cathodes of the zinc-steel couples.*

TABLE 4. *Comparison of minimum protective currents as indicated by current-potential curves with calculated values as average current*

Site	Zinc-steel area ratio	Age of couple at time of measurement of protective current	Protective current	Average current calculated from—			Effectiveness of protection[a]
				Measurements of galvanic current	Loss of weight of zinc cylinders	Loss of weight of unconnected steel rings	
		Years	*ma*	*ma*	*ma*	*ma*	*Percent*
71	1:20	0.73	0.4	0.5	0.5	.....	77
	1:10	.73	.3	.7	.6	0.6	87
	1:6.7	.....	.....	.7	.8	.....	87
72	1:20	0.13, 3.01, 5.18	0.4, 2.4, 1.2	.4	.3	.....	.....
	1:10	.13, 3.01, 5.18	.8, 1.0, 1.0	.9	.7	1.2	89
	1:6.7	.13, 3.01, 5.18	1.2, 0.8, 0.7	1.4	.8	.....	89
73	1:20	5.83	1.5	.....	3.0	.....	86
	1:10	.....	.....	.....	2.2	4.4	99
	1:6.7	.....	.....	.....	4.2	.....	98
74	1:20	.....	.....	.....	0.6	0.5	98
	1:10	[b] 5.82	[b] 1.5	.....	[b] .5	.....	[b] 13
	1:6.7	.....	.....	.....	.5	.....	99
75	1:20	.....	.....	.....	3.7	.....	97
	1:10	5.80	0.4	.....	4.6	2.1	98
	1:6.7	.....	.....	.....	5.0	.....	99
78	1:20	0	1.0	1.8	1.3	.....	97
	1:10	.....	.....	2.1	1.4	2.4	99
	1:6.7	.....	.....	2.1	1.9	.....	98

[a] Based on weight of unconnected specimen.
[b] Couple found on open circuit.

somewhat greater than the respective minimum values, as would be expected. This general agreement between the minimum and average values of current does not necessarily mean that the point on the current-potential curve at which the potential of the cathode departs from the constant potential indicates the value of the applied current that is just sufficient to reduce the corrosion currents to zero. In fact, it is altogether possible that considerably higher currents might have been required to effect this result initially. Prevention of corrosion at values of applied current somewhat less than the initial corrosion currents could readily occur if current applied over a long period of time so reduced the corrosiveness of the environment that the minimum current requirement was correspondingly reduced. In other words, while possibly underestimating the quantity of current initially necessary to eliminate the current associated with corrosion, the method of estimating the protective current gives due weight to the current-time effect in reducing the current required for protection.

Evidence that the continuous application of current cathodically tends to reduce the current required for protection is afforded by the data for site 75 (table 4) in which it is seen that after nearly 6 years the protective current is only from one-tenth to one-fifth of the average current, depending on the data used in calculating the average currents. Even if the protective current reported for this site is considered to be indicated by the intersection of projections of the horizontal part and the straight section of greatest slope (fig. 4), the value of the protective current estimated in this manner would only be doubled. Other evidence of the reduction in the required current with time is afforded by the data for site 73, and to a certain extent by the data for site 72, although these latter data are somewhat inconsistent.

It is realized, of course, that the procedure of attempting to interpret current-potential curves in terms of calculated values of average current is approximate at best. A much more satisfactory procedure would be to apply to a group of experimental cathodes a series of currents, the values of which would be based on the apparent minimum protective current as obtained from a current-potential curve. As a matter of fact, two installations based on this procedure are in operation at the present time.

VI. Summary

The cathodic protection of steel by means of zinc anodes has been investigated in eight soils. The cathode of the experimental galvanic couple was a steel ring having an area of 48 sq in. to which were connected from one to three zinc anodes to provide different area ratios of zinc to steel. In six of the eight environments, corrosion of the steel cathodes was prevented over the test periods of from approximately 3 to 6 years, although a greater area of zinc was required in certain soil environments than in others. The soil conditions that tended to inhibit the corrosion of the zinc anodes galvanically were high resistivity and high alkalinity.

Measurements of electrode potentials are interpreted in terms of the extent to which cathodic protection was provided. The increase in potential, which resulted when one or more zinc anodes

were connected to the iron rings, was found to indicate prevention of corrosion only for those cathodes whose potentials were already strongly anodic with respect to the reference electrode. Cathodes whose open-circuit potentials were less anodic were not protected when connection to zinc anodes produced similar changes in potential.

The minimum protective currents as obtained from current-potential curves for the cathodes were of the same order of magnitude as the average current of the galvanic couples calculated from direct measurements of current, from the loss in weight of the zinc anodes, and from the loss in weight of the unconnected steel rings. The general agreement between these values of the average current is interpreted as indicating that in the environments studied no more current is required for protection than is equivalent to the loss in weight produced by normal corrosion.

The authors gratefully acknowledge the material assistance received from the following individuals who cooperated in this project, either by providing the test sites, assisting in the installation of the tests, making the various electrical measurements, or by offering helpful suggestions relative to various phases of the investigation: C. B. Abbot, Colorado Interstate Gas Co.; C. L. Brockschmidt, formerly of Mississippi River Fuel Corp.; M. V. Carmichael, Southern Natural Gas Co.; Guy Corfield, Southern California Gas Co.; R. F. Hadley, Susquehanna Pipe Line Co.; Charles Kasper, formerly of the National Bureau of Standards; K. H. Logan, Cast Iron Pipe Research Association; D. W. Martin, Public Service Co. of New Mexico; G. R. Olson, United Gas Pipe Line Co.; G. I. Rhodes, Ford, Bacon and Davis Co.; Charles Turner (deceased), East Ohio Gas Co.

The authors are especially indebted to K. H. Logan for installing the tests, to R. F. Hadley for making possible the frequent electrical measurements made at sites 71 and 72, and for use of special electrical equipment, and to Guy Corfield and G. R. Olson for the numerous electrical measurements which they provided.

VII. References

[1] G. I. Rhodes, Cathodic protection or electrical drainage of pipe lines, Monograph, Natural Gas Dept. Am. Gas Assn. (1935).
[2] C. L. Brockschmidt, Elec. News (Petroleum Ind. Elec. Assn.) **11,** 31 (1942).
[3] O. C. Mudd Elec. News (Petroleum Ind. Elec. Assn.) **13,** 11 (1943).
[4] H. W. Wahlquist, Corrosion **1,** 119 (1945).
[5] C. L. Morgan, Petroleum Engr. **16,** 196 (1945).
[6] Carl Hering, Trans. Am. Inst. Elec. Engrs. **31,** 1949 (1912).
[7] R. H. Brown, and R. B. Mears, Trans. Electrochem. Soc. **74,** 15 (1938).
[8] W. J. Muller, Trans. Electrochem. Soc. **76,** 167 (1939).
[9] R. B. Mears and R. H. Brown, Trans. Electrochem. Soc. **74,** 35 (1938).
[10] U. R. Evans, L. C. Bannister, and S. C. Britton, Proc. Royal Soc. (London) **131,** 355 (1931).
[11] J. M. Pearson, Trans. Electrochem. Soc. **81,** 485 (1942).
[12] S. Ewing, Proc. Am. Gas Assn. 613 (1940).
[13] A. Hickling, Trans. Faraday Soc. **33,** 1540 (1937).

Washington, October 24, 1947.

U. S. Department of Commerce
National Bureau of Standards

Research Paper RP1877
Volume 40, April 1948

Part of the Journal of Research of the National Bureau of Standards

Disintegration of Antimony-124

By Irving Feister and Leon F. Curtiss

The radiations from radio antimony of 60-day half-period Sb^{124}, have been investigated in a magnetic lens electron spectrometer. The beta-ray spectrum was found to have two components with maximum energies of 0.57 ±0.02 and 2.24 ±0.05 million electron volts. The gamma-ray spectrum has two lines, one at 0.60 ±0.01 and the other at 1.69 ±0.02. million electron volts. It appears quite certain that the 0.60 Mev gamma ray originates from Sb^{124}, and therefore these measurements substantiate the disintegration scheme proposed by Meyerhof and Scharff-Goldhaber [1],[1] with a small revision of energies.

I. Introduction

The radiations from 60-day Sb^{124} have been studied by several investigators. Hales and Jordan [2] used a 180° spectrometer to study the beta spectrum of Sb^{124}. They report the presence of two components with maximum energies at 0.74±0.03 and 2.45±0.07 million electron volts (Mev). Miller and Curtiss [3], using a thin magnetic lens spectrometer, also observed a complex beta spectrum, but with maximum energies at 0.53 and 2.25 Mev.

The most recent investigation of the beta and gamma radiations is that of Meyerhof and Scharff-Goldhaber [1] by means of coincidence-absorption measurements. They report the presence of two beta-ray components with energies of 0.7 and 2.4 Mev; and two gamma rays with energies of 0.6 and 1.7 Mev. A table summarizing the results of previous studies of Sb^{124} is also given by them.

Although the gamma radiations from Sb^{124} had been studied by a number of investigators prior to these authors, none of them had reported the presence of a 0.6-Mev gamma ray. With one exception, these prior reports indicated only one gamma ray with energy about 1.7 Mev. The present paper provides further information regarding the origin of this 0.6-Mev gamma ray.

The energies of the beta and gamma rays from Sb^{124} reported here were obtained by means of a spectrometer of the thin magnetic lens type. This instrument has been described by Miller and Curtiss [4]. The results obtained are in partial agreement with those previously reported, but differ significantly in certain respects. It is believed that the type of spectrometer used by the authors provides a more accurate determination of the Sb^{124} beta and gamma energies than can be obtained from absorption measurements such as used by Meyerhof and Scharff-Goldhaber [1].

II. Preparation of Sources

To obtain radioactive Sb^{124} for these experiments, a sample of antimony, estimated to be about 99.95 percent pure, was prepared at the Bureau of Standards. This sample was then sealed in a quartz capsule and irradiated with slow neutrons in the Clinton Laboratories pile at Oak Ridge, Tenn. Since ordinary antimony consists of about 56 percent of Sb^{121} and 44 percent of Sb^{123}, the resultant reactions Sb^{121} (n, γ) and Sb^{123} (n,γ) produce a mixture of 2.8-day Sb^{122} and 60-day Sb^{124} [5].

The preparation of the beta and gamma sources used in the spectrometer has been described in detail in a previous paper [6]. The same methods were used here. To prepare a beta source, the antimony crystals were first ground up with a Carboloy mortar and pestle to a fine powder. A small amount of this powder was then deposited on a thin aluminum foil moistened with dilute glyptal solution.

The gamma source was prepared by placing a relatively large amount of the antimony crystals

[1] Figures in brackets indicate the literature references at the end of this paper.

in a brass capsule, the opening of which was then sealed with Apiezon-Q wax. A radiator of uranium foil (42 mg/cm^2) was used to convert the gamma rays from Sb^{124} into photoelectrons whose energy can be measured in the spectrometer.

III. Beta-Ray Spectrum of Sb^{124}

The beta-ray spectrum was determined about 6 months after receipt of the source from Oak Ridge. The amount of 2.8-day Sb^{122} left after this long an interval is completely negligible, so that the remaining activity must be due to 60-day Sb^{124}. Figure 1 shows the beta spectrum obtained. The quantity N represents the relative intensity over equal intervals of $H\rho$ (gauss-cm). It is equal to the number of counts per minute in the Geiger-Müller counter divided by $H\rho$.

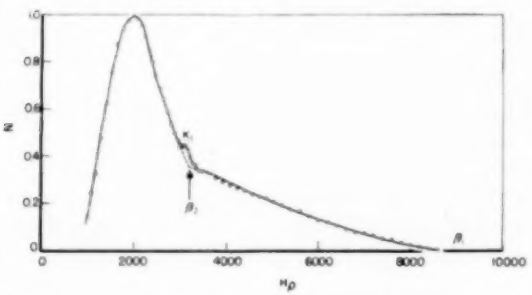

FIGURE 1. *Primary beta-ray spectrum of* Sb^{124} *showing the intensity plotted against* $H\rho$.

The K_1 peak is probably due to internal conversion electrons from a 0.60-Mev gamma ray.

The small K_1 peak in figure 1 is no doubt due to internal conversion electrons produced by a 0.60-Mev gamma ray, which will be discussed later. Omitting this peak, it is apparent that the beta spectrum of Sb^{124} consists of two components. The first part of the curve, up to the K_1 peak, is due to the sum of the two components; the remainder of the curve, beyond the K_1 peak, is due to the higher-energy component alone. Unfortunately, the K_1 peak occurs in the vicinity of the "break" in the beta distribution curve, which indicates the end point of the lower-energy beta-ray group. This tends to obscure the location of this end point.

If we neglect the K_1 peak, however, and extrapolate the parts of the curve immediately preceding and following this peak, their intersection is found to lie at $H\rho = 3{,}175 \pm 75$ gauss-cm. This corresponds to an energy of 0.57 ± 0.02 Mev. The higher-energy component approaches the $H\rho$ axis asymptotically, which makes its end point difficult to determine by direct inspection of figure 1. For this purpose, therefore, we make use of the Fermi plot shown in figure 2, which will be discussed in detail in section IV.

The Fermi plot again indicates clearly the presence of two beta-ray components. The K_1 peak of figure 1 has been omitted from figure 2, as indicated by the central broken portion of the curve. The extrapolated portions of this Fermi plot give the end points of the two beta components as 0.58 ± 0.02 Mev (in agreement with the value obtained from fig. 1) and 2.24 ± 0.05 Mev. These values are lower than those obtained by Hales and Jordan (0.74 and 2.45 Mev) [2], but agree within the limits of experimental error with those of Miller and Curtiss (0.53 and 2.25 Mev) [3].

The Fermi plot of figure 2 does not result in straight line curves, in contrast with the results of Hales and Jordan [2]. This, however, is not necessarily significant because of the following considerations:

1. The relatively long half-life of Sb^{124}, together with the high maximum energy of its beta spectrum, indicates that the transitions involved are

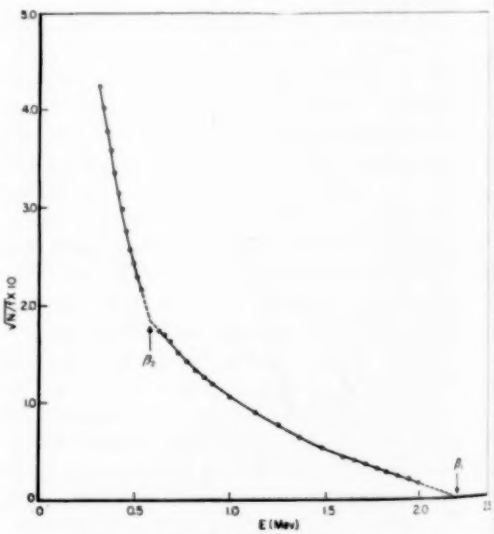

FIGURE 2. *Fermi plot of the data shown in figure 1.*

The original Fermi function $f(Z,\varphi)$ was evaluated for $Z=51$, not the usual Kurie approximation.

highly forbidden. The simple Fermi theory does not strictly apply to transitions of this type.

2. At the time the beta spectrum was measured the source had decayed through three half-lives, and its specific activity had decreased to about one-eighth of its initial value. Consequently, it was necessary to prepare a beta source whose thickness was such that the amount of absorption and scattering within the source cannot be considered entirely negligible. This would tend to distort the observed beta-ray spectrum.

IV. Fermi Plot

The plot in figure 2 is based on Fermi's theory of beta-ray emission. Starting with eq 42 of Fermi's paper [7], let

$$K=g^2\frac{256\pi^4}{[\Gamma(3+2S)]^2}\frac{m^5c^4}{h^7}\left(\frac{4\pi mc\rho}{h}\right)^{2S} \tag{1}$$

$$Q^*_{mn}=\int \psi_m^* u_n d\tau. \tag{2}$$

(See Fermi's paper for meaning of these expressions). For a given isotope, K is constant.

Also, we have

$$\sqrt{1+\eta_0^2}=E_0+1, \tag{3}$$

where

η_0 = maximum momentum of beta rays emitted in units of m_0c

E_0 = maximum energy of beta rays in units of m_0c^2

m_0 = rest mass of electron,

and similarly,

$$\sqrt{1+\eta^2}=E+1, \tag{4}$$

where η and E now refer to any electron with momentum η (equal to $H\rho/1700$) and energy E.

Substituting eq 1, 2, 3, and 4 in Fermi's eq 42, the probability of emission of an electron with momentum between η and $\eta+d\eta$ can be written

$$P(\eta)d\eta=K|Q^*|^2[\eta^2F(Z,\eta)](E_0-E)^2d\eta, \tag{5}$$

where

$$F(Z,\eta)=\eta^{2S}e^{\pi y}|\Gamma(1+S+iy)|^2 \tag{6}$$

$$S=\sqrt{1-\left(\frac{Z}{137}\right)^2}-1 \tag{7}$$

$$y=\frac{Z}{137}\frac{\sqrt{1+\eta^2}}{\eta}, \tag{8}$$

and Z is the atomic number.

According to Fermi, in case of "allowed" transitions the matrix element Q^* in eq 5 is of the order of unity. For "forbidden" transitions, however, $|Q^*|^2<<1$. In the latter case Q^* probably depends on the momentum η of the emitted beta rays, although the exact nature of this dependence is not known. As a first approximation, we shall assume that $|Q^*|^2$ is constant for all values of η.

Since the quantity N in the beta spectrum of figure 1 is proportional to $P(\eta)$, we have from eq 5

$$N\Delta\eta\propto f(Z,\eta)(E_0-E)^2\Delta\eta, \tag{9}$$

where

$$f(Z,\eta)=\eta^2F(Z,\eta). \tag{10}$$

Taking all the $\Delta\eta$'s equal throughout the beta spectrum, eq 9 may be written

$$\sqrt{\frac{N}{f}}\propto(E_0-E), \tag{11}$$

so that if we plot $\sqrt{N/f}$ against E, a straight-line curve is obtained which intersects the E axis at $E=E_0$. This graphical representation of the beta-ray spectrum is commonly referred to as a Fermi plot or Kurie plot, and is frequently used to determine the end point of a beta distribution.

It should be remembered, however, that eq 11 is based on the assumption that Q^* is independent of E, i. e.,

$$|Q^*|^2=\text{constant}. \tag{12}$$

For allowed transitions, eq 12 is true—at least approximately. For forbidden transitions, however, this is not necessarily true, and the Fermi plot need not be a straight line. Figure 2 indicates, therefore, that the beta transitions involved in the decay of Sb^{124} are of the forbidden type.

The Fermi function $f(Z,\eta)$ used in making a Fermi plot is given by eq 10 and 6. The factor $F(Z,\eta)$ in eq 5 is due to the effect of nuclear attraction upon the emitted beta ray. When $\eta>>Z/137$, $F(Z,\eta)\longrightarrow 1$. That is, for relatively high beta energies and light atoms, the effect of nuclear attraction is small.

A nonrelativistic treatment of the theory of beta emission leads to the expression

$$F(Z,\eta)=\frac{2\pi y}{1-e^{-2\pi y}}, \tag{13}$$

whereas the more rigorous relativistic theory leads to eq 6. According to Kurie, et al. [8], eq 13 is adequate for all light elements up to about

copper, $Z=29$ (provided η is not $>>1$). Hence in this case the Fermi function can be written

$$\left.\begin{aligned} f(Z,\eta)&=\eta^2\frac{2\pi y}{1-e^{-2\pi y}}\\ y&=\frac{Z}{137}\frac{\sqrt{1+\eta^2}}{\eta}\end{aligned}\right\} \tag{14}$$

For Sb^{124}, however, $Z=51$ and $\eta_0\cong 5$, so that the relativistic expression (eq 6) should be used. The Fermi function is then

$$f(Z,\eta)=\eta^{2+2S}e^{\pi y}|\Gamma(1+S+iy)|^2. \tag{15}$$

As $Z=51$, we have from eq 7

$$\left.\begin{aligned} \frac{Z}{137}&=0.37\\ S&=-0.072\\ 2+2S&=1.86\\ 1+S&=0.93\end{aligned}\right\} \tag{16}$$

The numerical values of $Z/137$ and S in eq 16 have been rounded off to two significant figures. Substituting from eq 16 in eq 15, we have for Sb^{124}

$$\left.\begin{aligned} f(\eta)&=\eta^{1.86}e^{\pi y}|\Gamma(0.93+iy)|^2\\ y&=0.37\frac{\sqrt{1+\eta^2}}{\eta}.\end{aligned}\right\} \tag{17}$$

This is the function that was used in the Fermi plot of figure 2. The values of $f(Z,\eta)$ obtained from eq 17 have been compared with the corresponding values given by the nonrelativistic expression (eq 14). It is worth noting that the differences between the two values vary from 0 to 15 percent for the range of momenta considered here.

V. Gamma-Ray Spectrum of Sb^{124}

The gamma-ray spectrum is shown in figure 3. The distribution represented by the full curve was obtained about 1 month after receipt of the source from Oak Ridge. The activity of the 2.8-day Sb^{122} had by this time decayed to less than 10^{-3} of its initial amount, and was therefore negligible in comparison with the 60-day Sb^{124} activity. The continuous distributions in figure 3 are due to Compton recoil electrons, mostly from the brass capsule containing the source; whereas the superimposed peaks are due to photoelectrons from the uranium radiator (the photoelectrons from the brass capsule are relatively negligible in number)[6].

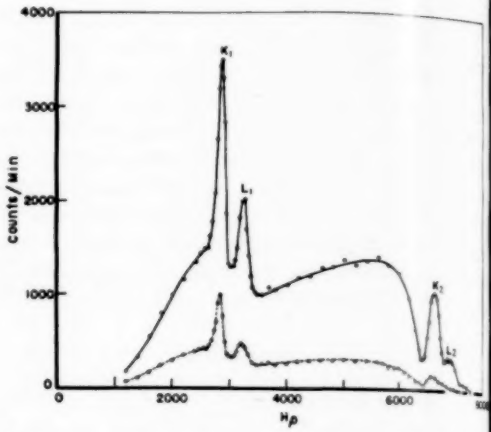

FIGURE 3. *Secondary electron spectrum produced by Sb gamma rays in uranium.*

K_1, L_1 are photoconversion lines of a 0.60-Mev gamma ray; K_2, L_2 are due to a 1.69-Mev gamma ray. Solid curve is gamma spectrum determined 1 month after preparation of source; broken curve is spectrum obtained months after preparation of source.

Figure 3 clearly shows the presence of two gamma rays, with energies of 0.60 ± 0.01 Mev and 1.69 ± 0.02 Mev. These values are obtained by adding the K-binding energy of uranium (0.113 Mev) to the energies of the K-photoelectrons ejected from the uranium radiator by the two gamma rays, as indicated by the location of the K_1 and K_2 peaks. A further check may be obtained by adding the L-binding energy of uranium (0.022 Mev) to the L-photoelectron energies indicated by the L_1 and L_2 peaks.

The energy of the 1.69 Mev gamma ray agrees within the limits of experimental error with the value 1.70 ± 0.02 Mev previously reported by Kruger and Ogle [9], and with the value 1.72 ± 0.03 Mev reported by Rall and Wilkinson [10]. The 0.60 Mev gamma ray, however, has not been reported by any investigators prior to Meyerhof and Scharff-Goldhaber [1]. This is difficult to understand, since figure 3 indicates that it is even more intense than the 1.69 Mev gamma ray.

Rall and Wilkinson [10] also reported a 0.61 Mev gamma ray, which they tentatively assigned to 30-day $Te^{122,124}$. Both half-life and identity of these isotopes were indicated as being in doubt.

This suggested the possibility that the 0.60 Mev gamma ray observed by us might be identical with the 0.61 Mev gamma ray reported by Rall and Wilkinson. To check this possibility, a chemical separation was made of the antimony and tellurium in the source about 9 months after its receipt from Oak Ridge. The separated tellurium fraction was then found to emit no detectable radiation. Had there been a 30-day $Te^{122,124}$ gamma activity in the tellurium fraction, it would almost certainly have been observed. We may safely conclude, therefore, that the 0.60 Mev gamma ray shown in figure 3 is not due to such an activity.

To determine whether the relative intensity of the 1.69 and 0.60 Mev gamma rays remains constant with time, the gamma spectrum was redetermined 4 months (2 half-lives of Sb^{124}) after its first measurement. This second determination is shown by the broken curve in figure 3. Comparison of the two curves indicates that the two gamma rays decay approximately at the same rate and are therefore probably both due to 60-day Sb^{124}.

VI. Disintegration Scheme of Sb^{124}

Meyerhof and Scharff-Goldhaber [1] have recently determined the relative intensities of the beta and gamma rays of Sb^{124} by means of Geiger-counter coincidences. Their measurements indicate that the relative intensity of the two beta-ray components is approximately 1:1, and that of the two gamma rays is about 2:1. According to them, the hard beta ray is followed by one gamma ray, whereas the soft beta ray is followed by two gamma rays. We were unable to make any accurate determination of relative beta- and gamma-ray intensities from our measurements. In general, however, the relative intensities indicated in figures 1 and 3 tend to agree with the values reported by these authors.

The beta- and gamma-ray energies determined by us, combined with the above data of Meyerhof and Scharff-Goldhaber, can be fitted into the disintegration scheme shown in figure 4. This is identical with the decay scheme proposed by them, except for the more accurate determination of the energies involved.

The authors thank E. W. Cannon and the Computation Laboratory of the National Bureau of Standards for the numerical evaluation of the original Fermi function for Z-51; and also A. Schwebel for the chemical separation of antimony and tellurium in the source.

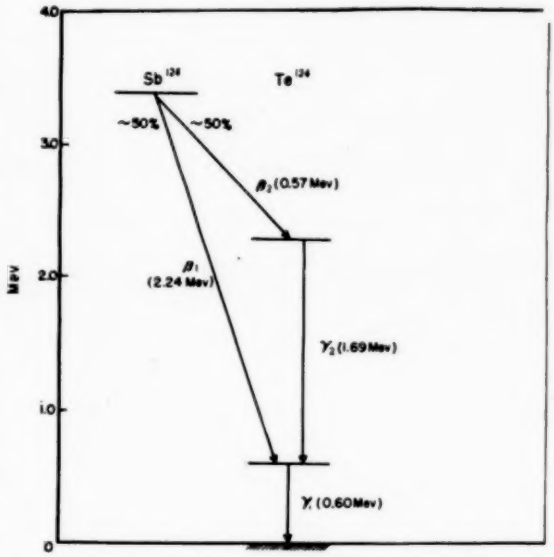

FIGURE 4. *Suggested disintegration scheme for* Sb^{124} *based on the observed beta- and gamma-ray spectra and on the coincidence measurements reported by Meyerhof and Scharff-Goldhaber* [1].

Beta transitions indicated above include energy equivalent of the electron mass.

VII. References

[1] W. E. Meyerhof and G. Scharff-Goldhaber, Phys. Rev. **72,** 273 (1947).
[2] E. B. Hales and E. B. Jordan, Phys. Rev. **64,** 202 (1943).
[3] L. C. Miller and L. F. Curtiss, Phys. Rev. **70,** 983 (1946).
[4] L. C. Miller and L. F. Curtiss, J. Research NBS **38,** 359 (1947) RP1778.
[5] J. J. Livingood and G. T. Seaborg, Phys. Rev. **55,** 414 (1939).
[6] I. Feister and L. F. Curtiss, J. Research NBS **38,** 411 (1947) RP1781.
[7] E. Fermi, Z. Physik **88,** 161 (1934).
[8] F. N. D. Kurie, J. R. Richardson, and H. C. Paxton, Phys. Rev. **49,** 368 (1936).
[9] P. G. Kruger and W. E. Ogle, Phys. Rev. **67,** 273 (1945).
[10] W. Rall and R. G. Wilkinson, Phys. Rev. **71,** 321 (1947).

WASHINGTON, October 22, 1947.

U. S. Department of Commerce
National Bureau of Standards

Research Paper RP1878
Volume 40, April 1948

Part of the Journal of Research of the National Bureau of Standards

Stabilization of Austenitic Stainless Steel

By Samuel J. Rosenberg and John H. Darr

A study was made of the resistance to intergranular attack of 23 18% Cr–10% Ni austenitic corrosion-resisting steels in 12 different initial conditions. Susceptibility to intergranular attack was determined after seven sensitizing treatments, followed by exposure for a maximum of 14 days in a boiling acidified copper sulfate solution.

It was found that maximum susceptibility to intergranular attack was developed by sensitizing either 8 or 21 days at 1,020° F. The straight carbon austenitic steels were quite vulnerable to attack, although decrease in carbon content decreased the degree of vulnerability. The columbium- and titanium-treated steels were satisfactorily resistant to attack provided the Cb/C or Ti/C ratios were sufficiently high. These ratios varied, depending on the initial condition of the steel. The carbon content of the treated steels had no influence upon the resistance to intergranular attack, the predominating factor being the Cb/C or Ti/C ratio.

I. Introduction

An undesirable characteristic of the austenitic stainless steels is their susceptibility to intergranular embrittlement after exposure to moderately elevated temperatures. This susceptibility to embrittlement may be decreased or eliminated, i. e., the steels may be stabilized against intergranular embrittlement, by the addition of titanium or columbium, usually in conjunction with a stabilizing heat treatment.

A diversity of opinion as to the relative amounts of titanium or columbium necessary for effective stabilization, the injurious effect of carbon content, and the necessity for stabilizing heat treatments, led the Bureau of Aeronautics, Navy Department, to request the National Bureau of Standards to undertake a study of factors affecting the stabilization of the 18–8 type of steels. This paper summarizes the results of such an investigation.

II. Theory of Sensitization and Stabilization

Intergranular embrittlement (or corrosion—the terms are usually used synonomously) may be considered as a disease of 18–8 steels, although it is not peculiar to these steels alone. Specifically, this type of corrosion is particularly pronounced in some 18–8 steels that have been subjected to moderately elevated temperatures (700° to 1,400° F) and are either simultaneously or subsequently subjected to corrosive conditions. Exposure to these elevated temperatures causes the precipitation of what are generally conceded to be chromium carbides at the grain boundaries, and steels having such carbide precipitation have been found to be more or less susceptible to intergranular corrosion, whereas steels that do not exhibit this structure are generally immune.

Annealed 18–8 stainless steel (quenched from temperatures in the neighborhood of 1,800° to 2,000° F) theoretically consists of metastable austenite, in this case a supersaturated solid solution of carbon or of chromium carbide in chromium-nickel austenite. Upon reheating to moderately elevated temperatures, chromium carbide (Cr_4C) precipitates at the grain boundaries. One school of thought believes that this precipitation reduces the chromium content of the metal near the grain boundaries to a level below that necessary to resist corrosion. This appears to be the most prevalent view. Others believe that internal strains resulting from the precipitation of carbides, and from the formation of alpha iron from the metastable austenite, are the cause of intergranular corrosion. Still another belief is

that the electrolytic effect resulting from a difference in potential between grains and grain boundaries is responsible. Regardless of the underlying theory, however, it is generally agreed that the presence of chromium carbides distributed in the form of a thin, nearly continuous network at the grain boundaries is an indication of material that is susceptible to intergranular corrosion. The larger isolated carbides that result after sufficient time at temperature has been allowed from coalescence of the precipitated carbides and for replenishment by diffusion of chromium in the depleted areas do not appear to be associated with intergranular corrosion.

The earliest efforts to prevent intergranular embrittlement were directed toward the manufacture of 18–8 with low carbon content on the theory that precipitation of chromium carbide would thereby be minimized or even eliminated [1, 2, 3].[1] It was also suggested that a treatment at about 1,600° F resulted in a decreased susceptibility to intergranular corrosion upon subsequent exposure at lower temperatures. This stabilizing (sometimes termed desensitizing) treatment was presumed to precipitate sufficient chromium carbides as coalesced particles, and also to permit diffusion of chromium, so that the amount of carbon that would be available to precipitate as fine chromium carbides at lower (sensitizing) temperatures would be negligible.

It was also reported that decreasing the austenitic grain size diminished the severity of intergranular attack [4] by providing extra grain boundary area for precipitation of carbides; that cold rolled material was more resistant to intergranular attack [3] because of the availability of numerous slip planes for the precipitation of carbides upon subsequent heating; and that the addition of elements that caused the formation of delta ferrite was also beneficial [5] in that, because of the lower solubility for carbides, precipitation occurred in the areas of delta ferrite.

The most commonly used method of preventing intergranular corrosion in 18–8 consists in adding a strongly carbide-forming element to the steel. The function of this element is to combine with the carbon, thus allowing the chromium to remain in solid solution in the austenite. To be effective this alloy carbide should be less soluble in the chromium-nickel austenite than is the chromium carbide. The two elements most frequently used are titanium and columbium [6, 7]. It is known that these elements are more strongly carbide forming than is chromium, and evidence is available that the titanium and columbium carbides are considerably less soluble in 18–8 austenite than is chromium carbide. Theoretically, if the carbon of 18–8 stainless steel is fixed by either of these stabilizing elements, that is, precipitated as TiC or CbC, no chromium carbide would precipitate at the grain boundaries upon subsequent reheating to sensitizing temperatures, and the steel thereafter would exhibit no intercrystalline embrittlement upon exposure to a corroding medium.

The atomic weight of carbon is 12.01, and that of titanium is 49.90, and since titanium forms a carbide corresponding to TiC, it is necessary, theoretically, to have about four times as much titanium as carbon in order to fix all the carbon as titanium carbide. Columbium has an atomic weight of 92.91, and as columbium forms a carbide corresponding to CbC, the theoretical minimum amount of columbium that must be added to fix the carbon is slightly less than eight times the amount of carbon.

Stabilization consists in reheating the Cb- or Ti-treated steels within the temperature range 1,550° to 1,800° F, usually at about 1,600° F. At these temperatures, the precipitation of titanium and columbium carbides within the austenitic grains is facilitated. The slight amount of carbon remaining in solid solution after this treatment is (theoretically) insufficient to cause any deleterious effects (in the form of Cr_4C precipitated at the grain boundaries) upon subsequent reheating to sensitizing temperatures.

III. Materials

Most of the steels used in this investigation were experimental melts, although a few commercial steels were included. The experimental steels were melted in an induction furnace and poured into 3-in. square big end up tapered molds equipped with hot tops. Each experimental heat weighed about 75 pounds, and all were made in the foundry of the Naval Research Laboratory. The ingots were shaped on all four sides as much as necessary to produce clean surfaces, following which they were hot forged to slabs about 3 in.

[1] Figures in brackets indicate the literature references at the end of this paper.

ide by 1 in. thick. Some of these ingots were rged at the Rustless Iron and Steel Division, merican Rolling Mill Co., Baltimore, Md.; all hers were forged at the Naval Research Laboratory. The slabs were surface ground on four sides nd rolled into 0.050-in. strip at the American olling Mill Co., Middletown, Ohio, the schedule f operations being as follows:

(1) Hot roll at 2,000° to 2,200° F to 0.125 in. and straighten.
(2) Anneal 6 minutes at 1,950° to 2,000° F and air cool.
(3) Pickle.
  (a) 2½ minutes in 10-percent H_2SO_4 at 190° F.
  (b) 45 minutes in caustic permanganate at 200° F.
  (c) 10 minutes in 1½-percent HF plus 10 percent HNO_3 at 130° F.
(4) Cold roll to 0.080 in. and straighten.
(5) Anneal 6 minutes at 1,950° to 2,000° F and air cool.
(6) Pickle.
  (b) and (c) only under (3) above.
(7) Cold roll to 0.050 in. and straighten.

The final strip thus had a cold reduction of 37½ ercent. Although the sequence of fabrication as not known, all commercial steels were rnished in cold rolled strips 0.050 in. thick, the me as the experimental steels.

Chemical analyses of all the steels were made on amples cut from the finished strip; these analyses re given in table 1. All experimental steels were ade to the base analysis of 18 percent chromium, 0 percent nickel, 1¼ percent manganese, and 40 percent silicon.

During the progress of this investigation a uestion was raised as to the effect of nitrogen on he Cb/C or Ti/C ratio. Analyses for nitrogen ere therefore made, both chemically and by acuum fusion. It is known that nitrogen combines with both titanium and columbium. The cid-soluble and acid-insoluble nitrogen can be eparated by treatment of the steel with dilute ulfuric acid. For purposes of calculation (as oted in table 1), it was assumed that all of the cid insoluble nitrogen was combined with either itanium or columbium, as the case might be. Considering the fact that the steels that contained o titanium or columbium also contained no acid insoluble nitrogen, this assumption appeared to be quite plausible. The revised percentages of titanium and columbium and the revised ratios of Ti/C and Cb/C were calculated after allowing for the amounts of titanium and columbium combined with the acid insoluble nitrogen and are included in table 1.

IV. Procedure

Specimens 3 in. long by ½ in. wide and 0.050 in. nominal thickness were taken longitudinally to the direction of rolling. A small hole was punched in one end of each specimen so that groups of specimens could be strung on wire for sensitizing treatments. All such treatments were carried out in furnaces of the vertical muffle type, electrically heated, and constructed especially for this work. The inside dimensions of the muffles were 4 in. diameter by 18 in. long. Temperature variations within the working length of each furnace were less than 10° F. Each furnace was controlled by an individual recording potentiometer controller.

Corrosion tests for development of intergranular embrittlement were conducted in a boiling acidified copper sulfate solution contained in 2-liter widemouthed Erlenmeyer flasks. These flasks were equipped with ground glass joints for fitting the reflux condensers. Specimens were laid in glass racks so that there was no metallic contact between specimens. No more than seven specimens were placed in an individual flask, and material of straight 18–10, 18–10 Cb, and 18–10 Ti was always segregated in different flasks. A minimum of 35 ml of acidified copper sulfate solution per square inch of surface area was used. The solution was changed every 48 hours at which time all specimens were examined; those showing definite evidence of intergranular attack were removed. Where evidence of attack, as indicated by a change in color of the solution, occurred in less than 2 days, the run was interrupted to remove the failed specimen or specimens, and the solution was changed. Maximum time of exposure in the acidified copper sulfate solution was 14 days.

Preliminary tests indicated the necessity of carefully controlling certain factors. The original choice of concentration for the boiling copper sulfate–sulfuric acid solution was 13 g of

TABLE 1. *Analyses of the test steels*

Steels designated by the prefix "S" are laboratory melts; those designated by the prefix "C" are commercial melts.

Steel No.	Percentage of—							Ratio		Percentage of nitrogen (vacuum fusion)	Percentage of nitrogen (chemical analysis)			Percentage (revised)[a]		Ratio (revised)[a]	
	C	Mn	Si	Cr	Ni	Cb	Ti	Cb/C	Ti/C		Total	Acid soluble	Acid insoluble (by difference)	Cb	Ti	Cb/C	Ti/C
C–1	0.025	0.70	0.50	19.7	8.8					0.041	0.039	0.039	0.000				
C–10	.026	.59	.40	17.2	12.6					.026	.026	.025	.001				
S–37	.044	1.10	.33	17.8	10.5					.049	.053	.053	.000				
S–4	.072	1.13	.45	18.0	10.2					.036	.036	.035	.001				
S–23	.113	1.11	.37	17.6	10.2					.041	.039	.039	.000				
S–26	.068	1.21	.37	17.8	10.0	0.50		7.4		.065	.061	.041	.020	0.37		5.4	
S–6	.070	1.23	.54	17.6	10.1	.61		8.7		.056	.054	.034	.020	.48		6.9	
S–12	.074	1.23	.38	17.9	10.0	.75		10.1		.051	.047	.024	.023	.60		8.1	
C–3	.090	1.69	.67	17.7	11.0	.71		11.8		.032	.035	.015	.020	.58		9.7	
S–27	.087	1.19	.40	17.8	10.1	.76		8.7		.059	.057	.030	.027	.58		6.7	
S–28	.115	1.22	.40	17.7	9.9	.92		8.0		.045	.045	.022	.023	.77		6.7	
S–17	.117	1.21	.40	18.0	10.1	1.14		9.7		.039	.040	.016	.024	.98		8.3	
S–18	.132	1.18	.40	17.9	10.1	1.47		11.1		.044	.046	.014	.032	1.26		9.5	
S–34	.067	1.17	.45	17.7	10.2		0.26		3.9	.031	.039	.001	.038		0.13		1.9
S–21	.071	1.49	.41	17.9	10.1		.32		4.5	.027	.031	.002	.029		.22		3.1
C–6	.064	1.32	.40	18.3	10.0		.35		5.5	.012	.013	.002	.011		.31		4.8
S–39	.065	1.23	.53	18.2	10.1		.36		5.5	.023	.023	.001	.022		.28		4.3
C–2	.070	1.52	.50	17.8	9.6		.50		7.1	.010	.010	.001	.009		.47		6.7
C–8	.075	1.25	.52	18.0	10.6		.59		7.9	.006	.007	.001	.006		.57		7.6
S–25	.082	1.23	.40	17.7	9.9		.37		4.5	.017	.022	.001	.021		.30		3.7
S–35	.107	1.29	.42	17.5	9.7		.44		4.1	.012	.016	.001	.015		.39		3.6
S–36	.109	1.35	.48	17.5	10.0		.54		5.0	.022	.018	.001	.017		.48		4.4
S–32	.105	1.44	.40	18.0	9.9		.61		5.8	.016	.017	.001	.016		.56		5.3

[a] The revised percentages of Ti and Cb were calculated by assuming that all of the acid insoluble nitrogen was combined as TiN or CbN. According to the atomic weights of these elements, 1 part of nitrogen will combine with 3.43 parts of titanium or 6.64 parts of columbium by weight. Multiplying these figures by the amount of acid insoluble nitrogen in the titanium- and columbium-treated steels, respectively, and subtracting the results from the amounts of titanium and columbium present in the steels gives the revised amounts of titanium or columbium available for combination with carbon. The revised Ti/C and Cb/C ratios were then obtained by dividing the revised percentages of titanium and columbium by the carbon contents.

$CuSO_4 \cdot 5H_2O$, 47 ml of concentrated H_2SO_4, and distilled water to make 1 liter of solution. This solution, which has been used by some investigators, corresponded to 0.8 percent of $CuSO_4$ and 8.2 percent of H_2SO_4, and the ratio of $CuSO_4$ to H_2SO_4 proved too low to prevent surface corrosion in many of the steels. Since the resultant corrosion complicated the evaluation of intergranular embrittlement, this solution was discarded in favor of that containing 100 g of $CuSO_4 \cdot 5H_2O$, 100 ml of concentrated H_2SO_4 (sp gr 1.84), and 900 ml of distilled water. This solution corresponded to 5.4 percent of $CuSO_4$ and 15.4 percent of H_2SO_4 by weight.

The scale that formed on specimens during sensitization was influenced by both time and temperature. In order to eliminate the variable which scale would introduce, it was decided to remove all scale. Polishing was tried and proved to be too time-consuming; pickling was therefore adopted with a schedule of operations as follows: (1) Pickle in 8 percent H_2SO_4+4 percent HCl at 160° F for 10 minutes; wash, scrub, and dry; (2) pickle in 10 percent HNO_3+1 percent HF at 160° F for 5 minutes; wash, scrub, and dry; (3) passivate in 20 percent HNO_3 at 125° F for 15 minutes; wash and dry.

To ascertain whether the method of scale removal influenced the susceptibility to intergranular attack, check tests were made on certain specimens both as pickled and as polished. These tests showed that the method of scale removal

nd no detectable effect on the specimens that ere extremely vulnerable to intergranular embrittlement. With specimens that were moderately vulnerable, it appeared that the extent of ntergranular attack was greater in specimens hat had been pickled than in specimens that has een polished. Typical microstructures of such pecimens after corrosion are shown in figure 1. ince it is frequently commercial practice to nish stainless steels by pickling, it appeared gical to test the steels as finished in that manner.

The susceptibility to intergranular attack of he various steels was determined for 12 different itial conditions, as listed in tables 2 to 24. A w steels were tested in only five different initial onditions, as may be seen from the particular ble involved.

In the first series of tests (carried out on the cold olled steels), specimens from each steel were sted in 16 sensitized conditions. Four sensitizg temperatures were used —840°, 1,020°, 1,200°, nd 1,380° F. Single specimens were held at each ensitizing temperature for 2 hours, 2, 8, and 21 ays. After exposure to the boiling copper sulfate olution, it was apparent that certain of these ensitizing treatments were quite innocuous and ould be discarded. It was decided, therefore, o decrease the number of sensitizing conditions o seven in all—these were 21 days at 840° F; hours, 2, 8, and 21 days at 1,020° F; and 2 hours nd 2 days at 1,200° F. A control specimen, not ensitized, was included in each series.

Evaluation of intergranular embrittlement was ade by observations of: (a) change in electrical esistivity, (b) loss in metallic ring when the test pecimen was dropped on a steel plate, (c) extent f cracks occurring after bend tests of 180°, and d) appearance of the corroded sections under the icroscope. The interpretation of these various sts was frequently influenced by the personal ctor, particularly in cases where only slight vidence of failure existed. Frequently, also, vidence of failure by one method was not corroborated by another.

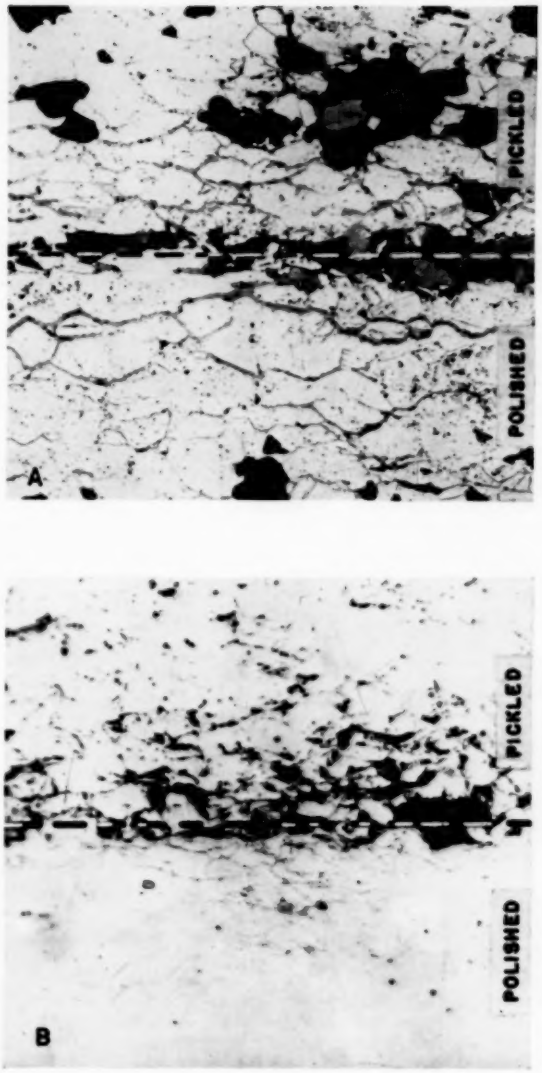

FIGURE 1. *Effect of method of scale removal on susceptibility to intergranular attack.*

A, Extremely vulnerable material after 2 days in the boiling acidified copper sulfate solution. Unetched. ×100. *B*, Less vulnerable material after 6 days in the boiling acidified copper sulfate solution. Unetched. ×500.

778365—48——5

TABLE 2. *Effects of various treatments upon the susceptibility to intergranular attack of steel C–7*

(Carbon=0.025%—no stabilizing element)

Treatment of steel subsequent to cold-rolling		Sensitizing treatment							
Annealing	Stabilizing	None	21 days at 840° F	2 hours at 1,020° F	2 days at 1,020° F	8 days at 1,020° F	21 days at 1,020° F	2 hours at 1,200° F	2 days at 1,200° F
None	None	A	A	A	D−	E+	D−	A	A
Do	½ hour at 1,600° F, A. C	A	A−	A	C	D−	D−	A	A
½ hour at 1,800° F, W. Q	None	A	A	A	DE	DE	E	A−	A
Do	½ hour at 1,600° F, A. C	A	A	A	B	DE	E+	A	A
Do	2 hours at 1,600° F, A. C	A	A−	A	B	DE	DE	A−	A
½ hour at 1,800° F, A. C	None	A	A	A	C−	D	CD	A−	A
Do	1 hour at 1,600° F, A. C	A	A	A	C−	D	D	A	A−
3 min. at 1,975° F, W. Q	None	A	A	A	CD	D	CD	A	A
Do	1 hour at 1,600° F, A. C	A	A	A	BC	CD	CD	A	A
3 min at 1,975° F, A. C	None	A	A	A	B−	DE	C	A	A
Do	½ hour at 1,600° F, A. C	A	A	A	D+	D	D	A	A−
Do	2 hours at 1,600° F, A. C	A	A	A	C−	D−	D+	A−	A−

TABLE 3. *Effect of various treatments upon the susceptibility to intergranular attack of steel C–10*

(Carbon=0.026%—no stabilizing element)

Treatment of steel subsequent to cold-rolling		Sensitizing treatment							
Annealing	Stabilizing	None	21 days at 840° F	2 hours at 1,020° F	2 days at 1,020° F	8 days at 1,020° F	21 days at 1,020° F	2 hours at 1,200° F	2 days at 1,200° F
None	None	A	B+	A	B−	A	A−	A−	A
Do	½ hour at 1,600° F, A. C	A	A	A−	DE	E	E	A−	B−
½ hour at 1,800° F, W. Q	None	A−	A	A	E+	E	E	AB	C−
Do	½ hour at 1,600° F, A. C	A	A	A	E+	E	E	A	B−
Do	2 hours at 1,600° F, A. C	A−	A	A	E+	E	E	A−	BC
½ hour at 1,800° F, A. C	None	A	A	A	E+	E	E	AB	CD
Do	1 hour at 1,600° F, A. C	A	A	A	E	E	E	AB	C
3 min at 1,975° F, W. Q	None	A	A	A	E	E	E	A−	A−
Do	1 hour at 1,600° F, A. C	A	A	A	E+	E	E	A−	BC
3 min at 1,975° F, A. C	None	A	A	A	D+	E	E	A	BC
Do	½ hour at 1,600° F, A. C	A	A	A	D+	E	E	A	C−
Do	2 hours at 1,600° F, A. C	A	A	A	D	E	E	A	C−

TABLE 4. *Effect of various treatments upon the susceptibility to intergranular attack of steel S–37*

(Carbon=0.044%—no stabilizing element)

Treatment of steel subsequent to cold-rolling		Sensitizing treatment							
Annealing	Stabilizing	None	21 days at 840° F	2 hours at 1,020° F	2 days at 1,020° F	8 days at 1,020° F	21 days at 1,020° F	2 hours at 1,200° F	2 days at 1,200° F
None	None	A	AB	A	E+	E	D+	AB	A
Do	½ hour at 1,600° F, A. C	A	D	AB	E	E	E	B+	A
½ hour at 1,800° F, W. Q	None	A	A−	A	E+	E	E	D+	D−
Do	½ hour at 1,600° F, A. C	A	A	A−	DE	E	E	A	E
Do	2 hours at 1,600° F, A. C	A	A−	A−	CD	E	E	BC	D

TABLE 5. *Effect of various treatments upon the susceptibility to intergranular attack of steel S–4*

(Carbon=0.072%—no stabilizing element)

Treatment of steel subsequent to cold-rolling		Sensitizing treatment							
Annealing	Stabilizing	None	21 days at 840° F	2 hours at 1,020° F	2 days at 1,020° F	8 days at 1,020° F	21 days at 1,020° F	2 hours at 1,200° F	2 days at 1,200° F
None	None	A	D+	DE	E	E	E	E	A
Do	½ hour at 1,600° F, A. C	B	E	E	E	E	E	CD	A
½ hour at 1,800° F, W. Q	None	A	A−	A	E	E	E	E	E
Do	½ hour at 1,600° F, A. C	DE	E	E	E	E	E	E	E
Do	2 hours at 1,600° F. A. C	D	E	E	E	E	E	E	E+
½ hour at 1,800° F, A. C	None	A	D	A	E	E	E	E	E
Do	1 hour at 1,600° F, A. C	C−	F	E	E	E	E	E	D
3 min at 1,975° F, W. Q	None	A	A	A	DE	E	E	E	E
Do	1 hour at 1,600° F, A. C	D	E	E+	E	E+	E+	DE	E
3 min at 1,975° F, A. C	None	A	A	A	D	E	E	E	E
Do	½ hour at 1,600° F, A. C	C	D	D	E	E	E	E	E
Do	2 hours at 1,600° F, A. C	C+	E+	E+	E+	E	E	E	E

TABLE 6. *Effect of various treatments upon the susceptibility to intergranular attack of steel S–23*

(Carbon=0.113%—no stabilizing element)

Treatment of steel subsequent to cold-rolling		Sensitizing treatment							
Annealing	Stabilizing	None	21 days at 840° F	2 hours at 1,020° F	2 days at 1,020° F	8 days at 1,020° F	21 days at 1,020° F	2 hours at 1,200° F	2 days at 1,200° F
None	None	A	D	DE	E	E	E	E	A
Do	½ hour at 1,600° F, A. C	C+	E	E	E+	E	E+	D	A
½ hour at 1,800° F, W. Q	None	A	B+	D+	E	E	E	E	E
Do	½ hour at 1,600° F, A. C	E+	E+	E	E+	E+	E	E	E
Do	2 hours at 1,600° F, A. C	D	E	E	E	E	E+	E	BC

TABLE 7. *Effect of various treatments upon the susceptibility to intergranular attack of steel S–26*

(Carbon=0.068%, columbium=0.50%; Cb/C=7.4)

Treatment of steel subsequent to cold-rolling		Sensitizing treatment							
Annealing	Stabilizing	None	21 days at 840° F	2 hours at 1,020° F	2 days at 1,020° F	8 days at 1,020° F	21 days at 1,020° F	2 hours at 1,200° F	2 days at 1,200° F
None	None	A	B+	A−	D	B+	A	A	A
Do	½ hour at 1600° F, A. C	A	A	A	D	DE	D+	A	A
½ hour at 1,800° F, W. Q	None	A	A	A	E+	E	E	A	A
Do	½ hour at 1,600° F, A. C	A	A	A	D	E+	E+	A	A
Do	2 hours at 1,600° F, A. C	A	A	A	D+	E+	E	A	A
½ hour at 1,800° F, A. C	None	A	A	A	DE	E	E+	AB	A
Do	1 hour at 1,600° F, A. C	A	A	A	E+	E+	E+	A−	A
3 min at 1,975° F, W. Q	None	A	A	A	C−	E	E	BC	A−
Do	1 hour at 1,600° F, A. C	A	A	A	D	DE	D	A−	A
3 min at 1,975° F, A. C	None	A	A	A	E+	E+	E	A	A−
Do	½ hour at 1,600° F, A. C	A	A	A	DE	E	E+	A−	A−
Do	2 hours at 1,600° F, A. C	A	A	A	D−	E	E+	A−	A−

TABLE 8. *Effect of various treatments upon the susceptibility to intergranular attack of steel S–6*

(Carbon=0.070%, columbium=0.61%; Cb/C=8.7)

Treatment of steel subsequent to cold-rolling		Sensitizing treatment							
Annealing	Stabilizing	None	21 days at 840° F	2 hours at 1,020° F	2 days at 1,020° F	8 days at 1,020° F	21 days at 1,020° F	2 hours at 1,200° F	2 days at 1,200° F
None	None	A	B	AB	B+	AB	AB	A–	A
Do	½ hour at 1,600° F, A. C	A	A	A	C–	C–	B	A	A
½ hour at 1,800° F, W. Q	None	A	A	A	C+	D–	E+	A	A
Do	½ hour at 1,600° F, A. C	A	A	A	D+	E+	E+	A	A
Do	2 hours at 1,600° F, A. C	A	A	A	C–	E+	D–	A	A
½ hour at 1,800° F, A. C	None	A	A	A	BC	D	C	A	A
Do	1 hour at 1,600° F, A. C	A	A	A	D	D–	D–	A	A
3 min at 1,975° F, W. Q	None	A	A	A	B+	E	E	A	A
Do	1 hour at 1,600° F, A. C	A	A	A	C	E	D	A	A
3 min at 1,975° F, A. C	None	A	A	A	C	DE	E+	A–	A–
Do	½ hour at 1,600° F, A. C	A	A	A	D	E+	E	A–	A–
Do	2 hours at 1,600° F, A. C	A	A	A	DE	DE	E	A	A–

TABLE 9. *Effect of various treatments upon the susceptibility to intergranular attack of steel S–12*

(Carbon=0.074%, columbium=0.75%; Cb/C=10.1)

Treatment of steel subsequent to cold-rolling		Sensitizing treatment							
Annealing	Stabilizing	None	21 days at 840° F	2 hours at 1,020° F	2 days at 1,020° F	8 days at 1,020° F	21 days at 1,020° F	2 hours at 1,200° F	2 days at 1,200° F
None	None	A	AB	A–	B+	A	A–	A	A
Do	½ hour at 1,600° F, A. C	A	A	A	A	A	A	A	A
½ hour at 1,800° F, W. Q	None	A	A	A	A	A	A–	A	A
Do	½ hour at 1,600° F, A. C	A	A	A	A	A	A–	A	A
Do	2 hours at 1,600° F, A. C	A	A	A	A	A	A	A	A
½ hour at 1,800° F, A. C	None	A	A	A	A	A–	A–	A	A
Do	1 hour at 1,600° F, A. C	A	A	A	B+	B	B–	A–	A
3 min at 1,975° F, W. Q	None	A	A	A	A	B	D+	A	A
Do	1 hour at 1,600° F, A. C	A	A	A	B+	B	B	A	A
3 min at 1,975° F, A. C	None	A	A	A	A–	AB	C–	A	A
Do	½ hour at 1,600° F, A. C	A	A	A	AB	C–	C	A	A
Do	2 hours at 1,600° F, A. C	A	A	A	C+	C	C	A	A–

TABLE 10. *Effect of various treatments upon the susceptibility to intergranular attack of steel C–3*

(Carbon=0.060%, columbium=0.71%; Cb/C=11.8)

Treatment of steel subsequent to cold-rolling		Sensitizing treatment							
Annealing	Stabilizing	None	21 days at 840° F	2 hours at 1,020° F	2 days at 1,020° F	8 days at 1,020° F	21 days at 1,020° F	2 hours at 1,200° F	2 days at 1,200° F
None	None	A	A–	A	A	A	A–	A	A–
Do	½ hour at 1,600° F, A. C	A	A	A	A	A	A	A	A
½ hour at 1,800° F, W. Q	None	A	A	A	A	A	A	A	A
Do	½ hour at 1,600° F, A. C	A	A	A	A	A–	A–	A	A
Do	2 hours at 1,600° F, A. C	A	A	A	A	A	A	A	A
½ hour at 1,800° F, A. C	None	A	A	A	A	A	A	A	A
Do	1 hour at 1,600° F, A. C	A	A	A	A	A–	A–	A–	A
3 min at 1,975° F, W. Q	None	A	A	A	A	A	A	A	A
Do	1 hour at 1,600° F, A. C	A	A	A	A	A	A	A	A
3 min at 1,975° F, A. C	None	A	A	A	A	A	A	A–	A
Do	½ hour at 1,600° F, A. C	A	A	A	A	A	A	A	A
Do	2 hours at 1,600° F, A. C	A	A	A	A	A	A	A	A

TABLE 11. *Effect of various treatments upon the susceptibility to intergranular attack of steel S–27*

(Carbon=0.087%, columbium=0.76%; Cb/C=8.7)

Treatment of steel subsequent to cold-rolling		Sensitizing treatment							
Annealing	Stabilizing	None	21 days at 840° F	2 hours at 1,020° F	2 days at 1,020° F	8 days at 1,020° F	21 days at 1,020° F	2 hours at 1,200° F	2 days at 1,200° F
None	None	A	B+	A	B	A	A	A−	A
Do	½ hour at 1,600° F, A. C	A	A	A	C−	C	AB	A	A
½ hour at 1,800° F, W. Q	None	A	A	A	D	DE	E+	A	A
Do	½ hour at 1,600° F, A. C	A	A	A	D	E+	E+	A	A
Do	2 hours at 1,600° F, A. C	A	A	A	CD	E+	D	A	A

TABLE 12. *Effect of various treatments upon the susceptibility to intergranular attack of steel S–28*

(Carbon=0.115%, columbium=0.92%; Cb/C=8.0)

Treatment of steel subsequent to cold-rolling		Sensitizing treatment							
Annealing	Stabilizing	None	21 days at 840° F	2 hours at 1,020° F	2 days at 1,020° F	8 days at 1,020° F	21 days at 1,020° F	2 hours at 1,200° F	2 days at 1,200° F
None	None	A	B	A−	C−	B+	A−	A−	A
Do	½ hour at 1,600° F, A. C	A	A	A	D+	D+	BC	A	A
½ hour at 1,800° F, W. Q	None	A	A	A	DE	E	E	A	A
Do	½ hour at 1,600° F, A. C	A	A	A	D	E+	E+	A	A
Do	2 hours at 1,600° F, A. C	A	A	A	C−	E+	DE	A	A
½ hour at 1,800° F, A. C	None	A	A	A	DE	DE	E+	A−	A
Do	1 hour at 1,600° F, A. C	A	A	A	D	DE	D−	B+	A
3 min at 1,975° F, W. Q	None	A	A	A	D+	E	E	B−	A
Do	1 hour at 1,600° F, A. C	A	A	A	CD	E	C−	A−	A
3 min at 1,975° F, A. C	None	A	A	A	E+	DE	E	A−	A
Do	½ hour at 1,600° F, A. C	A	A	A	D−	E+	E+	A−	A
Do	2 hours at 1,600° F, A. C	A	A	A	E+	E+	DE	A−	A−

TABLE 13. *Effect of various treatments upon the susceptibility to intergranular attack of steel S–17*

(Carbon=0.117%, columbium=1.14%; Cb/C=9.7)

Treatment of steel subsequent to cold-rolling		Sensitizing treatment							
Annealing	Stabilizing	None	21 days at 840° F	2 hours at 1,020° F	2 days at 1,020° F	8 days at 1,020° F	21 days at 1,020° F	2 hours at 1,200° F	2 days at 1,200° F
None	None	A	B+	A−	AB	AB	A−	A	A
Do	½ hour at 1,600° F, A. C	A	A	A	A	A	A	A	A
½ hour at 1,800° F, W. Q	None	A	A	A	A	A	B+	A	A
Do	½ hour at 1,600° F, A. C	A	A	A	AB	B	AB	A	A
Do	2 hours at 1,600° F, A. C	A	A	A	A	A	A	A	A
½ hour at 1,800° F, A. C	None	A	A	A	A	AB	A	A	A
Do	1 hour at 1,600° F, A. C	A	A	A	BC	BC	B+	A	A
3 min at 1,975° F, W. Q	None	A	A	A	A−	C+	D+	A	A
Do	1 hour at 1,600° F, A. C	A	A	A	B+	B	B	A	A
3 min at 1,975° F, A. C	None	A	A	A	A−	B−	CD	A	A
Do	½ hour at 1,600° F, A. C	A	A	A	B+	D	C	A−	A
Do	2 hours at 1,600° F, A. C	A	A	A	C−	C	C	A−	A−

TABLE 14. *Effect of various treatments upon the susceptibility to intergranular attack of steel S–18*

(Carbon = 0.132%, columbium = 1.47%; Cb/C = 11.1)

Treatment of steel subsequent to cold-rolling		Sensitizing treatment							
Annealing	Stabilizing	None	21 days at 840° F	2 hours at 1,020° F	2 days at 1,020° F	8 days at 1,020° F	21 days at 1,020° F	2 hours at 1,200° F	2 days at 1,200° F
None	None	A	A	A	A−	A−	A−	A−	A
Do	½ hour at 1,600° F, A. C	A	A	A	A	A	A	A	A
½ hour at 1,800° F, W. Q	None	A	A	A	A	A	A−	A	A
Do	½ hour at 1,600° F, A. C	A	A	A	A	A	A−	A	A
Do	2 hours at 1,600° F, A. C	A	A	A	A	A	A	A	A
½ hour at 1,800° F, A. C	None	A	A	A	A	A	A	A	A
Do	1 hour at 1,600° F, A. C	A	A	A	A−	B+	A−	A	A
3 min at 1,975° F, W. Q	None	A	A	A	A	A	B	A	A
Do	1 hour at 1,600° F, A. C	A	A	A	A	A−	A−	A	A
3 min at 1,975° F, A. C	None	A	A	A	A−	A−	B+	A	A
Do	½ hour at 1,600° F, A. C	A	A	A	A	B+	B	A	A
Do	2 hours at 1,600° F, A. C	A	A	A	A	A−	A−	A	A

TABLE 15. *Effect of various treatments upon the susceptibility to intergranular attack of steel S–34*

(Carbon = 0.067%, titanium = 0.26%; Ti/C = 3.9)

Treatment of steel subsequent to cold-rolling		Sensitizing treatment							
Annealing	Stabilizing	None	21 days at 840° F	2 hours at 1,020° F	2 days at 1,020° F	8 days at 1,020° F	21 days at 1,020° F	2 hours at 1,200° F	2 days at 1,200° F
None	None	A	C+	B	D−	E+	DE	B+	A
Do	½ hour at 1,600° F, A. C	A	E+	D	E	E	E+	A−	A
½ hour at 1,800° F, W. Q	None	A	A	A	E	E	E	DE	C−
Do	½ hour at 1,600° F, A. C	A	E	D	E	E	E	B	B
Do	2 hours at 1,600° F, A. C	A	D	D+	E	E	E	C+	A−
½ hour at 1,800° F, A. C	None	A	A	A	E	E	E	DE	CD
Do	1 hour at 1,600° F, A. C	A	C	B−	E	E	E	C+	A
3 min at 1,975° F, W. Q	None	A	A	A	C+	E	E	E+	F
Do	1 hour at 1,600° F, A. C	AB	D+	CD	E+	E	E	C−	D+
3 min at 1,975° F, A. C	None	A	A	A	B−	E+	E	E+	F
Do	½ hour at 1,600° F, A. C	A	BC	B+	E	E	E	C	F
Do	2 hours at 1,600° F, A. C	A−	B−	B−	DE	E	E	C+	CD

TABLE 16. *Effect of various treatments upon the susceptibility to intergranular attack of steel S–21*

(Carbon = 0.071%, titanium = 0.32%; Ti/C = 4.5)

Treatment of steel subsequent to cold-rolling		Sensitizing treatment							
Annealing	Stabilizing	None	21 days at 840° F	2 hours at 1,020° F	2 days at 1,020° F	8 days at 1,020° F	21 days at 1,020° F	2 hours at 1,200° F	2 days at 1,200° F
None	None	A	C−	B	D	DE	D	B+	A
Do	½ hour at 1,600° F, A. C	A	AB	AB	E+	E+	E+	A−	A
½ hour at 1,800° F, W. Q	None	A	A	A	E	E	E	D	A−
Do	½ hour at 1,600° F, A. C	A	CD	B	E	E	E	A	A
Do	2 hours at 1,600° F, A. C	A	A−	AB	E+	E+	E	AB	A−
½ hour at 1,800° F, A. C	None	A	A	A	E	E	E	D+	B+
Do	1 hour at 1,600° F, A. C	A	B+	A−	CD	D−	D	BC	A
3 min at 1,975° F, W. Q	None	A	A	A	D+	E	E	E	DE
Do	1 hour at 1,600° F, A. C	A	BC	B+	E+	E	E	B−	B
3 min at 1,975° F, A. C	None	A	A	A	DE	E+	E+	DE	E+
Do	½ hour at 1,600° F, A. C	A	AB	AB	E+	E	E	BC	CD
Do	2 hours at 1,600° F, A. C	A−	A−	B	D−	E	E	BC	C

TABLE 17. *Effect of various treatments upon the susceptibility to intergranular attack of steel S–39*

(Carbon=0.065%, titanium=0.36%; Ti/C=5.5)

Treatment of steel subsequent to cold-rolling		Sensitizing treatment							
Annealing	Stabilizing	None	21 days at 840°F	2 hours at 1,020°F	2 days at 1,020°F	8 days at 1,020°F	21 days at 1,200°F	2 hours at 1,020°F	2 days at 1,200°F
None	None	A	B+	A	A−	B+	A	A	A−
Do	½ hour at 1,600° F, A. C	A	A	A	A	A	A	A	A
½ hour at 1,800° F, W. Q	None	A	A	A	A−	C−	C−	A−	A
Do	½ hour at 1,600° F, A. C	A	A	A	AB	B−	BC	A	A
Do	2 hours at 1,600° F, A. C	A	A	A	B−	BC	BC	A−	A
½ hour at 1,800° F, A. C	None	A	A	A	BC	C−	CD	AB	A
Do	1 hour at 1,600° F, A. C	A	A	A	BC	BC	B	A	A
5 min at 1,975° F, W. Q	None	A	A	A	A	E+	E	A−	A−
Do	1 hour at 1,600° F, A. C	A	A	A	B	C	BC	A−	A−
5 min at 1,975° F, A. C	None	A	A	A	AB	D+	E	A	A−
Do	½ hour at 1,600 F, A. C	A	A	A	AB	D	D	A	A
Do	2 hours at 1,600° F, A. C	A	A	A	C+	C+	CD	A	A−

TABLE 18. *Effect of various treatments upon the susceptibility to intergranular attack of steel C–6*

(Carbon=0.064%, titanium=0.35%, Ti/C=5.5)

Treatment of steel subsequent to cold-rolling		Sensitizing treatment							
Annealing	Stabilizing	None	21 days at 840°F	2 hours at 1,020°F	2 days at 1,020°F	8 days at 1,020°F	21 days at 1,020°F	2 hours at 1,200°F	2 days at 1,200°F
None	None	A	A	A	A	A−	A	A	A
Do	½ hour at 1,600° F, A. C	A	A	A	A	A	A	A	A
½ hour at 1,800° F, W. Q	None	A	A	A	A−	AB	C−	A	A
Do	½ hour at 1,600° F, A. C	A	A	A	A−	A−	A−	A	A−
Do	2 hours at 1,600° F, A. C	A−	A−	A	A	A	A−	A	A
½ hour at 1,800° F, A. C	None	A	A	A	AB	C	C−	A−	A
Do	1 hour at 1,600° F, A. C	A	A	A	A−	BC	B−	A	A
5 min at 1,975° F, W. Q	None	A	A	A	A	D	D−	A	A−
Do	1 hour at 1,600° F, A. C	A	A	A	AB	B	C−	A	A
5 min at 1,975° F, A. C	None	A	A	A	A	D+	E+	A	B
Do	½ hour at 1,600° F, A. C	A	A	A	B+	CD	D	A	A−
Do	2 hours at 1,600° F, A. C	A	A	A	C+	C+	C+	A	A−

TABLE 19. *Effect of various treatments upon the susceptibility to intergranular attack of steel C–2*

(Carbon=0.070%, titanium=0.50%; Ti/C=7.1)

Treatment of steel subsequent to cold-rolling		Sensitizing treatment							
Annealing	Stabilizing	None	21 days at 840°F	2 hours at 1,020°F	2 days at 1,020°F	8 days at 1,020°F	21 days at 1,020°F	2 hours at 1,200°F	2 days at 1,200°F
None	None	A	C−	A	AB	A	B−	A	A
Do	½ hour at 1,600° F, A. C	A	A	A	A	A	A	A	A
½ hour at 1,800° F, W. Q	None	A	A	A	A	A	A	A	A
Do	½ hour at 1,600° F, A. C	A	A	A	A	A	A	A	A
Do	2 hours at 1,600° F, A. C	A	A	A	A	A	A	A	A
½ hour at 1,800° F, A. C	None	A	A	A	A	B+	B+	A	A
Do	1 hour at 1,600° F, A. C	A	A	A	A	A	A−	A−	A
5 min at 1,975° F, W. Q	None	A	A	A	A	BC	D	A	A
Do	1 hour at 1,600° F, A. C	A	A	A	A	A	A−	A	A
5 min at 1,975° F, A. C	None	A	A	A	A	B+	D+	A	A
Do	½ hour at 1,600° F, A. C	A	A	A	A	A−	A−	A	A−
Do	2 hours at 1,600° F, A. C	A−	A−	A	A	A−	A	A	A

TABLE 20. *Effect of various treatments upon the susceptibility to intergranular attack of steel C–5*

(Carbon=0.075%, titanium=0.59%; Ti/C=7.9)

Treatment of steel subsequent to cold-rolling		Sensitizing treatment							
Annealing	Stabilizing	None	21 days at 840° F	2 hours at 1,020° F	2 days at 1,020° F	8 days at 1,020° F	21 days at 1,020° F	2 hours at 1,200° F	2 days at 1,200° F
None	None	A–	B+	A	A	AB	B+	A	A
Do	½ hour at 1,600° F, A. C	A	A	A	A	A	A	A	A
½ hour at 1,800° F, W. Q	None	A	A	A	A	A	A	A	A
Do	½ hour at 1,600° F, A. C	A	A	A	A–	A	A	A	A
Do	2 hours at 1,600° F, A. C	A	A	A	A	A	A	A	A
½ hour at 1,800° F, A. C	None	A	A	A	A–	A	A	A	A
Do	1 hour at 1,600° F, A. C	A	A	A	A	A	A–	A–	A
3 min at 1,975° F, W. Q	None	A	A	A	A	A	A–	A	A
Do	1 hour at 1,600° F, A. C	A	A	A	A	A	A	A	A
3 min at 1,975° F, A. C	None	A	A	A	A	A	B	A	A
Do	½ hour at 1,600° F, A. C	A	A	A	A	A	A	A	A
Do	2 hours at 1,600° F, A. C	A	A	A	A	A–	A–	A	A

Table 21. Effect of various treatments upon the susceptibility to intergranular attack of steel S–25

(Carbon=0.082%, titanium=0.37%; Ti/C=4.5)

Treatment of steel subsequent to cold-rolling		Sensitizing treatment							
Annealing	Stabilizing	None	21 days at 840° F	2 hours at 1,020° F	2 days at 1,020° F	8 days at 1,020° F	21 days at 1,020° F	2 hours at 1,200° F	2 days at 1,200° F
None	None	A	C D	B	C–	D+	B+	A	A
Do	½ hour at 1,600° F, A. C	A	AB	A	E+	E+	D+	A–	A
½ hour at 1,800° F, W. Q	None	A	A	A	E	E	E	B	A–
Do	½ hour at 1,600° F, A. C	A	B–	A–	E	E+	E	A–	A
Do	2 hours at 1,600° F, A. C	A	A	A–	DE	DE	E+	A–	A–

TABLE 22. *Effect of various treatments upon the susceptibility to intergranular attack of steel S–35*

(Carbon=0.107%, titanium=0.44%; Ti/C=4.1)

Treatment of steel subsequent to cold-rolling		Sensitizing treatment							
Annealing	Stabilizing	None	21 days at 840° F	2 hours at 1,020° F	2 days at 1,020° F	8 days at 1,020° F	21 days at 1,020° F	2 hours at 1,200° F	2 days at 1,200° F
None	None	A	E+	D+	DE	C+	B	A	A
Do	½ hour at 1,600° F, A. C	A	AB	A–	DE	E	D	A–	A
½ hour at 1,800° F, W. Q	None	A	A	A	E	E	E	D	A
Do	½ hour at 1,600° F, A. C	A	C	B	E	E	E	A	A
Do	2 hours at 1,600° F, A. C	A	A	A	DE	E+	E	AB	A–
½ hour at 1,800° F, A. C	None	A	A	A	D–	E	DE	B–	A
Do	1 hour at 1,600° F, A. C	A	B+	A–	D	DE	D	BC	A
3 min at 1,975° F, W. Q	None	A	A	A	C–	E	E	E	DE
Do	1 hour at 1,600° F, A. C	A	B+	AB	D–	E	E	B–	AB
3 min at 1,975° F, A. C	None	A	A	A	DE	E	E	D–	E+
Do	½ hour at 1,600° F, A. C	A	B	A	DE	E	E	B+	C+
Do	2 hours at 1,600° F, A. C	A	B+	B	D–	E	E	B	C+

TABLE 23. *Effect of various treatments upon the susceptibility to intergranular attack of steel S–36*

(Carbon=0.109%, titanium=0.54%; Ti/C=5.0)

Treatment of steel subsequent to cold-rolling		Sensitizing treatment							
Annealing	Stabilizing	None	21 days at 840° F	2 hours at 1,020° F	2 days at 1,020° F	8 days at 1,020° F	21 days at 1,020° F	2 hours at 1,200° F	2 days at 1,200° F
None	None	A	B−	A	D−	B+	B+	A	A
Do	½ hour at 1,600° F, A. C.	A	A	A	A	A	A	A	A
½ hour at 1,800° F, W. Q.	None	A	A	A	C+	C	E+	A	A
Do	½ hour at 1,600° F, A. C.	A	A	A	A	A	A	A	A
Do	2 hours at 1,600° F, A. C.	A	A	A	A	A	A	A	A
½ hour at 1,800° F, A. C.	None	A	A	A	B−	C+	BC	AB	A
Do	1 hour at 1,600° F, A. C.	A	A	A	B	B	A−	A	A
5 min. at 1,975° F, W. Q.	None	A	A	A	B+	E+	E	C+	A
Do	1 hour at 1,600° F, A. C.	A	A	A	A−	A−	B	A	A
5 min. at 1,975° F, A. C.	None	A	A	A	C+	DE	E	A−	A
Do	½ hour at 1,600° F, A. C.	A	A−	A	A−	BC	B−	A	A
Do	2 hours at 1,600° F, A. C.	A	A	A	C+	BC	C−	A−	A−

TABLE 24. *Effect of various treatments upon the susceptibility of intergranular attack of steel S–32*

(Carbon=0.105%, titanium=0.61%; Ti/C=5.8)

Treatment of steel subsequent to cold-rolling		Sensitizing treatment							
Annealing	Stabilizing	None	21 days at 840° F	2 hours at 1,020° F	2 days at 1,020° F	8 days at 1,020° F	21 days at 1,020° F	2 hours at 1,200° F	2 days at 1,200° F
None	None	A	B+	A	C	AB	B+	A	A
Do	½ hour at 1,600° F, A. C.	A	A	A	A	A	A	A	A
½ hour at 1,800° F, W. Q.	None	A	A	A	A	B+	C−	A	A−
Do	½ hour at 1,600° F, A. C.	A	A	A	A	A	A	A	A
Do	2 hours at 1,600° F, A. C.	A	A	A	A	A	A	A	A
½ hour at 1,800° F, A. C.	None	A	A	A	B+	B	A	A	A
Do	1 hour at 1,600° F, A. C.	A	A	A	A	B	AB	A	A
5 min. at 1,975° F, W. Q.	None	A	A	A	A−	D	D	A	A
Do	1 hour at 1,600° F, A. C.	A	A	A	A−	A−	A−	A	A
5 min. at 1,975° F, A. C.	None	A	A	A	B+	C+	DE	A	A
Do	½ hour at 1,600° F, A. C.	A	A	A	A−	B+	B−	A	A
Do	2 hours at 1,600° F, A. C.	A	A	A	A−	B	BC	A	A

V. Results and Discussion

All specimens were examined for carbide distribution subsequent to sensitizing. The type of distribution of the precipitated carbides was not an infallible indication of the resistance to intergranular attack. Steels in which the carbides were distributed randomly were usually resistant to intergranular attack. However, steels that contained carbides at the grain boundaries, even though these carbides were distributed as a continuous network, either were or were not susceptible to intergranular attack, depending on the time-temperature relation during sensitization. Frequently the microstructures of susceptible and unsusceptible specimens of the same steel appeared quite similar. A rather striking illustration of this statement is shown in figure 2. This figure shows the microstructure of a straight carbon (0.09%) austenitic steel, initially as cold rolled, after sensitizing 2 hours at 1,200° F (fig. 2, A) and after sensitizing 2 days at 1,200° F (fig. 2, B). Both micrographs show a precipitation of carbides at the grain boundaries and on various slip planes, and it is evident that the microstructures resulting from the two treatments are indistinguishable. The behavior of these two specimens after exposure to the boiling acidified copper sulfate solution, however, differed radically (fig. 2, c). The left side of the micrograph, which corresponds to specimen A, was exposed 2 days and suffered severe intergranular corrosion. The right side of the micrograph, which corresponds to specimen

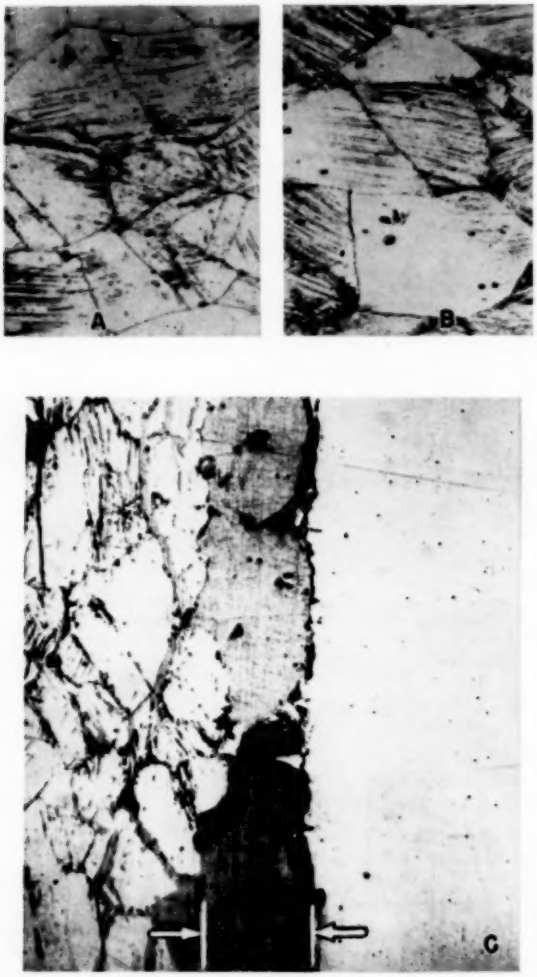

FIGURE 2. *Structure of straight carbon (0.09%) austenitic stainless steel, initially as cold-rolled, before and after exposure to the boiling acidified copper sulfate solution.*

A, Sensitized 2 hours at 1,200° F. Heavy carbide precipitation at grain boundaries and on slip planes. Etched electrolytically 10 minutes in 10-percent sodium cyanide. ×500. *B*, Sensitized 2 days at 1,200° F. Heavy carbide precipitation at grain boundaries and on slip planes. Etched electrolytically in 10-percent sodium cyanide. ×500. *C*, Specimens *A* and *B* after exposure to boiling acidified copper sulfate solution. Left side of micrograph, which corresponds to *A*, was exposed 2 days and suffered severe intergranular attack. Right side of micrograph, which corresponds to *B*, was exposed 14 days and showed no evidence of intergranular attack, yet both had the same type of carbide precipitation. The massive gray globules attached to specimen shown on left of *C* are particles of copper deposited from the acidified copper sulfate solution. Unetched. ×250.

B, was exposed 14 days and showed no evidence whatever of intergranular attack.

As a total of well over 2,500 individual specimens were tested, it is obviously impractical to present a detailed account of the test data pr cured. All data were assembled in tabular for for study. The performance of each specime was then rated on the basis of each of the fo methods of evaluation (electrical resistivit metallic ring, bend test, and microstructure aft corrosion). An arbitrary system of appraisal w used, as follows:

A. Completely immune to intergranular attac Electrical resistivity, no increase; metallic rin no impairment; bend test, no evidence of crack microstructure, no evidence of intergranular a tack.

B. Practically immune to intergranular attac Electrical resistivity, not more than 12 perce increase; metallic ring, slightly dead; bend te slight cracks; microstructure, slight intergranul attack in extreme surface layers only.

C. Moderately vulnerable to intergranular a tack: Electrical resistivity, more than 12 perce but not more than 25 percent increase; metall ring, slight; bend test, cracked; microstructur moderately severe intergranular attack in surfa layers only.

D. Vulnerable to intergranular attack: ele trical resistivity, more than 25 percent increas metallic ring, dead; bend test, broke; microstru ture, intergranular attack.

E. Extremely vulnerable; Same as D, b occurring in a few days.

The four ratings obtained for each individu specimen were then averaged by assigning n merical values to the ratings (A=4, B=3, C= D=1, E=0) and converting to the appropria letter symbol. Plus or minus signs were used t indicate averages falling slightly above or belo letters, respectively, and averages falling midwa between two letters were denoted by both letter These averages were then used to prepare tabl 2 to 24, inclusive, which summarize qualitativel the performance of each steel after various an nealing, stabilizing, and sensitizing treatment The averaged letter symbols may be considere as an order of merit, bearing in mind that th differences between A and B are rather slight, an those between D and E are very large. Sinc specimens were exposed to the boiling acidifie copper-sulfate solution for a maximum time of days, specimens that were rated B and C, and i many cases even D, might have been rated s satisfactory had they been subjected to the co

ding solution for the more or less standardized ne of only 2 days.

A noteworthy feature shown by these tables is at the sensitizing temperature of 1,200° F, ich is commonly specified, is too high to effect aximum susceptibility to intergranular attack. posure to a sensitizing temperature of 1,020° F much more effective, provided the time of exsure is quite long. A period of 8 or 21 days at 20° F appeared to be the most severe sensitizg treatment of those used. It was not unusual steels that showed complete immunity to intergranular attack after sensitizing either 2 hours or days at 1,200° F to be definitely vulnerable to tergranular attack after sensitizing for either 8 21 days at 1,020° F. It is possible that a orter period of time at a temperature higher an 1,020° F, but lower than 1,200° F, would be ually effective in causing maximum sensitizaon. This possibility, however, was not explored ring this investigation.

Considering the steels that contained no stabilizg elements (tables 2 to 6, inclusive), it is apparnt that all of these were quite vulnerable to tergranular attack after certain sensitizing atments. Decrease in carbon content decreased e degree of vulnerability, but even the two very w-carbon steels tested were quite susceptible to attack. The ratio of chromium to nickel in steel C–1 (table 2) was such that, in the presence of low carbon, appreciable amounts of delta ferrite were present in the microstructure. Steel C–10 (table 3) contained lower chromium and higher nickel so that no delta ferrite existed. This latter steel proved generally to be the more susceptible to intergranular attack except that, in the initially cold-rolled condition, it was practically immune.

The performance of the individual columbium- and titanium-treated steels may be studied by reference to the appropriate table, but a more readily comprehensible presentation is given in table 25. In this table only the worst averaged rating of each steel, as presented in tables 7 to 24, inclusive, is used. The steels are arranged in table 25 in order of Cb/C or Ti/C ratio without regard to the carbon content. It will be observed that, for all 12 initial conditions studied, the performance of the steels improves as the Cb/C or Ti/C ratios increase. Apparently the carbon content within the range studied (0.06 to 0.13%) had little, if any, effect upon susceptibility to intergranular attack, the predominating factor being the Cb/C or Ti/C ratio. The ratings of the various steels, as given in table 25, are plotted, as an order of merit, against the Cb/C and Ti/C ratios in figures 3 and 4.

TABLE 25. *Qualitative rating of resistance of test steels to intergranular attack* [a]

Steel No.	Percentage of C	Ratio		Cold-rolled (37½%)		Annealed ½ hr at 1,800° F, W. Q.			Annealed ½ hr at 1,800° F, A. C.		Annealed 3 min at 1,975° F, W. Q.		Annealed 3 min at 1,975° F, A. C.		
		Cb/C	Ti/C	No stabilizing treatment	Stabilized ½ hr at 1,600° F, A. C.	No stabilizing treatment	Stabilized ½ hr at 1,600° F, A. C.	Stabilized 2 hr at 1,600° F, A. C.	No stabilizing treatment	Stabilized 1 hr at 1,600° F, A. C.	No stabilizing treatment	Stabilized 1 hr at 1,600° F, A. C.	No stabilizing treatment	Stabilized ½ hr at 1,600° F, A. C.	Stabilized 2 hr at 1,600° F, A. C.
	0.068	7.4	.....	D	DE	E	E+	E	E	E+	E	DE	E	E	E
	.115	8.0	.....	C−	D+	E	E+	E+	E+	DE	E	E	E	E+	E+
	.070	8.7	.....	B	C−	E+	E+	E+	D−	D−	E	E	E+	E	E
	.087	8.7	.....	B	C−	E+	E+	E+							
	.117	9.7	.....	B+	A	B+	B	A	AB	BC	D+	B	CD	D	C−
	.074	10.1	.....	B+	A	A−	A−	A	A−	B−	D+	B	C−	C−	C
	.132	11.1	.....	A−	A	A−	A−	A	A	B+	B	A−	B+	B	A−
	.060	11.8	.....	A−	A	A	A−	A	A	A−	A	A	A−	A	A
	.067	.....	3.9	E+	E	E	E	E	E	E	E	E	E	E	E
	.107	.....	4.1	E+	E	E	E	E	E	DE	E	E	E	E	E
	.071	.....	4.5	DE	E+	E	E	E	E	D−	E	E	E+	E	E
	.082	.....	4.5	D+	E+	E	E	E+							
	.109	.....	5.0	D−	A	E+	A	A	C+	B	E	B	E	BC	C−
	.065	.....	5.5	B+	A	C−	BC	BC	CD	BC	E	C	E	D	CD
	.064	.....	5.5	A−	A	C−	A−	A−	C−	BC	D−	C−	E+	D	C+
	.105	.....	5.8	C	A	C−	A	A	B	B	D	A−	DE	B−	BC
	.070	.....	7.1	C−	A	A	A	A	B+	A−	D	A−	D+	A−	A−
	.075	.....	7.9	B+	A	A	A−	A	A−	A−	A−	A	B	A	A−

[a] This table was prepared from tables 7 to 24, inclusive, using only the worst averaged rating of each steel in each initial condition. For instance, steel S–26, cold-rolled and stabilized ½ hour at 1,600° F, was rated DE as tested after sensitizing 8 days at 1,020° F (see table 7). Although for all other conditions of sensitization the ratings were higher than DE, this worst rating was used in this summary table.

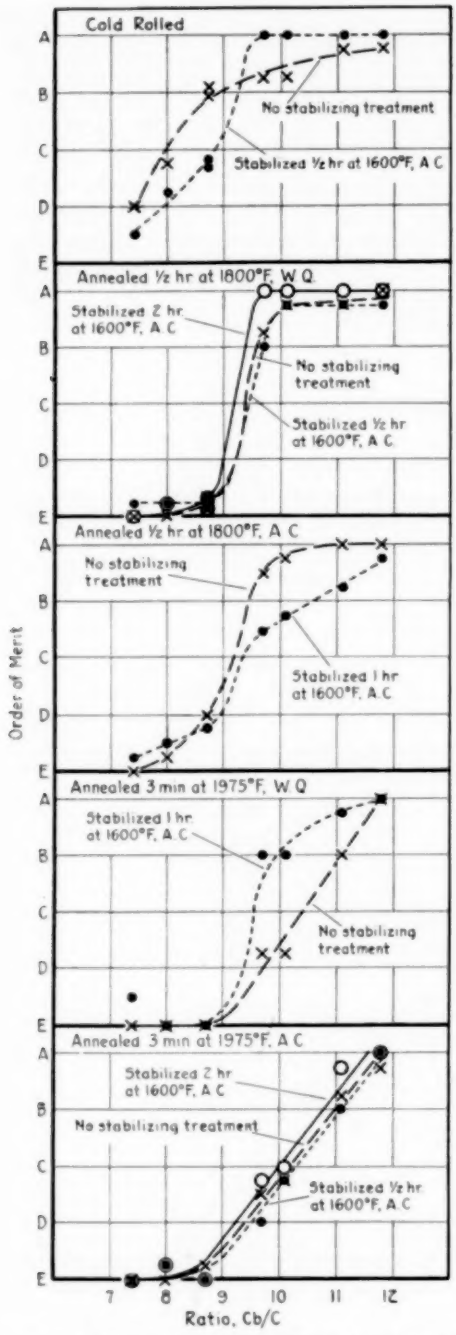

FIGURE 3. *Influence of ratio of* Cb/C *and of initial heat treatment upon resistance to intergranular attack.*

See page 334 for explanation of significance of letters representing order of merit.

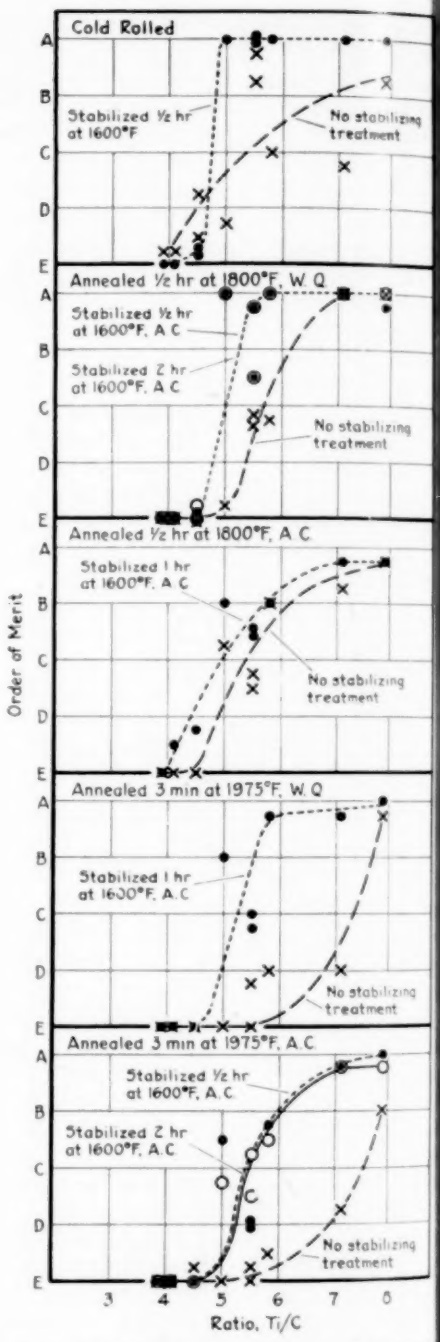

FIGURE 4. *Influence of ratio of* Ti/C *and of initial treatment upon resistance to intergranular attack.*

See page 334 for explanation of significance of letters representing order of merit.

regardless of the initial condition of the steels, ...ase in Cb/C or Ti/C to the higher ratios had ...arkedly beneficial effect upon the resistance to ...granular embrittlement. The ratio required ...ubstantial immunity varied with the initial ...tion of the steel. Of the initial conditions ...ed, those conferring maximum immunity to ...granular attack were as cold rolled or as ...ched from 1,800° F in water. Increase in ...aling temperature from 1,800° to 1,975° F ...ired the resistance to intergranular attack. ...deleterious effect of higher annealing temper... upon susceptibility to intergranular attack ...been shown by other investigators [8]. Air ...ing instead of water quenching after annealing ...also detrimental. The stabilizing treatment ...eared to be quite necessary for the titanium-...ted steels but was generally of only slight ...fit to the columbium-treated steels. In fact, ...superimposed stabilizing treatment appeared ...ally to be detrimental to the columbium-...ted steels as air cooled from 1,800° F. The ...n indicated no significant differences between ...bilizing periods of ½ and 2 hours at 1,600° F.

VI. Summary and Conclusions

...ata are presented on the resistance to inter-...ular embrittlement of 23 austenitic corrosion-...sting steels (18% Cr—10% Ni base composition) ...2 different initial conditions. Susceptibility to ...rgranular attack was determined after seven ...ferent sensitizing treatments, followed by a ...imum of 14 days exposure in a boiling ...ified copper sulfate solution. The following ...clusions appear warranted:

1. Of the various sensitizing treatments utilized, ...imum susceptibility to intergranular attack ...s developed by either 8 or 21 days at 1,020° F. ...e commonly used sensitizing treatment of 2 ...rs at 1,200° F was ineffective in developing ...eptibility in any but the most vulnerable ...els.

2. The straight carbon austenitic corrosion-...sting steels were very susceptible to intergran-...r embrittlement. The susceptibility decreased ...the carbon content decreased but, with the ...eption of one low-carbon steel in the cold-...ed condition only, even the very low carbon ...els (0.025% C) were vulnerable regardless of ...at treatment.

3. In the columbium- and titanium-bearing steels, carbon content within the range of 0.06 to 0.13 percent had no influence upon the resistance to intergranular attack, except insofar as it influenced the Cb/C or Ti/C ratios. Steels having similar ratios of stabilizing element to carbon had approximately the same degree of susceptibility to intergranular attack regardless of the carbon content.

4. Both the columbium- and titanium-treated steels exhibited greater resistance to intergranular attack as cold rolled or annealed at 1,800° F and water quenched than as annealed at 1,800° F and air cooled, or as annealed at 1,975° F and either water quenched or air cooled.

5. Stabilizing heat treatments at 1,600° F had a negligible effect upon the resistance to intergranular embrittlement of the columbium-treated steels. The performance of the titanium-treated steels carrying the higher ratios of Ti/C, however, was markedly improved by such treatments. Variation in time of the stabilizing treatments from ½ to 2 hours had no effect.

6. When properly treated, substantially complete immunity to intergranular attack may be obtained with a minimum ratio of Cb/C = 10 and Ti/C = 5. For more "fool-proof" immunity, it is believed that these ratios should be 12 and 8 respectively.

It should be emphasized that the data and conclusions given in this paper refer only to the susceptibility of the test steels to intergranular attack as developed under test conditions considerably more severe than those normally used.

The authors are indebted to Lt. Dennis J. Carney and James Darby, Naval Research Laboratory, for assistance in melting the experimental steels; to G. N. Goller, Rustless Iron and Steel Division, American Rolling Mill Co., Baltimore, Md., for forging many of the steels; to M. E. Carruthers and H. I. White, American Rolling Mill Research Laboratory, Middletown, Ohio, for assistance in rolling the experimental steels; to J. L. Hague and J. T. Sterling, National Bureau of Standards, for the chemical and vacuum fusion analyses, respectively, and to Albert Lewis, National Bureau of Standards, for assistance in the early phases of the work.

This investigation was made possible by the generous support of the Bureau of Aeronautics, Navy Department, and the friendly cooperation of N. E. Promisel and B. A. Kornhauser of that Bureau.

VII. References

[1] B. Strauss, H. Schottky, and J. Hinnüber, Z. anorg. Chem. **188,** 309 (1930).

[2] Robert H. Aborn and Edgar C. Bain, Trans. Am. Soc. Steel Treating **18,** 837 (1930).

[3] E. Houdremont and P. Schafmeister, Arch. Eisenhüttenswsen **1,** 187 (1933).

[4] H. D. Newell, Trans. Am. Soc. Steel Treating **19,** 673 (1932).

[5] P. Payson, Trans. Am. Inst. Mining Met. Engineers **100,** 306 (1932).

[6] E. C. Bain, R. H. Aborn, and J. J. B. Rutherford, Trans. Am. Soc. Steel Treating **21,** 481 (1933).

[7] Frederick M. Becket and Russell Franks, Trans. Am. Inst. Mining Met. Engineers **113,** 143 (1934).

[8] L. B. Pfeil and D. G. Jones, J. Iron Steel Inst. **127,** 337 (1933).

WASHINGTON, December 16, 1947.